NTNU – Trondheim
Norwegian University of
Science and Technology

Effect of Surface Chemistry and Physical Properties of Carbon Nanotubes on the Adsorption of Polycyclic Aromatic Hydrocarbons in Aqueous Solutions

Muhammad Ramzan

Environmental Toxicology and Chemistry
Submission date: May 2013
Supervisor: Rudolf Schmid, IKJ
Co-supervisor: Oyvind Mikkelson, IKJ
Andrew Booth, SINTEF

Norwegian University of Science and Technology
Department of Chemistry

NTNU

Effect of Surface Chemistry and Physical Properties of Carbon Nanotubes on the Adsorption of Polycyclic Aromatic Hydrocarbons in Aqueous Solutions

KJ3910 – Master Thesis in Environmental Chemistry

CREDITS – 60

Muhammad Ramzan

Supervisors:

Rudolf Schmid
Department of Chemistry
NTNU

Øyvind Mikkelsen
Department of Chemistry
NTNU

Co-Supervisor:

Andrew Booth
Material and Chemistry
SINTEF

May 22, 2013

DEPARTMENT OF CHEMISTRY

ACKNOWLEDGEMENT

This thesis is written in collaboration with the Department of Chemistry NTNU and SINTEF Marine Environmental Chemistry. The experimental work of this thesis has taken place from September 2012 to April 2013 in the laboratories of SINTEF Sealab Trondheim.

My thesis would not have reached its completion without the aid of a group of people especially my supervisors Andy Booth, Rudolf Schmid and Øyvind Mikkelsen. Their talents and knowledge have always inspired me to work through all the obstacles I have faced during the project work.

A warm thanks to the SINTEF Sealab staff for creating a welcoming environment for me to execute my laboratory practices. I would like to thank to Marianne Unaas, Kjesrti Almas and especially Lisbet Sørensen and Berit Glomstad for giving me the needed training in the use of instruments, procedures and analytical software.

A huge thanks to Dr. Calin Marioara of SINTEF Materials and Chemistry Trondheim for providing TEM analysis of the carbon nanotubes and Dr. Aud I Spjelkavik of SINTEF Materials and Chemistry Oslo for providing me the BET and Total pore volume measurements. Thanks to Berit Glomsatd for sample preparations for Zeta potential and DLS measurements.

I would like to thank again Lisbet Sørensen and Berit Glomsatd for being excellent partners in conversations and frustrations.

ABSTRACT

Adsorption behavior of seven different carbon nanotubes (CNTs) towards polycyclic aromatic hydrocarbons (PAHs) was studied in moderately hard reconstituted water (MHRW) with and without dissolved natural organic matter (NOM). At one concentration, adsorption of phenanthrene towards these CNTs was determined using negligible depletion solid phase micro extraction (nd-SPME) followed by GC-MS analysis. The single walled carbon nanotubes (SWCNTs) showed much higher adsorption than all other CNTs. Functionalized multi-walled CNTs showed lower adsorption potential than their non-functionalized (MWCNTs) analogue. The adsorption potential of CNTs is affected by the type and extent of functionalization. Presence of NOM reduced phenanthrene adsorption towards the CNTs from 26-88 % of what was observed in MHRW. NOM decreases the adsorption potential of CNTs according to the type and extent of functionalization. The results suggest that increased diameter of MWCNTs might have supporting effect for the adsorption potential of CNTs for phenanthrene. The study could not find a clear correlation between the adsorption potential of the CNTs and one of the single parameter like specific surface area (SSA), outer diameter (OD), total pore volume (V_T) and length of the CNTs. The CNTs characterization results in this study seem to differ from manufacturer's specifications for these CNTs.

TABLE OF CONTENTS

List of Abbreviations

BET	Brunauer, Emmet and Teller
CNTs	Carbon nanotubes
DLS	Dynamic light scattering
EDX	Energy dispersive X-rays spectrometry
GC-MS	Gas chromatography-Mass spectrometry
MHRW	Moderately hard reconstituted water
MWCNTs	Multi walled carbon nanotubes
Nd-SPME	Negligible depletion solid phase micro-extraction
NOM	Natural organic matter
OD	Outer diameter
PAHs	Polycyclic aromatic hydrocarbons
PDMS	Polydimethylsiloxane
Phe	Phenanthrene
Pyr	Pyrene
Phe_{free}	Phenanthrene free concentration
SEM	Scanning electron microscopy
SSA	Specific surface area
SWCNTs	Single walled carbon nanotubes
SPME	Solid phase microextraction
TEM	Transmission electron microscope
VT	Total pore volume
ZP	Zeta potential

List of Figures

List of Tables

Chapter 1
Project Description

Carbon nanotubes (CNTs) represent a new group of materials with increasing application in new technologies. As a result, there is increased potential for their release to the environment. Concerns have risen regarding the possible negative effects CNTs might have on environmental and human health, and several studies have investigated the toxicity of these materials. More recently, the interaction between CNTs and environmentally relevant pollutants has received attention. CNTs exhibit a strong sorption affinity to hydrophobic organic contaminants (HOCs) and may influence their fate, bioavailability, and toxicity.

The current study focuses on the physical and chemical properties of CNTs and their interaction with HOCs. CNTs will be dispersed in synthetic natural water samples and phenanthrene will be selected as a representative PAH for use in the study. Known concentrations of phenanthrene will be spiked into the dispersions of the CNTs with and without dissolved natural organic matter (NOM). The aim of the project is to study the adsorption behavior of the selected PAH to CNTs with different physical and chemical properties.

In this project, two main parameters will be investigated to determine their effect upon adsorption characteristics:

- CNT surface chemistry (pure carbon CNTs, hydroxyl, carboxylic acid and amine functionalized analogues)

- CNT physical properties (single-walled CNTs, multi-walled CNTs, different lengths and diameters)

NOM will be used as stabilizing agent in the dispersion of CNTs in aqueous solutions. The use of NOM will also increase the environmental relevance of the experiments conducted.

After an exposure period to the CNTs, the remaining freely dissolved concentration of phenanthrene (phe_{free}) in the aqueous phase will be quantified by negligible depletion solid-phase micro-extraction (nd-SPME) followed by GC-MS analysis. A reduction in the freely dissolved concentration of a compound is evidence of adsorption to the CNTs and a reduction in potential bioavailability.

A wide range of CNTs are commercially available. Some of those selected for use in this study exhibit different physical properties (number of walls, length and diameter), which will be assessed for their impact on phenanthrene adsorption. In addition to different physical properties, CNTs with a range of surface chemistries are also available. CNTs with hydroxyl, carboxylic acid and amines substituents will be studied to determine what effect these surface chemistry has on adsorption behavior. The Selected CNTs will exhibit surface chemistries ranging from hydrophobic (no substituents) to hydrophilic (polar substituents).

Chapter 2
Introduction

2.1 Background Information

2.1.1 Global carbon nanotubes (CNTs) production statistics

Following the accidental discovery of CNTs (Iijima 1991) increasing number of potential applications are being suggested. Owing to their properties such as high electrical and thermal conductivity, small diameters, large aspect ratios, excellent mechanical strength and a tip surface area near to the theoretical limit, carbon nanotubes are replacing a variety of materials already in use. Currently more than 100 companies are producing carbon nanotubes with more than 1000 companies and research institutions active in CNTs related research and development. Increasing market demand has resulted in production of hundreds of tons of CNTs per annum (Patel 2011). In 2010, estimated production of CNTs was reported as 2500 metric tons (MT). In 2011, 32.5% compound annual growth rate (CAGR) was forecasted in the production of CNTs, shown in Figure 2.1.

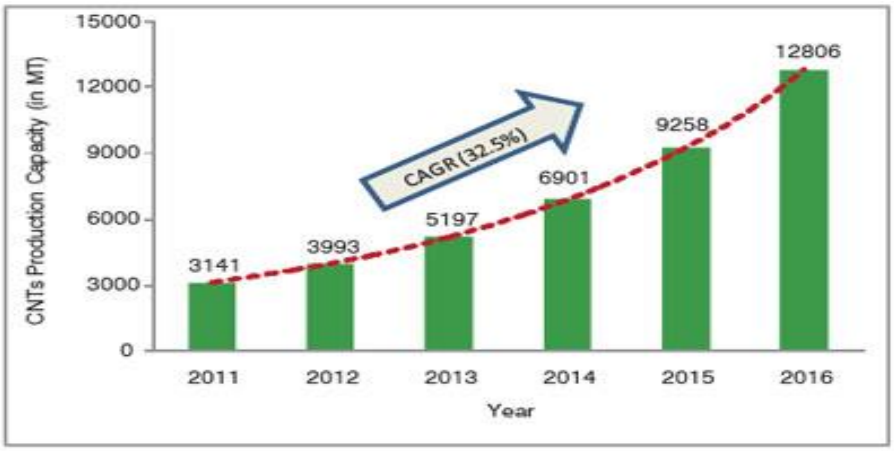

Figure 2.1. Five years forecast (2011-2016) for global CNTs production market (Patel 2011).

Plastics, composites, electrical, electronics and energy industries are the main consumers of CNTs currently. Racquets, ice hockey sticks, surf boards, golf clubs, mass transportation fuel system components, battery electrode additives, master batches and plastic additives are the CNTs enabled products already in consumer hands and it is expected that in the future will be much more dependent on carbon nanotubes. The electrical, electronics and energy industries are actively engaged in making more efficient CNTs enabled nano-electromechanical systems (NEMS), power transmission cables, super-capacitor electrodes, photovoltaic devices, Field effect transistors, and interconnects and transparent conducting films. The aerospace and automobile sectors are expected to use CNTs in their structural composites. The medical industry is focusing on more efficient and target oriented CNTs enabled drug and gene delivery systems. The present use and the expected future applications will lead to even

higher production of CNTs (Patel 2011) and increased risk of their release to the environment.

2.1.2 CNTs Release Pathways to the Environment:

CNTs can enter the environment through accidental releases from the production facilities or during the life cycle of CNTs incorporated in composite materials. During the life cycle of a nano-composites, CNTs can potentially be released to the environment by degradation (bio, photo, thermo or hydrolytic), incineration, washing or by mechanical mechanisms (abrasion, scratching, sanding). Release of CNTs from nano-composites through mechanical means has not been studied yet. Washing and falling rain onto the surface of nano-composites materials can release the loosely bound CNTs on the polymer surface to the environment illustrated in **Error! Reference source not found.**.

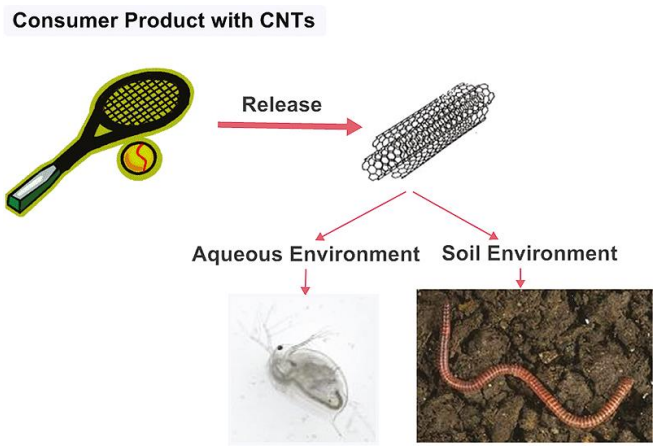

Figure 2.2. Carbon nanotubes environmental release pathways

(Petersen, Zhang et al. 2011)

Loss of polymer by degradation of the nano-composites surface causes more exposure of the CNTs and more likelihood of their release to the environment. Degradation of the matrix in nano-composites causes chain scissions and cross linking in the polymers leading the nano-composites to be more brittle. It also increases the likelihood of CNTs release from the nano-composites (Petersen, Zhang et al. 2011).

Another exposure route is the effluent of wastewater treatment facilities. Gottschalk and colleagues suggest that CNTs released into a sewer system mostly originate from CNTs containing textiles as a result of tailoring, finishing, use and degradation of these products or as a result of their use in research and development(Gottschalk, Sonderer et al. 2010). The quantity of CNTs released from a treatment facility as a part of effluent, depends on the efficiency of the CNTs removal system which is not well documented (Petersen, Zhang et al. 2011). In another study Gottschalk and colleagues assumed CNTs removal efficiencies of wastewater treatment facilities from 96.3% to 99.7% depending on natural organic matter present (Gottschalk, Sonderer et al. 2009). Holbrook and colleagues reported removal efficiencies of MWCNTs from 10%-85% which was dependent of influent CNTs concentration and coagulant type and dosage (Holbrook, Kline et al. 2010).

A lot of focus has been given to the development of new applications of CNTs but data regarding release pathways of CNTs and their fate and effect is mostly limited. Some studies have been conducted regarding the estimated release of CNTs through various routes to the air, soil, water and sediments. The available data is mostly concerned with

polymer/composite based CNT materials because they are commercially available (Petersen, Zhang et al. 2011).

2.1.3 Environmental concerns of CNTs

Although CNTs have potential for use in many applications and exhibit special physical and chemical properties, increasing use and production has also increased the potential for their release to the environment. Researchers have identified serious health and environmental risks regarding their release to the environment. The primary risk comes from the toxicity of the CNTs themselves, owing to their nano size, CNTs can enter into cells (Shi Kam, Jessop et al. 2004) and can cause damage to humans (Cui, Tian et al. 2005), animals (Warheit, Laurence et al. 2004) and plants (Miralles, Johnson et al. 2012).

CNTs have a very high sorption capacity for toxic substances because of their high surface area (Long and Yang ; Li, Wang et al. 2002) which can make them even more toxic (Yang, Zhu et al. 2006). The fate, transportation and transformation of toxic substances in the environment may also be affected by CNTs (Chen, Johnson et al. 2005; Sander and Pignatello 2005; Yang, Zhu et al. 2006). Yang and colleagues reported that adsorption of PAHs to CNTs is reversible and high adsorption capacity and reversible adsorption of PAHs might be a serious environmental and public health risk if PAH-adsorbed CNTs are inhaled (Yang and Xing 2007).

The potential effects of CNTs to the environment can be summarized as:

- CNTs are toxic themselves because of their nano structures and shape,
- CNTs may have enhanced toxicity due to high sorption capacity of toxic substances
- Transportation and potential release of contaminants from CNT-sorbate in environments which may initially be contaminant free.

2.1.4 Interaction of CNTs with organic compounds

The potential of CNTs for the sorption of organic contaminants is both a serious environmental concern but also a reason why CNTs have found potential application in the removal of organic pollutants from the environment. Therefore, it is critical to understand the interactions between organic contaminants and CNTs for both environmental hazards and environmental applications of CNTs (Chen, Duan et al. 2007). The Understanding of interactions between toxic compounds and CNTs is very important and useful for the risk assessment of CNTs (Yang, Zhu et al. 2006).

The outermost surface, inner cavities, interstitial channels and grooves of CNTs are the four possible sites for adsorption to CNTs (Zhao J.J 2002). The availability of these absorption sites is dependent on the morphology and functionalities of CNTs, molecular morphology and functional groups of the contaminants and environmental conditions

(Pan and Xing 2008). CNTs can vary in shape, size, surface area, diameter, curvature, chirality, number of walls, functional group, extent of functionalization, surface oxide contents, and impurities (metal, and amorphous carbon) which makes sorption to CNTs, a complex phenomenon (Chen, Duan et al. 2007; Pan and Xing 2008). Environmental conditions (pH, ionic strength and NOM) affect both CNTs and the organic contaminant and hence the interaction between them (Pan and Xing 2008). A very limited number of systematic studies has been conducted so far, which included a variety of pristine and functionalized CNTs to characterize and compare the adsorption behavior of CNTs in environmental conditions. Adsorption mechanisms will be better understood if the adsorption studies are performed under relevant environmental conditions (Pan and Xing 2008). This currently represents a significant knowledge gap.

2.2 Project aims and objectives

The aim of this MSc project is to study the adsorption behavior of commercially available CNTs with PAHs in environmental conditions.

There are two main objectives to this thesis.

- To assess how different functionalities on the surface of CNTs affect the adsorption behavior of CNTs
- To characterize how the number of walls, diameter and length affects the adsorption behavior of CNTs.

Chapter 3

Theoretical Back ground

3.1 Carbon nanotubes (CNTs)

Carbon nanotubes (CNTs) are long, thin, concentric hollow cylinders of one or more rolled grapheme sheets (Iijima 1991). Like graphite, graphene, diamond, fullerene and amorphous carbon, carbon nanotube (CNT) is one of the allotropic forms of carbon. Crystal structures of different allotropes of carbon are illustrated in Figure 3.1. Three dimensional (3D); a and b are diamond and graphite respectively, two dimensional (2D); c is graphene sheet, one dimensional (1D); d is CNT, zero dimensional (0D); e is buck balls.

A Graphene is an individual sheet of graphite while CNT is rolled up graphene sheet as illustrated in Figure 3.2. These sheets are rolled up at discrete chiral angles. In combination, both rolling angle and radius of CNT determine the properties of CNTs (In-Youp Jeon, Dong Wook Chang et al. 2011).

Figure 3.1. Crystal structures of different allotropes of carbon

(Katsnelson 2007).

Carbon atoms in CNTs are sp^2 hybridized and each carbon atom is joined to three carbon atoms like in graphite. CNTs are one dimensional having aspect ratio greater than 1000 (In-Youp Jeon, Dong Wook Chang et al. 2011).

Typical lengths of CNTs range from 1 to 100 μm and diameters range from 1 to 25 nm (Iijima 1991). Recent research has made it possible to make nanotubes much longer ranging to centimeters. Under high pressure, nanotubes merge together, with change of some sp^2 bonds to sp^3 bonds, thus producing greater length nanotubes (In-Youp Jeon, Dong Wook Chang et al. 2011).

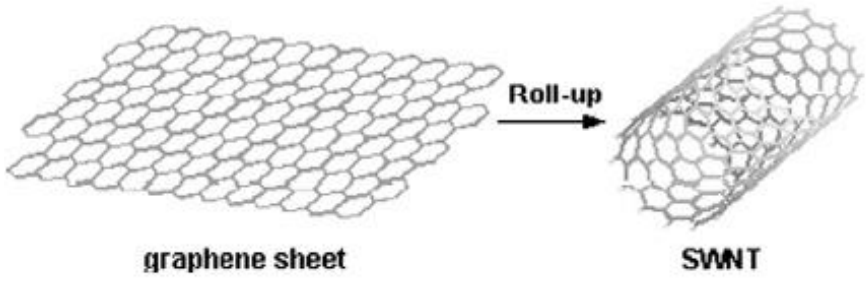

Figure 3.2. Rolling of graphene sheet into SWCNT illustrated.

(Aqel, El-Nour et al. 2012)

3.1.1 Types of CNTs

Carbon nanotubes can possibly be grouped in three ways.

1. **Number of walls:**

Single walled carbon nanotubes (SWCNTs), double walled carbon nanotubes (DWCNTs), multi walled carbon nanotubes (MWCNTs) are

the three types of CNTs on are three possible types of CNTs on the basis of number of walls, illustrated in Figure 3.3.

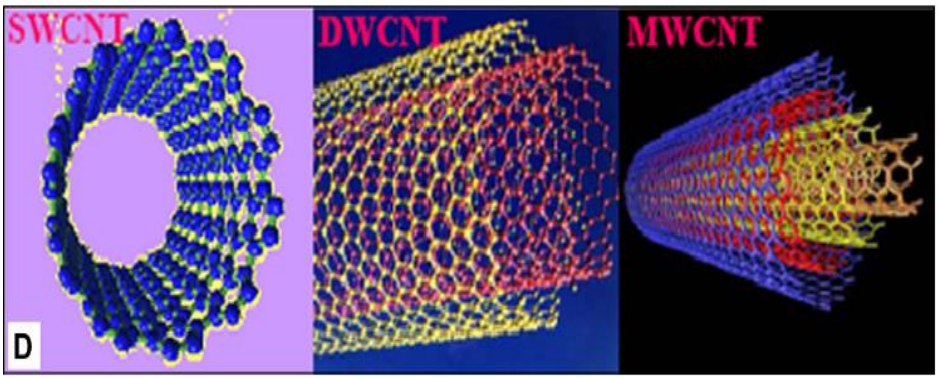

Figure 3.3. Three possible types of CNTs based on the number of walls.

(Aqel, El-Nour et al. 2012)

2. Structure:

Based on how the graphene sheet is oriented on rolling SWCNT can be classified as zigzag, armchair and chiral depending on the direction of hexagons in a CNT(Aqel, El-Nour et al. 2012). MWCNTs may have a mixture of all these. Getting MWCNTs with only one configuration is still a major challenge (University of Wisconsin 2008).

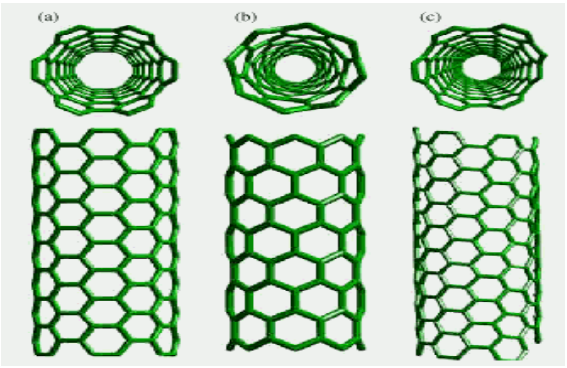

Figure 3.4. Directions of hexagons in a CNT a= armchair, b= zigzag, c= chiral

(University of Wisconsin 2008)

3. Functionalization:

Commercially available CNTs are heavily entangled bundles which are highly resistant to dispersion in aqueous or organic media (In-Youp Jeon, Dong Wook Chang et al. 2011) and are extremely resistant to wetting. It is also difficult to make composites of insoluble CNTs. Functionalization helps improve solubility, accessibility and makes possible to combine the unique properties of CNTs with other materials. Functionalization can be achieved by both covalent and non-covalent means. Derivitization of CNTs by modifying the external surface is called exohedral functionalization while modifying the inner cavity of the CNTs is called endohedral functionalization.

(a). Covalent exohedral functionalization

Linking entities like carboxylic, hydroxyl, amine, halo or group on carbon scaffold of CNTs by covalent bonding is called covalent functionalization. The possible sites are side walls or termini of the tubes

(i). Side wall functionalization: Involves functionalization directly on the side walls and is associated with change of hybridization from sp^2 to sp^3 resulting in simultaneous loss of conjugation.

(ii). Defect Functionalization: functionalization on defect sites of CNTs is called defect functionalization. Possible defect sites on CNTs are the open ends or holes in side walls, or terminated groups for example the –COOH or pentagon or hexagon irregularities (stone wall defects) in the hexagon graphene framework. Oxygenated sites resulting from oxidative purification of CNTs are also considered as defects sites.

(b). Non-covalent functionalization: Involves supramolecular complexation using Van der Waals or pi-stacking as adsorption forces. In this case, an extended pi network of CNTs is preserved improving the interfacial properties of CNTs while leaving the desired properties unchanged. Polymers, surfactants, biomolecules and aromatic compounds are non-covalently functionalized using pi-stacking and hydrophobic interactions.

(c). Endohedral functionalization: Involves trapping of nanoparticles inside the cavity of CNTs which is done in two ways.

(i). CNTs are treated with suspensions of nanoparticles which can penetrate the tubes and stay inside the CNTs. The incorporation of fullerenes is an example.

(ii). CNTs are filled with a material which reacts with the CNTs and then produces the nanoparticles. Creation of nanothreads of gold and platinum by treating SWCNTs with corresponding perchlorometallic acids at high temperatures is an example (Hirsch and Vostrowsky 2005).

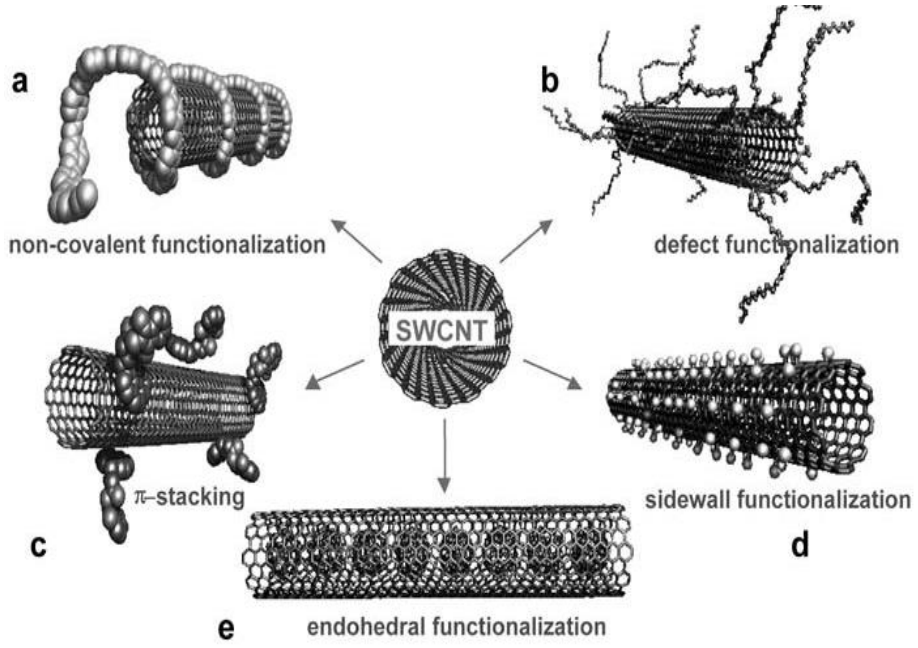

Figure 3.5. Different possibilities for the functionalization of CNTs

a:non-covalent exohedral functionalization with polymers, **b**:defect group functionalization, **c**:non-covalent exohedral functionalization through pi-stacking, **d**:side wall functionalization, **e**:endohedral functionalization, in this case C_{60} in SWCNT (Hirsch and Vostrowsky 2005).

3.2 Characterization techniques for CNTs

Characterization of carbon nanotubes either for industrial applications or adsorption studies is very important. There are two main reasons for this. Carbon nanotubes may contain a number of impurities depending on the method of production and subsequent purification technique used.

In all commonly acknowledged methods, CNTs contain graphene, amorphous carbon, smaller fullerenes and metal catalysts as impurities (Ebbesen 1997). Because CNTs are insoluble, purification methods are also not sufficiently efficient to get 100% homogeneous CNTs. Application of purification techniques not only removes impurities but also modifies the surface chemistry of CNTs. For example in acid treatment CNTs remain suspended while the acid dissolves the metal catalyst leaving carbonaceous materials un-separated. Oxidative treatment is effective in oxidizing and removing the carbonaceous impurities but also oxidizes the CNTs to some extent. Surface oxide contents of CNTs greatly affect their aggregation properties in aqueous environments and also their adsorption potential. The presence of impurities influences the properties of CNTs possibly affecting their adsorption behavior (Mawhinney, Naumenko et al. 2000; Hu, Bhowmik et al. 2001). No single method is available which can produce all carbon nanotubes of exact parameters even in the same batch. Carbon nanotubes produced differ in diameter, length, chirality, defects and numbers of walls in case of MWCNTs (Mawhinney, Naumenko et al. 2000; Hu, Bhowmik et al. 2001).

Techniques for bulk production of CNTs in a controlled way are still underdevelopment and present lots of challenges. Purification techniques also may result in the modification of CNTs where different purification techniques give different results (Aqel, El-Nour et al. 2012). Therefore, it is required to determine all the properties of CNTs including the qualitative and quantitative analysis of impurities present, to better understand the adsorption behavior of CNTs and

consider the role of each factor in adsorption. Table 3.1 summarizes the recommended techniques for the characterization of CNTs.

Table 3.1. Important recommended techniques for the characterization of CNTs (Florian and Asmus 2011)

Technique	**Metrics**
TEM	diameter, length, agglomeration, composition, impurities, surface contaminations, uniformity, chirality
SEM	length, agglomeration, composition, impurities, surface contaminations, uniformity
EDX	Impurities, contaminations
BET	porosity, surface area

Whilst there are large number of potential techniques which can be used in the characterization of CNTs and other nanomaterial, typically characterization is dependent upon those techniques which are available at a specific research facility. The techniques used to characterize the CNTs used in this study are described below.

3.2.1 Transmission electron microscopy (TEM):

The Working principle of a transmission electron microscope (TEM) is the same as a light microscope except that a TEM makes use of electrons. Due to the small de-Broglie wave length of electrons, TEM resolution is thousand times better than a light microscope. It is possible view objects in the order of Angstroms and even details down to the atomic level.

Electrons from the source at the top of the microscope travel through the column in vacuum and are focused by magnetic lenses and pass through a very thin layer of the specimen supported on a mesh called grid. Some of Incident electrons are scattered depending on the density of the part of the specimen.

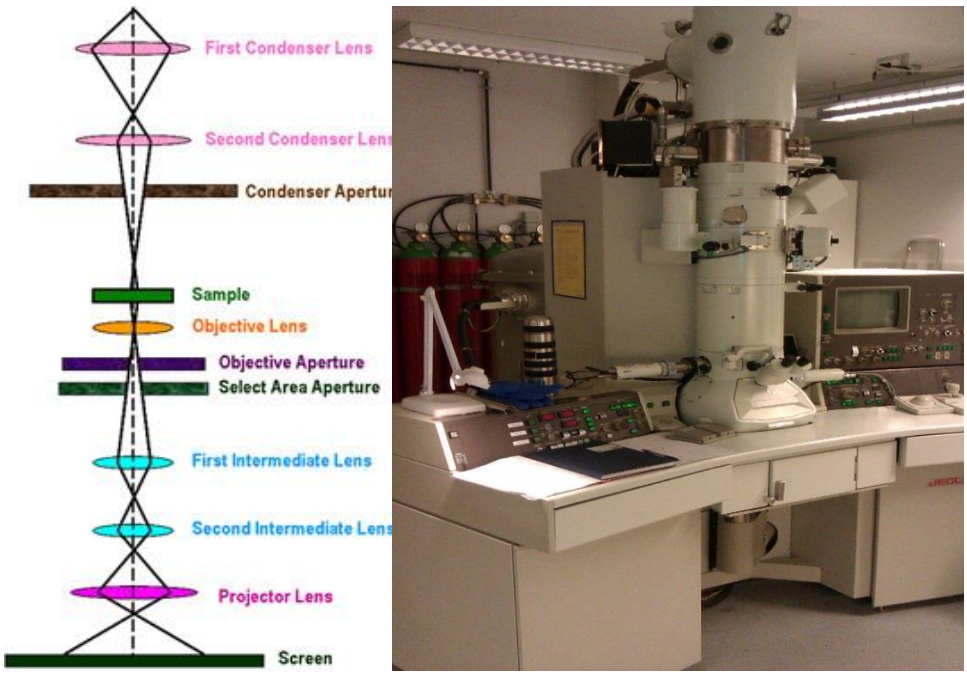

Figure 3.6. Schematic of a Transmission electron microscope (TEM)

Left image shows layout of components of a basic TEM(Ding). Image on right is Jeol JEM 2010F: the TEM used in current study (image courtesy SINTEF Trondheim Norway).

Scattered electrons disappear from the beam while transmitted electrons make the image of the specimen which is magnified and focused on a fluorescent screen, a layer of photographic film or CCD camera at the bottom of the TEM. The denser parts of the specimen

appear darker because of more scattering of the incident electrons (Egerton 2005).

The electron source in a TEM is an electron gun which either uses a hair pin or spike shaped tungsten filament or single crystal of lanthanum borohydride. When electron gun is connected to high voltage i.e 100-300 kV, it generates electrons either by thermal process called thermionic emission or by electrostatic field and the process is called field emission. The focusing, movement and manipulation of the electron beam is done by electromagnetism which forms electromagnetic lenses. The condenser lenses are responsible for primary beam formation, the objective lenses are responsible for electron beam through the sample and the project lenses expand the beam on the imaging device (Egerton 2005).

Transmission electron microscopy has been applied to reveal the internal structure of carbon nanotubes. Diameters of SWCNTs and MWCNTs, the number of walls and inter wall distances of MWCNTs are measured using high resolution transmission electron microscope (Journet, Maser et al. 1997; Kiang, Endo et al. 1998). TEM images of two MWCNTs involved in the current study are given in Figure 3.7.

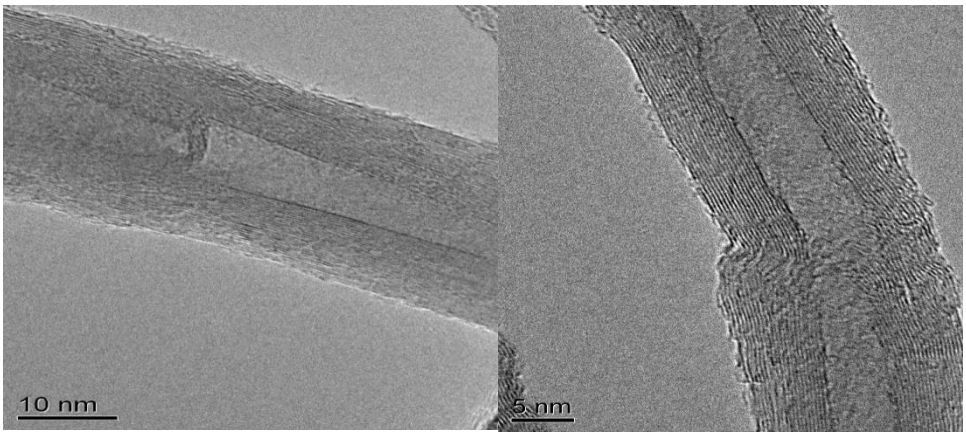

Figure 3.7. TEM images of two MWCNTs from samples involved in the current study.

3.2.2 Scanning electron microscopy (SEM):

Scanning electron microscopy (SEM) is considered a non-destructive technique widely used for the studying morphology, topography and chemical composition of solid materials. An accelerated beam of electrons interacts with a solid specimen and generates a variety of signals. Each signal is a result of a particular interaction and carries specific information. The most commonly used signals are secondary electrons (SE), back scattered electrons and X-rays (Egerton 2005).

Secondary electrons (SE) are the atomic electrons of the solid sample which are released as a result of the inelastic scattering of the electrons from the incident beam (called primary electrons). From law of conservation of energy, energy lost by a primary electron is gained by the electron causing inelastic scattering. Secondary electrons produced under a certain depth lose their energy as a result of inelastic collisions with other atomic electrons in the bulk. Only SEs produced near the surface are able to escape to the vacuum and reach the detector. The depth from which electrons are able to escape to the

vacuum depends on the energy of the incident electrons and the atomic number of the element present in the bulk. In the case of heavier elements fewer SEs reach the detector so heavier elements appear darker in the SEM images. As a result, signals produced by SEs reveal topographical information of the specimen (Egerton 2005). Figure 3.8 shows an SEM image of MWCNTs-COOH involved in the current study.

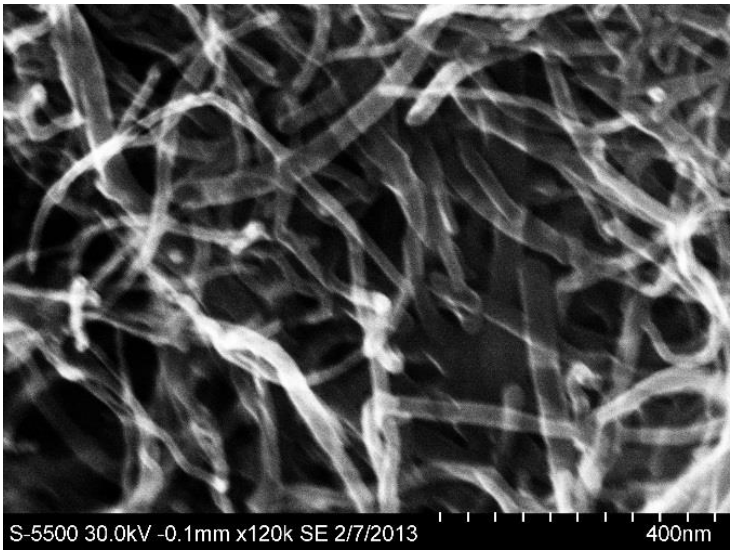

Figure 3.8. An SEM image of MWCNTs-COOH involved in this study

Image was taken from Hitachi S-5500 S(T)EM at NTNU nanolab Norway.

Some of the primary electrons change their trajectory as they interact with the sample surface without significant changes in their kinetic energy and are called back scattered electrons (BSE). The larger the atom, the more is the back scattering there is. Larger atoms have greater cross sectional area and hence higher probability of backscattering. Therefore in BSE images, high intensity areas are comprised of heavier elements while low intensity areas show

elements with lower atomic number. BSE detectors are placed above the sample based on scattering geometry of the incident beam (Goodge 2013). Signals below the sample are only observed if the thickness of the sample is small enough. Figure 3.9 illustrates the electron matter interaction arising from the impact of an electron beam.

Once the different portions of a surface are identified, the instrument provides the facility to focus the beam on one specific portion and the resulting X-rays can be used for elemental analysis. EDXs will be discussed below separately.

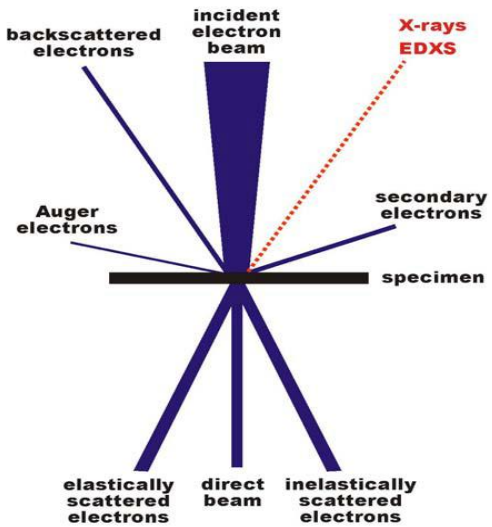

Figure 3.9. Scheme of electron matter interactions

(Krumeich)

When scanning technique is combined with the transmitted electron signals, the technique is termed as scanning transmission electron microscopy or STEM. Dedicated STEM instruments are available. A TEM is also equipped with scanning coils and can work in scanning mode

also. An SEM instrument is also provided with transmitted electron detector and the instrument can work as an SEM as well as STEM and is mentioned as S(T)EM. Spatial resolution in electron microscopy depends on the dimensions of electron probe. (Egerton 2005). Scheme of an SEM is shown in Figure 3.10.

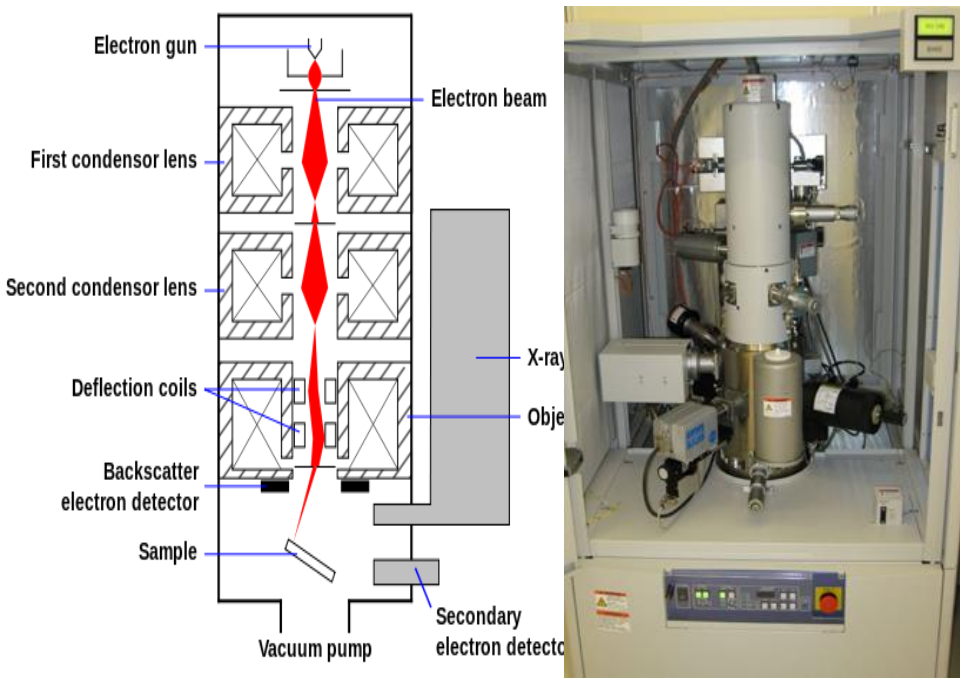

Figure 3.10. Scheme of a Scanning electron microscope (SEM)

Left is schematic image of a SEM. Right is Hitachi S-5500 S(T)EM at NTNU nanolab Norway used in current study.

3.2.3 Energy Dispersive X-Ray Spectroscopy (EDX):

X-rays are emitted when an electron beam interacts with a material. Emission of the X-rays from an element involves electronic transitions in its inner shells. Energy of the emitted X-rays depends on the energy

difference of the two orbitals involved in electronic transition, which is characteristic for each element due to its nuclear charge and electronic structure. Figure 3.11 illustrates the emission of X-rays from an element due to interaction with an electron beam.

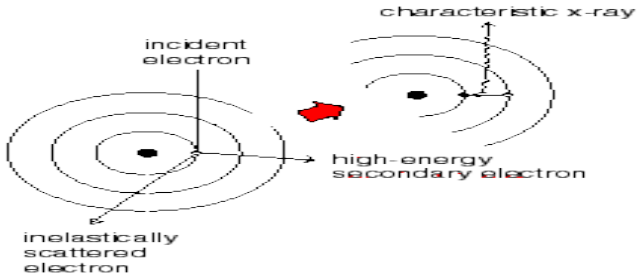

Figure 3.11 Illustration of the emission of X-rays

Hence every element has its characteristic X-ray spectrum. Each element in the sample can be identified by a particular X-ray and measuring the intensity of this X-ray makes its quantitative analysis possible. This technique is called X-ray spectrometry. The name “energy dispersive X-ray spectrometry (EDX)” comes because of the detector used which identifies X-rays based on their energy not the wavelength (NORON Instruments.).

3.2.4 Zetasizer

Zetasizer can measure the particle size and zeta potential of the particles in suspension. Concept of zeta poetical and the working principle of the instrument are briefly explained below.

When dispersed in aqueous systems, most particles acquire a charge on their surface. It happens either by ionization of already present functional groups on the surface or by the adsorption of charged

species present in the aqueous system. The charge on the surface of the particle modifies the distribution of ions in the system. The ions in the system with an opposite charge to the surface, arrange themselves around the surface in a layer which is different from the bulk distribution of ions and is termed as an electrical double layer. Figure 3.12 shows an electrical double layer around a spherical particle with negatively charged surface and potential drop as a function of distance.

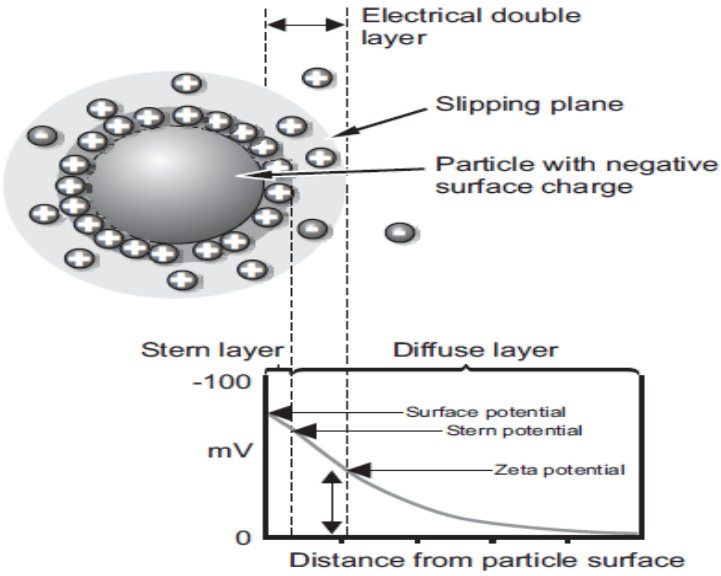

Figure 3.12. Representation of an electrical double layer around a spherical particle its Zeta potential

When the particle moves in the bulk solution because of Brownian motion or an electrical force this layer moves with the particle that's why its plane is called slipping plane. The potential of slipping plane is called zeta potential. A large zeta potential is indicative of greater repulsions between particles of same sign of zeta potential. Smaller particles with high zeta potential will have greater repulsive forces which will keep them apart and will keep them stable as suspension.

Zeta potential is pH dependent and is much smaller than the potential at the particle surface and it may be opposite in sign to that. Zeta potential is not possible to measure directly. The particles in the suspension are forced to move under the influence of an electric field and their velocity is measured using Doppler's frequency or phase shift in the incident laser beam. When phase shift is used to find electrophoretic mobility, the technique is called phase analysis light scattering (PALS). Zeta potential is calculated using particles equilibrium velocity under the applied electric field referred as electrophoretic mobility (Malver Instruments.). Electrophoretic mobility is directly proportional to zeta potential of the particle (Sakshat Virtual Labs).

3.2.5 "Brunauer, Emmet and Teller" Theory (BET)

The Surface area of a solid powder like material be determined using BET theory. According to BET, adsorption of a gas on a solid adsorbent surface occurs in multilayers and the total volume all the layers or the total volume of a gas adsorbed to the surface is correlated to the volume of its monolayer. The volume of monolayer of adsorbate can further be correlated to the surface area of adsorbent using cross sectional area of adsorbate gas molecules.

Degassing of the sample before BET analysis is compulsory in a way that its surface properties are not modified to a considerable extent. Adsorption of nitrogen at constant temperature but different pressures is usually measured (Particle analyticle 2013).

3.3 Negligible depletion solid phase micro-extraction (nd-SPME)

Negligible depletion solid phase micro-extraction (nd_SPME) is a sample preparation technique. The term negligible depletion is specified when solid phase micro-extraction (SPME) is performed under certain conditions. The concept of SPME and negligible depletion is explained below.

3.3.1 Solid phase micro-extraction (SPME)

Solid phase micro-extraction involves the extraction of analytes from the sample matrix to a liquid or solid coating supported on glass or fused silica fiber An SPME fiber is shown in Figure 2.1, coating and inside core can be seen clearly.

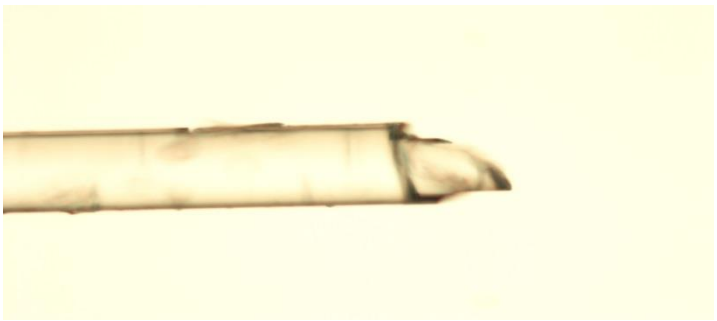

Figure 3.13. SPME fiber showing coating and inside core.

The transport of the analytes begins as the coated fiber is brought in contact with the sample. When the distribution equilibrium is achieved, it is considered that the maximum extraction is achieved because once the equilibrium is achieved there is no net gain in the quantity of the analytes extracted by the fiber. The quantity of the

analyte extracted by the fiber is directly proportional to the initial concentration of the analyte in the sample. The fiber is then analyzed to determine the concentration of the analyte in the sample. The extraction can interrupted prior to equilibrium at some fixed interval and the fiber can be analyzed. The latter determinations are called pre-equilibrium determinations. Equilibrium determinations are easy to perform. To get reproducible data in pre-equilibrium determinations, constant agitation conditions, temperature and careful extraction timings are required p.15 (Pawliszyn. 1997).

Since SPME is an equilibrium technique, the extraction by the fiber is not exhaustive. The fiber extracts a very small amount of the analyte from the matrix. This makes SPME a special and very useful for studying the natural systems where it can facilitate speciation without disturbing the equilibrium of the system p.16 (Pawliszyn. 1997).

3.3.2 nd-SPME

If SMPE meets the following three criteria then SPME is termed as negligible depletion solid phase micro-extraction (nd-SPME).

1. the extracted quantity of a particular analyte by the fiber is negligible as compared with the total amount present in the matrix
2. There is equilibrium between the bound and freely dissolved concentration of the analyte in the matrix
3. The binding matrix doesn't affect the extraction

The 1st point is the most important one. Only freely dissolved concentrations of the analytes are available for distribution to the

SPME fiber. This makes nd-SPME technique widely used to determine the free concentrations of the analytes even in very complex mixtures like in environmental samples for speciation, bioavailability interpretation (Heringa and Hermens 2003).

Since depletion cannot be zero so there should be set some limit. Researchers have proposed different limits. Vaes and colleagues have set this limit < 5% (Vaes, Urrestarazu Ramos et al. 1996), Górecki and Pawliszyn proposed <1% (Gorecki and Pawliszyn 1997) and Poerschmann proposed <10% (Poerschmann, Zhang et al. 1997).

3.3.3 Modes of SPME

SPME is performed in three modes. The choice of the mode is dependent on the volatility of the analyte and the nature of the matrix.

3.3.3.1 Direct Immersion SPME

In the direct immersion mode SPME fiber is directly inserted in the sample and the transport of the analyte is directly from the sample matrix to the fiber. The position of the fiber while immersed in the sample matrix does not make any difference. Once the fiber is in the matrix, the quantity of the analyte extracted is always the same, provided that all other conditions are kept constant p.16 (Pawliszyn. 1997). Direct immersion mode is referred as DI-SPME

3.3.3.2 Head Space SPME

In the head space mode, the analytes are transported to the fiber through the air above the sample matrix. It allows protection of the fiber from the interferences due to sample matrix. It also allows

modifications in the sample matrix, like pH changes, without damaging the fiber p. 16 (Pawliszyn. 1997).

3.3.3.3 Membrane protected SPME

The SPME fiber can be closed in semi permeable membrane which can allow the transport of the analyte molecules to and from, avoiding the large molecular weight interferences from the sample matrix. The large molecular weight compounds like humic acids can adsorb and block the fiber surface p. 16 (Pawliszyn. 1997). It can leading to higher equilibrium times and erroneous results. If these large molecular weight interferences also have adsorbed analyte, that can also be a part of the determination leading to erroneous results. The latter effect is termed is as fouling of the SPME fiber.

3.3.4 Experimental verifications for SPME

Nature of the coating material and thickness of the coating, temperature, agitation condition, pH, salt concentrations are the important parameters for SPME. Coating material selection depends on the nature of the analyte. Polydimethylsiloxane (PDMS) is widely used coating material for non-polar hydrophobic organic compounds like PAHs. Thickness of the coating affects the equilibrium time or speed of the analysis. The total amount extracted by the fiber depends on the volume of coating. Agitation conditions affect the mass transfer rate and determine the extraction rate and equilibrium time from aqueous samples p. 89 (Pawliszyn. 1997). Temperature is very important parameter and affects the coating/sample distribution

coefficient of the analyte. Salt concentration and pH affect SPME in similar fashion to solvent extraction p. 24 (Pawliszyn. 1997).

3.4 Gas chromatography-Mass spectrometry (GC-MS)

GC-MS is a hyphenated technique which couples the good separation quality of gas chromatography with the high resolution of mass spectrometry. The coupled GC-MS technique was pioneered in the 1950's by Fred W. McLafferty and Roland S. Gohlke (Gohlke and McLafferty 1993) and has since found a wide range of applications. Compared to other hyphenated chromatography and spectroscopic techniques (e.g. CE-MS, LC-MS and LC-NMR), GC-MS offers low costs and unsurpassed chromatographic reproducibility and resolution. Gas chromatography and mass spectrometry are explained below separately.

3.4.1 Gas chromatography (GC)

Gas chromatography (GC) is an important analytical method widely used in laboratories around the world. It's a frequently used method to separate and analyze volatile compounds ranging from 2 to above 1000 Da (McNair H.M. and Miller J.M 2011). In GC the mobile phase is an inert gas, such as nitrogen, helium or hydrogen, the main function of which is to carry the sample through the column. The stationary phase is a solid or a liquid coated on a solid support or directly on the column wall. In gas chromatography compounds are separated based on differences in vapor pressure and differences in retention time

which is due to interactions of analyte with the stationary phase (Poole C.F. 2003).

3.4.1.1 Gas Chromatograph

A gas chromatograph has several parts which are important for a successful separation. These parts are the carrier gas reservoir and the carrier gas, the flow control, the injector port, the column, the column oven, and the detector as well as a computer program to convert the detector signals into a chromatogram. Figure 3-14 shows a schematic setup of a gas chromatograph.

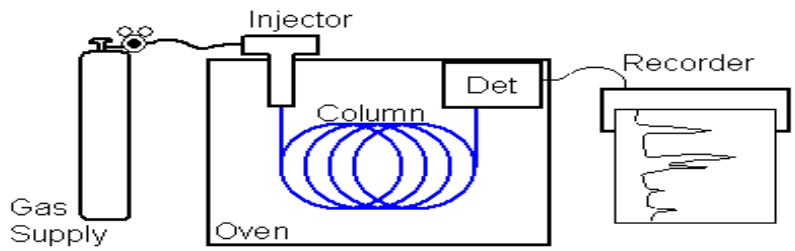

Figure 3.14. Schematic setup of a simplified gas chromatograph (KU Chemistry).

3.4.1.2 Carrier gas and flow control

Helium, nitrogen and hydrogen are all gasses that are used as carrier gasses in gas chromatography. The primary function of the carrier gas is to carry the sample through the column. The choice of carrier gas is based on efficiency, time availability, cost and safety as well as compatibility with the detector. The carrier gas reservoir is connected to the system at the sample injection chamber where the carrier gas is mixed with the sample vapor. The carrier gas flow is controlled by a flow controller or pressure regulator placed between the carrier gas reservoir and the sample injection chamber (Poole C.F. 2003).

3.4.1.3 Syringe, valves and sample inlets

The sample is typically introduced by a micro-syringe through a rubber septum. The sample is introduced into an injection chamber where it is vaporized and mixed with the carrier gas.

In split-less injection the entire sample is transferred into the heated injection port. The sample is heated and led into the cold column. Split-less injection is dependent on refocusing mechanisms, such as cold trapping or solvent effects, to avoid band broadening. An advantage with the split-less injection is increased sensitivity compared with split injection, which makes this type of injection mode better for trace analysis. The disadvantage of split-less injection is time demand and the need for a temperature controlled program.

Other sample inlets are the direct injection, programmed temperature vaporizer injection and cold on-column injection (Miller J.M. 2005).

3.4.1.4 Column

The column is the heart and soul of the chromatographic system. There are two main types of columns usually used in GC, packed columns and open tubular (capillary) columns. The dimensions within and between these two groups varies much, from short and broad preparative columns to long and thin columns in capillary GC. For analytical work the capillary column is the mostly used. Capillary columns used in GC have a length ranging from 10 to 100 meters, with inner diameter from 0.1-0.5 mm.

Considerable loss of stationary phase may occur due to evaporation if the stationary phase is not thermally stable and ideally having a boiling point of more than 100 ˚C higher than the maximum working temperature. Loss of stationary phase due to evaporation is called Column bleeding which can offer problems in chromatographic separations and detection of the anlyte. This is due to the high temperatures encountered in GC which can be as high as 400˚C. Bonded and cross-linked stationary phases, increase the column life and prevent column bleeding (Holler, Skoog et al. 2007).

3.4.1.5 Detectors

Several detectors have been used in GC, such as mass spectrometer, the electron capture detector (ECD), the flame ionization detector (FID), and the nitrogen-phosphorous detector (NPD), thermal conductivity detector (TCD) etc. These detectors are described below, while the ever more used mass spectroscopy (MS) detector is described separately later. Each detector has its own advantages and disadvantages (Holler, Skoog et al. 2007).

3.4.2 Mass spectrometry

Mass spectrometry is a micro-analytical tool that can provide more structural information about a unit analyte than any other known analytical technique. Structural determination and compound characterization is based on the measured mass-to-charge (m/z) ratio of an analyte molecule. The sample molecules are first ionized by an ion source, before they are analyzed in the mass analyzer. A schematic showing the device setup is given in Figure 2. Ionization may cause the

analyte particles to fragment, producing characteristic fragments with specific masses that can be used for either quantitative or qualitative analysis. Qualitative analysis offers structural determination, while quantitative analysis provides information about the concentration. (Throck Watson J. 2007).

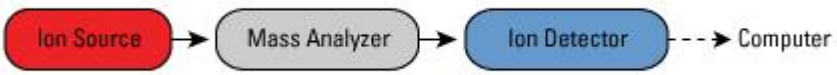

Figure 3.15. Scheme of the basic components of a mass spectrometer (Thermo Scientific).

A brief description of the components of a mass spectrometer is given below.

3.4.2.1 Ion Source

The ion source produces ions in gas phase. There are many different ionization methods currently available, electron ionization (EI) and chemical ionization (CI) being the most common for gaseous molecules. The choice of ion source depends on physical and chemical properties of the analyte and the internal energy transfer during the ionization process. The EI is a highly energetic ionization technique, which typically offers extensive fragmentation. The advantage is that fragmentation patterns are reproducible meaning that comparison of unknown fragmentation patterns to known ones are possible using spectral databases. However, massive fragmentation may lead to the disappearance of the molecular ion, making characterization of the molecule difficult. (Edmond de Hoffman 2007)

3.4.2.2 Mass analyzer

A mass analyzer is a device that separates ions based on only their m/z ratio independent of their chemical conformation.

Several types of mass analyzers are in use e.g. magnetic or pure electric, scanning or non-scanning, trapping or non-trapping, quadruple mass filter, quadruple ion trap and Fourier transform ion cyclotron resonance. All are based on electromagnetism.

The quadruple mass analyzer is based on a combination of direct current (DC) and radio frequency (RF) in four symmetrically arranged parallel rods. Diagonally aligned rods are electrically connected to make a pair. At any given time the two pairs have a potential of same magnitude, but with opposite signs. When accelerated ions enter in quadruple, they are affected by the applied electrical field according to their m/z ratio. Heavy ions have low charge density and will therefore be less influenced by the attractions and repulsions. They travel through the quadruple mainly under the influence of the DC electrodes, while the lighter ions are more influenced by the changes in the AC electrodes due to high charge density. In other words, the ratio between the DC and RF current determines the trajectory of ions which makes it possible to direct ions of appropriate masses to the exit slit towards the detector. A full scan run can be done by changing the ratios of DC and AC in both pairs of a quadruple (Miller J.M. 2009). An explanatory picture of the quadruple device in given in Figure 3.16

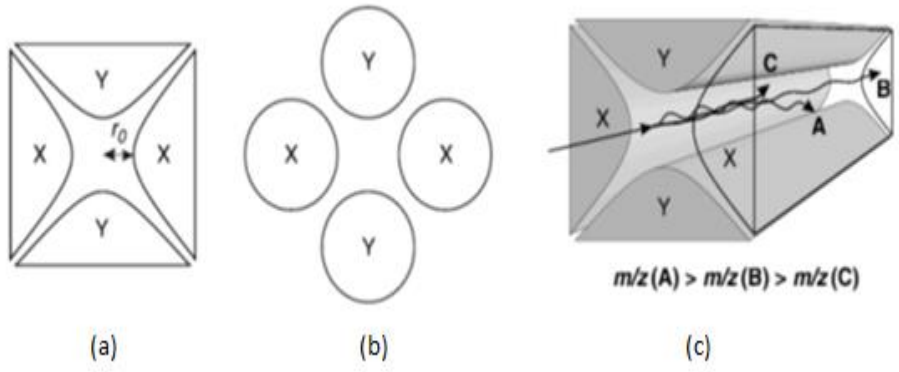

Figure 3.16. . Scheme of a quadrupole mass analyzer;

The fig. illustrates (a) hyperbolic cross-section. The two x-poles have RF current channeling through them, while the two y-poles have DC current channeling through them. (b) Cross-section of cylindrical rods. (c) The principle of a quadrupole mass analyzer. The x-poles and the y-poles act as a high and low pass filter respectively, meaning that molecule A and C are not permitted through the quadrupole since they are not within the allowed m/z range (Rolf Ekman, Dominic M. Desiderio et al. 2002).

3.4.2.3 Detector

The detectors in MS convert the energy of incoming particles into electrical signals. The energy is registered by electronic devices and transferred to a computer that translates these electrical signals into mass spectrometric information about the analyte. The signal received by the detector is generally low, so the energy of the incoming particles is usually amplified by the structural configuration of the detector. When ions from the mass analyzer strike the detector, the energy of the impact causes a secondary emission of electrons or photons depending on the nature of the detector (Rolf Ekman, Dominic M. Desiderio et al. 2002) p49-50. Several types of detectors are available for mass spectrometers. The choice of a particular detector is

made by considering the design of the instrument in connection with analytical applications (Edmond de Hoffman 2007).

Chapter 4
Experimental

This chapter details the experimental work completed to accomplish the goals of this study. The experiments are divided into three sections. The first section is dedicated to the characterization of carbon nanotubes. The second section deals with the experimental to study the equilibrium times for different components of the system while the third part deals with the experiments performed to study the adsorption behavior of the different CNTs.

4.1 Test materials

4.1.1 Carbon nanotubes (CNTs)

The CNTs used in the study include one type of pristine single walled CNTs (SWCNTs), three pristine multi-walled CNTs with different physical properties and three multi-walled CNTs with –COOH, -OH, -NH_2 surface functionalities. The non-functionalized or pristine MWCNTs were specified as MWCNTs-1, MWCNTs-2 and MWCNTs-3 in this study. While the functionalized MWCNTs were specified as MWCNTs–OH, MWCNTs-COOH and MWCNTs–NH_2. According to the manufacturer's specifications MWCNTs-2 are non-functionalized analogue of the functionalized ones in this study. The CNTs were used as received from the supplier as the main focus is the adsorption behavior of commercially available CNTs which will enter the natural

environment without any further modification (Zhang, Shao et al. 2009).

All CNTs used in this study were purchased from Timesnano (Chengdu Organic Chemicals Co. Ltd., Chinese Academy of Sciences) China. The manufacturer specifications are given in the 4.1.

Table 4.1. CNTs specifications as given by the manufacturer

	Purity (wt. %)	SSA (BET) m2/g	OD (nm)	Length (μm)	Functionalization wt %
SWCNTs	>95	>380	<2	5-30	0.0
MWCNTs-1	>95	>500	<8	10-30	0.0
MWCNTs-2	>95	>233	8-15	50	0.0
MWCNTs-3	>95	>110	20-30	10-30	0.0
MWCNTs-COOH	>95	>233	8-15	50	2.56
MWCNTs-OH	>95	>233	8-15	50	5.58
MWCNTs-NH2	>95	>233	8-15	50	0.45

4.1.2 Suwannee river natural organic matter (SR-NOM)

Since back ground solution chemistry can affect the interaction of CNTs and Polycyclic aromatic hydrocarbon (Zhang, Shao et al. 2010) we chose SR-NOM solution in moderately hard reconstituted water (MHRW) was selected as the back ground solution in experiments. The MHRW-SR-NOM solution will be referred to as NOM solution here-after. This whole solution represents natural surface water environments. Hence the study will be helpful to understand the adsorption potential and behavior of CNTs in natural fresh water systems.

Suwannee river natural organic matter (SR-NOM) was purchased from IHSS, USA.

4.1.3 Polycyclic aromatic hydrocarbons (PAHs):

Phenanthrene (phe) and pyrene (pyr) were selected for use in the study. Research grade phenanthrene (99.5%) and pyrene (99%) and were purchased from Sigma Aldrich.

4.2 Chemicals, reagents and other materials

Disposable solid phase micro extraction (SPME) fibers were purchased from Poly Micro Industries (Phoenix, AZ, USA).These SPME fibers had a total diameter of 170 which comprised of a silica core of 110 µm diameter and 30 µm thick PDMS coating making a volume of 0.132 µL PDMS.

GC grade n-Hexane and dichloromethane (DCM) were purchased from Sigma Aldrich. Reagent grade KCl, $NaHCO_3$, $MgSO_4.7H_2O$ and $CaSO_4.2H_2O$ were also purchased from Sigma Aldrich.

4.3 Characterization of CNTs:

This section deals with the instrument details, operating conditions and the sample preparations for the characterization of carbon nanotubes.

4.3.1 Transmission electron microscopy (TEM) analysis

The purity, diameter and number of walls of CNTs were revealed by Jeol2010F TEM (Jeol Ltd. Tokyo, Japan) operated at 200 kV in low and high resolution moods. Prior to analysis the CNTs were dispersed in ethanol with sonication. The samples for TEM study were prepared by taking a droplet of the dispersion and placing it onto Leci™ carbon coated grid and dried in air.

4.3.2 EDX analysis

Qualitative metal analysis was achieved by using high angle annular dark field scanning TEM and EDX. The samples on the Leci™ grid were first mapped by Z-contrast achieved by high angle annular dark field scanning TEM and then qualitatively analyzed by an EDX spectroscope (Oxford Instruments, Oxfordshire, UK) in analytical mode. The Jeol2010 TEM was equipped with both detectors.

4.3.3 Surface area and total pore volume (V_T) determination

BET and total pore volume analysis was performed at SINTEF facility in Oslo using Belsorp Mini II instrument (BEL Japan Inc.) Samples were outgassed under vacuum at 80 ˚C for 18 hrs and at 100 ˚C for 1hr. Nitrogen gas was used as the adsorbate at 77K.

4.3.4 Zeta potential and Particle size measurement

Zeta potential and hydrodynamic diameters of CNTs were determined using a Malvern Zetasizer Nano-ZS ZEN3600 (Malvern Instruments, Worcestershire, UK) in another SINTEF facility by SINTEF staff. The instrument was fitted with a 633 nm laser source capable of 0.6 nm to 6 µm measurement range for particle size. Clear disposable polystyrene cuvettes were used for zeta potential measurement while reusable green disposable capillary cells were used for aggregate size distribution.

Sample preparation was done by taking the exact weight some value around 1 mg of each CNTs in a 250 mL glass bottles. A 25 mL aliquot of NOM solution was added and the sample was sonicated for 6-7 min using an ultra-sonication bath. That was repeated three more times but at the last addition of NOM solution, the volume was adjusted to achieve a CNT concentration of exactly 10 mg/L. The samples were then left to settle for 24 hr before the supernatant was taken out and used for the measurements.

One set of samples in Milli-Q water was also prepared but with no addition of NOM, following exactly the same procedure.

4.4 Preparation of Standards and Solutions

4.4.1 Stock solutions:

1mg/mL stock solutions of phenanthrene and pyrene were prepared in *n*-hexane for GC-MS standards and in methanol for use as working sample solutions and phenanthrene free-concentration (phe_{free}) standards. Phenanthrene and pyrene were separately weighed to a value close to 4mg and the exact weight was noted, then a volume of *n*-Hexane or methanol was added to each vial to make a final concentration of 1mg/mL. The vials were left overnight wrapped in aluminum foil at room temperature to make sure that phenanthrene and pyrene were completely dissolved.

4.4.2 Working sample solutions

Working sample solutions of 100 µg/L phe and pyr for studying adsorption behavior of CNTs were prepared by spiking 100 µL of 1mg/mL phenanthrene or pyrene stock solution in methanol to the sample solutions under study.

4.4.3 GC-MS analysis calibration standards

GC-MS calibration standards 0.001, 0.01, 0.05, 0.1, 0.5, 1.0, 2.5, and 5.0 µg/mL were prepared by appropriate dilutions of 1mg/mL stock solutions in *n*-hexane.

4.4.4 Moderately hard reconstituted water (MHRW)

MHRW was prepared by according to modified APHA method (U.S. Environmental Protection Agency 1993). Instead of a plastic carboy, a glass bottle was used. No additional aeration of the solution was done during the preparation. In 9 L of Milli-Q water 1.2274 g of $MgSO_4.7H_2O$, 0.96 g of $NaHCO_3$ and 0.04 g KCl were dissolved. The bottle was kept open and agitated overnight. A 0.7586 g of $CaSO_4.2H_2O$ was dissolved in 0.5 L Milli-Q water in separate flask and then added to the bottle with 9 L water. The combined solution was agitated for 24 hr while the bottle was kept open.

4.4.5 NOM Solution

Suwannee river water natural organic matter (SR-NOM) was added to the MHRW prepared as in 4.5.4 to give a concentration of 20 mg/L. After stirring for 24 hr with magnetic stirrer, the solution was filtered using 0.2 µm cellulose membrane filter. The pH of the resulting SR-NOM solution was 7.63±0.02. The resulting NOM concentration was not quantified, but the same MHRW-SR-NOM solution was used for each type of CNTs. The MHRW-SR-NOM here-after will be referred to as NOM solution.

4.5 Negligible depletion solid phase micro-extraction (nd-SMPE) Procedure

The nd-SPME used to extract dissolved PAH analytes from aqueous samples in all experiments is modified from that reported by Hu et al.,(Hu, Liu et al. 2008). The PDMS coated SPME fiber was cut into 1 cm pieces and all the pieces thoroughly rinsed three times with acetone and then with freshly prepared Milli-Q water. A 250 mL volume of each sample to be extracted for PAH analytes was placed in 500 mL bottles. A single PDMS fiber was inserted into each bottle and the bottle capped with a Teflon seal. All the bottles were placed in incubator shaker at 25±2 ˚C and 125 rpm in the dark. After specified time points (described in each experiment), each sample was withdrawn from the shaker and drained. The fiber was taken out of the bottle using tweezers, cleaned with a moist tissue and transferred to a 1 mL GC vial for desorption. The desorption of PAHs partitioned to the PDMS coating was achieved using 1 mL *n*-hexane and leaving for 24 hr. The *n*-hexane extracts were analyzed on GC-MS.

The choice of the parameters and SPME and conditions in this study was subjected to available facilities.

4.6 GC-MS Analysis

GC-MS analysis was conducted using an Agilent 6890 N GC system fitted with an auto chromatograph was fitted with a 60 m x 0.25 mm silica capillary column with a 0.25 µm film thickness of 5% diphenyl/95% dimethylpolysiloxane. A pulsed split less inlet at an initial temperature of 320 ˚C was used to inject 1 µL sample volume. Helium (grade 6.0) was used as the carrier gas at a flow rate of 1.1 mL/min. The initial column temperature was 40^{O}C with an initial hold for 1 min followed by a ramp rate of 12^{O}C/min to the final temperature of 325 ˚C with a final hold for 20 minutes. The MSD was operated in Electron ionization (EI) mode at 70 eV and an ion source temperature of 310 ˚C. Suitable GC-MS standards were also analyzed with the samples as external calibration standards for GC-MS analysis. The quantitation and confirmation ions were respectively 178 and 176 were for phe, and 202 and 101 for (chromatogram in appendix……)

4.7 Phenanthrene free concentration (phe_{free}) Calibration procedure

The phe_{free} calibration curve to enable calculation of dissolved phenanthrene concentration in the test samples was obtained by an external calibration method. Aqueous phenanthrene standards 1, 2, 5, 10, 25, 50, 75, 100, and 150 µg/L were prepared by spiking the phenanthrene stock solution (in methanol) to MHRW. These standards were extracted by negligible depletion solid phase micro extraction (nd-SPME) and analyzed by GC-MS as described in 4.5 and 4.6

respectively and were treated with the samples in the same way. This also covered the losses due to evaporation and adsorption to glassware. The phe_{free} calibration curve was obtained by plotting GC-MS responses against concentrations of aqueous phe standards (Ouyang and Pawliszyn 2008).

4.8 Investigation of partition equilibrium time between aqueous PAHs and PDMS Coated SPME fiber

4.8.1 Aim:

The aim of the experiment was to determine the extraction equilibrium time between PDMS coated fiber and two PAHs phenanthrene and pyrene.

4.8.2 Method

The SPME of 100 µg/L working solution of phenanthrene and pyrene was carried out for 1, 3, 24, 48 and 72 hr for phenanthrene and 1, 4, 5 and 6 days for pyrene. The SPME procedure was followed as described in 4.5. The fibers for each time point were extracted with *n*-hexane and analyzed by GC-MS as described in 4.5 and 4.6. The GC-MS responses were plotted against corresponding time points. The increased exposure of PDMS fiber to the analyte during SPME produced increasing GC-MS responses until the partitioning of phe or pyr to the PDMS fiber reached to the equilibrium state.

4.9 Study of adsorption equilibrium time between CNTs and aqueous PAHs

4.9.1 Aim:

The aim of this experiment was to determine the adsorption equilibrium time of PAHs to the CNTs suspended in MHRW.

4.9.2 Method:

The equilibrium time study was done using the SWCNTs. Two different concentrations of only SWCNTs carbon were attempted with slightly different methodology to estimate the equilibrium time for adsorption of PAHs to the CNTs. Both methods are describes below (a, b). Phe was used in one method, pyr in the other. This choice of pyr and phe for each method was random.

(a). A 10 L suspension of SWCNTs at a concentration of 50 mg/L SWCNTs was prepared by agitation using a magnetic stirring bar. After 24 hr of agitation, it was assumed that stable aggregate sizes are achieved in the suspensions and phenanthrene was spiked to achieve a concentration 100 µg/L. The bottle was wrapped in aluminum foil and the sample was kept agitated using magnetic stirring bar. After 2, 4, 26, 50, 72, 96, 120 and 148 hr 800 mL volume was subsampled into a separate bottle, while keeping the mixture well stirred in the 10 L bottle to ensure the CNTs remained dispersed homogeneously. The subsample bottle was capped, wrapped in aluminum foil and allowed

the CNTs to settle for 24 hr before the supernatant layer was decanted into a beaker. Triplicate samples of 250 mL after each time point were prepared from the decanted supernatant in 500 mL bottles. Each set of triplicates was extracted for 24 hr by SPME as described in 4.5. The n-hexane extract vials from each time point were stored in the refrigerator at 4 ˚C until collection of n-hexane extract from last time point. All n-hexane extracts were kept in the dark normalized for temperature before they were analyzed by GC-MS described in 4.6.

A decrease in GC-MS responses is linked with decrease in phe_{free} because of the adsorption of phe to CNTs until the equilibrium is achieved between aqueous phe and CNTs in the suspensions.

(b). A 10 L suspension of SWCNTs at a concentration of 0.5 mg/L was prepared as described above. After 24 hr stirring, the mixture was spiked with pyrene, to achieve a concentration 100 µg/L. The whole mixture was stirred for two hr to ensure homogeneous mixing of pyrene. The mixture was then split into 250 mL volumes in 500 mL bottles. Triplicates of these subsamples were kept allowing the adsorption of pyrene to the CNTs for 1, 2, 3, 4, 5 and 6 days. All bottles were placed in shaker at 25 C and 125 rpm for the each time point. Each set of triplicates after specified adsorption time was extracted for 24 hr by SPME as described in 4.5. No prior settling of CNTs was allowed. The n-hexane extracts from each time point were kept in the refrigerator until collection of *n*-hexane extract from last time point. All *n*-hexane extracts were kept in the dark normalized for temperature and analyzed by GC-MS described in 4.6.

4.10 Study of adsorption of phenanthrene to Carbon nanotubes

4.10.1 Aim:

In this experiment the adsorption of aqueous phenanthrene to seven different carbon nanotubes dispersed in MHRW with and without the presence of NOM was studied. The aim of the study was to explore the effects of diameter, number of walls, length and surface functionalization of the CNTs. It was hypothesized that the interaction of the CNTs with NOM can change their adsorption pattern.

4.10.2 Method

4.10.2.1 In MHRW:

All CNTs were carefully and accurately weighed to approximately 0.5 mg using weighing boats made of glass. The exact weight was noted. Weighing glass boats were used because it makes possible to transfer and rinse all CNTs from glass material. All CNTS were transferred to separate 1 L amber glass bottles and weighing containers were rinsed with MHRW. The volume of MHRW was adjusted to achieve a concentration of 0.5 mg/L CNTs of each type of CNTs in each bottle. Individual solutions were prepared for each CNTs type.

The CNTs in each bottle were stirred using magnetic stirring bars for period of one week for equilibration between NOM and the CNTs. All bottles were spiked with phenanthrene stock solution (in methanol) to achieve 100 µg/L phenanthrene in each bottle. The matrix was stirred

and equilibrated for another week. Changes in the system due to bio-decomposition of NOM were not considered.

Triplicate samples of 250 mL in 500 mL bottles from each 1 L bottle were made for each CNTs type. Phenanthrene was extracted from all triplicate samples using 5 day SPME. as described in 4.5. PDMS fibers were removed for extraction in n-hexane. Any CNTs adsorbed to the fiber were wiped using wet tissue. The n-hexane extracts were analyzed by GC-MS as described in 4.5. The remaining dissolved phenanthrene concentration was calculated from phe_{free} calibration curve constructed as described in 4.7. Controls with MHRW and NOM solution containing 100 µg/L phenanthrene were also run simultaneously. These were set as reference points for comparison of adsorption to each CNTs type representing matrix.

4.10.2.2 In NOM Solution

The experiment was repeated but this time with CNTs in MHRW only without any NOM. As a result the one week equilibration step between CNTs and NOM was not required. The remaining steps were performed exactly the same way as in 4.10.2 (a).

Chapter 5

Results

5.1 Characterization of Carbon nanotubes

5.1.1 TEM and EDX

TEM images confirmed that the SWCNTs, in most cases, were defect-free Figure 5.1 (a). It was impossible to follow one given tube along all its length to say that it is entirely defect-free, but the amount of defects is assumed to be quite low. However, the SWCNT batch does not contain only SWCNTs, lots of double-walled, and to a lesser extent three-walled and four-walled CNTs were also observed. It could not be determined that what fraction of each is present in the sample. This is because most of the tubes were bundled together onto long filaments (like wires in an electrical cable) and finding individual tubes was a challenge. Figure 5.1, Figure 5.2 show TEM images of perfect SWCNT, a three-walled CNT and entangled SWCNTs in the SWCNTs sample.

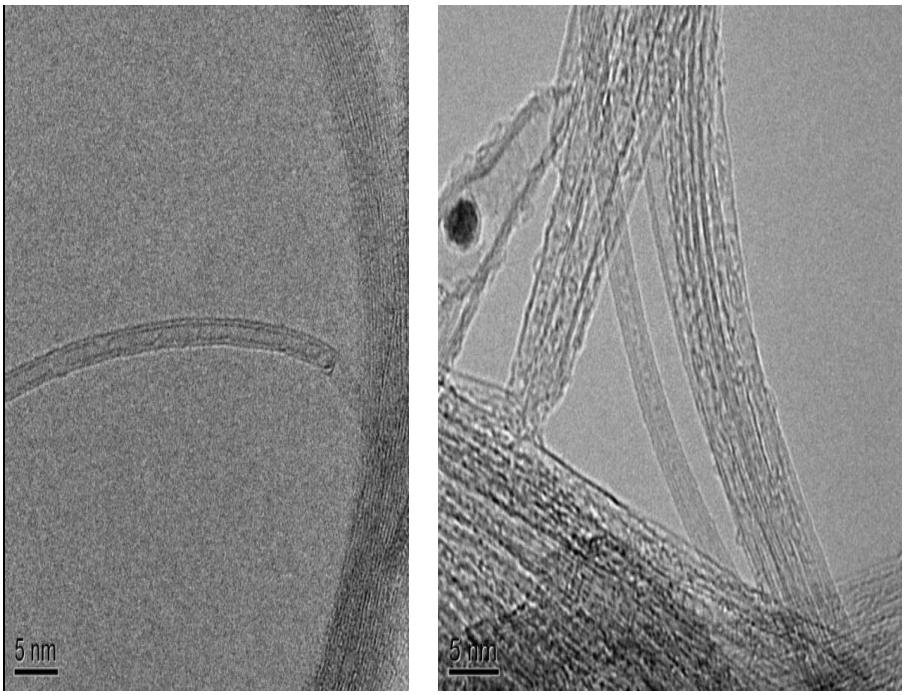

(a) (b)

Figure 5.1. TEM image of (a). Defect free SWCNT (b). Encapsulated metal impurities in a SWCNT

The TEM images of the MWCNTs-1 sample revealed the presence of impurities in the form of disordered graphitic material and large conglomerates of failed CNTs from the fabrication process (a TEM image taken is shown in Figure 5.3. a). SWCNTs were also observed. The majority of the CNTs observed, looked damaged, with broken or fractured walls and open ends (one representing TEM image in Figure 5.3. b).

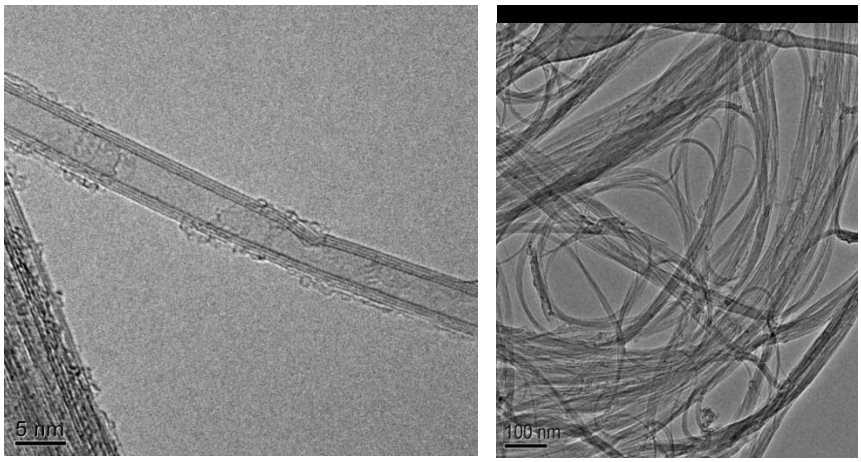

(a) (b)

Figure 5.2. TEM image of (a) Three-walled CNT in SWCNTs sample (b) Entangled SWCNTs.

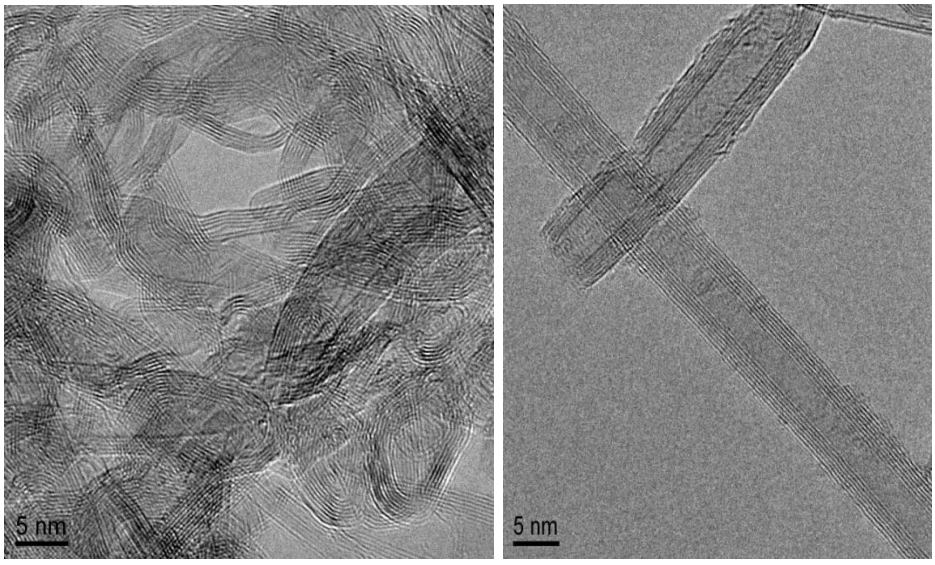

(a) (b)

Figure 5.3. TEM image of (a). Failed fabrication of CNTs in MWCNTs-1 (b). CNT with open end in MWCNTs-1.

MWCNTs-3, MWCNTs-COOH, MWCNTs-OH and MWCNTs-NH_2 samples did not dispersed well in ethanol during sample preparation. As a result, TEM images of theses CNTs showed big clumps of badly entangled CNTs. The MWCNTs-OH observed, in most cases, were not really concentric cylinders, but stacked cones. Most of the walls had defects (Figure 5.4. a). High magnification images of MWCNTs-COOH exhibited wall defects in the outer region in some areas (Figure 5.4. b) while the inner walls were intact. More TEM images for each CNTs type can be found in the Appendix B.

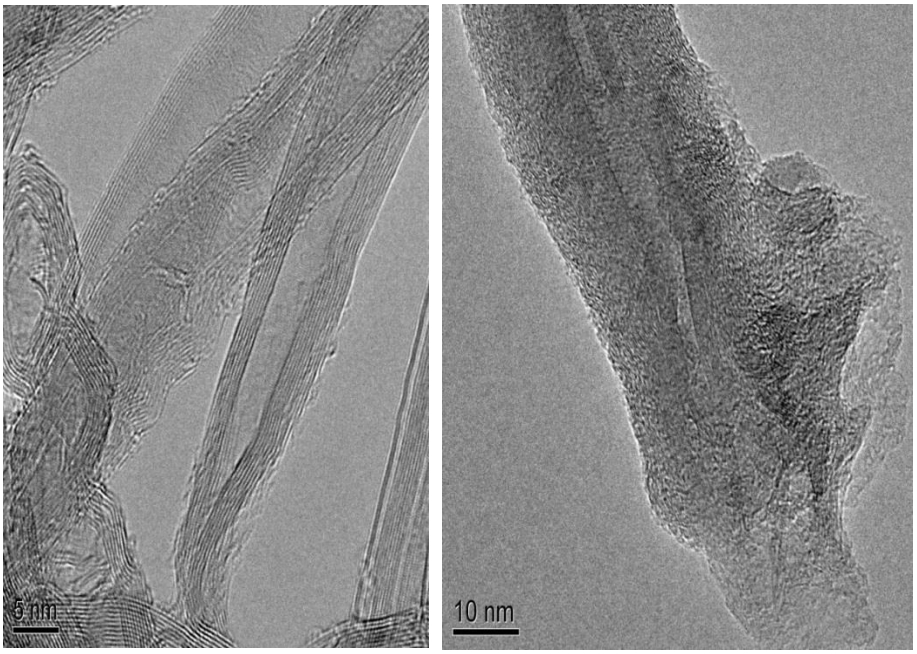

(a) (b)

Figure 5.4. TEM image of (a). Low quality MWCNT-OH exhibiting concentric cones. (b). CNT with wall defects in MWCNTs-COOH sample

The EDX studies revealed the presence of metal particles in the SWCNTs sample. The particles up to a size of 10 nm and mainly

consisted of Co or Mo whilst those up to the particles up to a size of 0.5 microns consisted mainly of Cr and Fe. Traces of Ni, Al, Mg and Si were also found. The small particles were encapsulated by the tubes while the large particles were attached to clumps of CNT material (one representing TEM image shown in Figure 5.5).

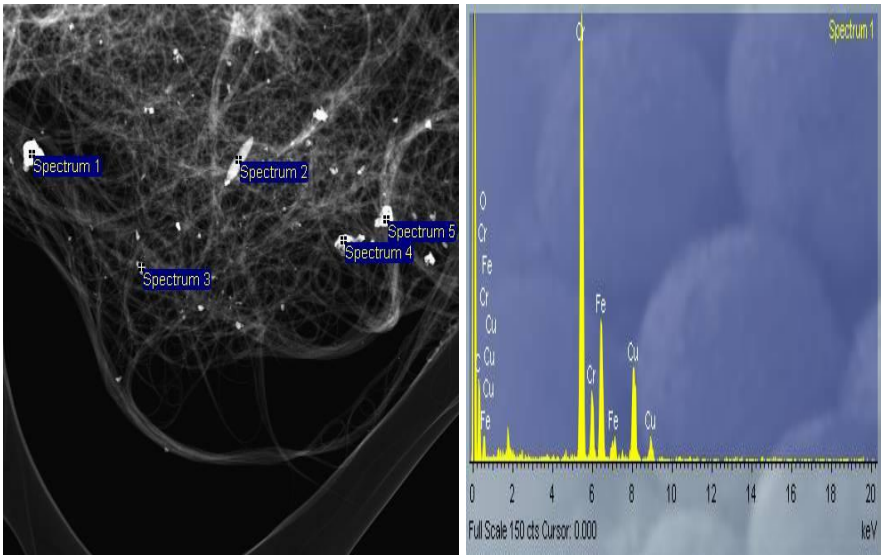

(a) (b)

Figure 5.5. (a). High angle high annular dark filed image of SWCNTs (b). EDX spectrum of metallic impurities in SWCNTs

The EDX study of MWCNTs-1 showed metallic particles, up to 10 nm which consisting mainly of Co, with traces of Mo. Most of the metal was encapsulated in the graphitic material.

The MWCNTs-3 sample contained Ni particles, with sizes ranging from 2 to 20 nm. The MWCNTs-2 and MWCNTs-OH, MWCNT-NH2 and MWCNT-COOH contained both Ni and Fe particles ranging in size from

1 nm to 10 nm. Compared with other CNT types, more particles in the MWCNTs-OH were observed encapsulated in the graphitic material.

The diameters of CNTs were measured from high resolution TEM images. The observed diameters were spread over a range in each CNTs type sample. The average diameter per CNT in each CNTs type is represented graphically in Figure 5.6. The observed statistics can be found in Appendix B.

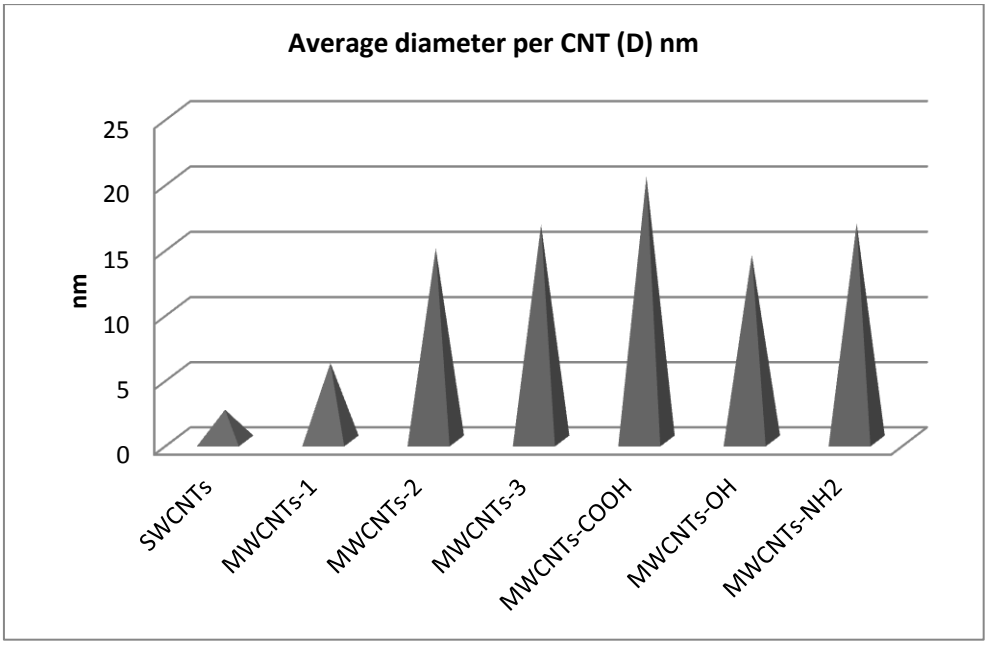

Figure 5.6. Results of average diameter per CNT in each CNTs type sample as measured from HRTEM images

5.1.2 Surface area (BET):

The measured specific surface area (SSA) for given CNT types ranged from 467 to 137 m^2/g. The highest value was 467 for SWCNTs. The MWCNTs-1 type had SSA value 428 m^2/g which was close to SWCNTs.

The MWCNTs-3 and MWCNTs-OH types had SSA values 175 and 161 respectively close to each other. The SSA values for MWCNTs-2, MWCNTs-NH2 and MWCNTs-COOH were 140, 142 and 137 respectively. A graphical representation of the specific surface areas determined is given in the Figure 5.7. Adsorption desorption isotherms and experimental data for BET measurements is given in the Appendix.

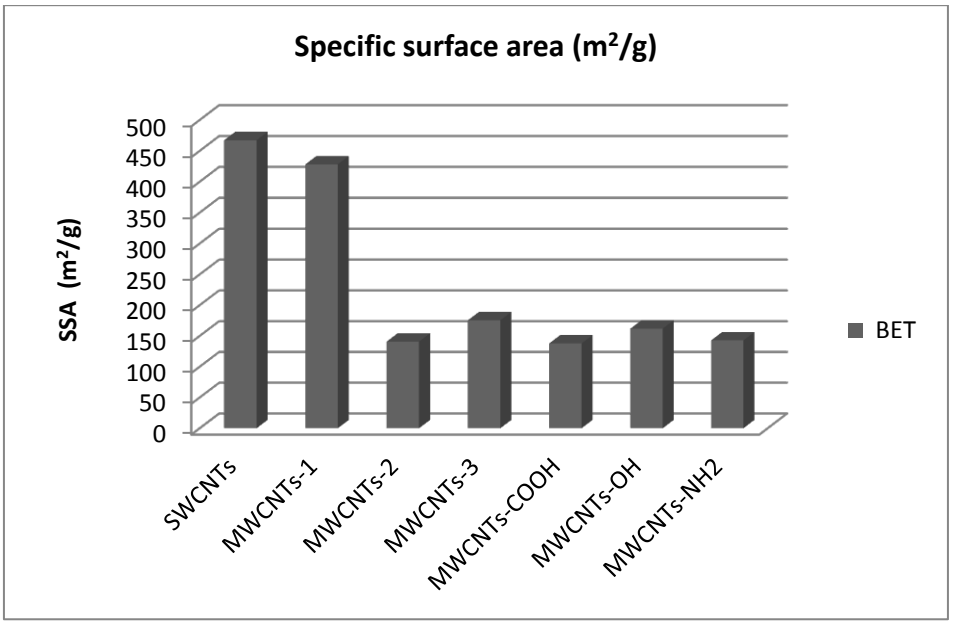

Figure 5.7. Results of BET measurements for SSA

5.1.3 Total pore volume (V_T):

The total pore volume measured ranged from highest 1.53 cm^3/g for SWCNTs to the lowest 0.71 cm^3/g for MWCNTs-1. The MWCNTs-NH2 had V_T value 1.50 cm^3/g which is very close to the SWCNTs. Similarly the MWCNTs-3 and MWCNTs-COOH had very close V_T values which were 1.31, 1.33 cm^3/g. The MWCNTs-OH and MWCNTs-2 had V_T 1.24

and 1.28 cm^3/g respectively in close proximity to each other. Figure 5.8 represents these results.

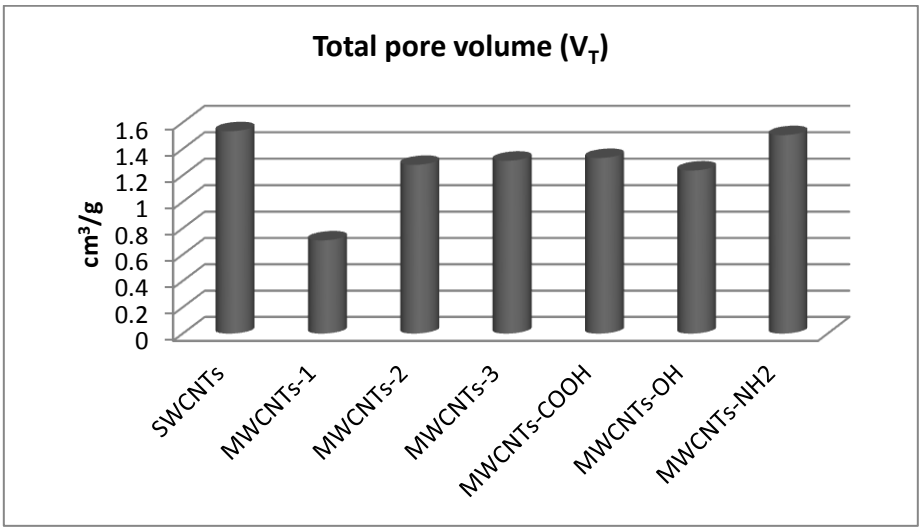

Figure 5.8. Results of total pore volume of CNTs

5.1.4 Zeta potential (ZP) and Particle size:

The CNTs suspensions in NOM solutions were less negatively charged than in Milli-Q water except SWCNTs. The CNTs suspensions in NOM are more negatively charged than NOM alone.

ZP values of CNTs in NOM ranged from -11.2 (±2.1) mV for MWCNTs-1 to -18.9 (±0.4) mV for MWCNTs-COOH. The MWCNTs-OH, and SWCNTs had ZP values -18.5 (±0.5) and -18.3 (±0.4) mV respectively. The MWCNTs-3 and MWCNTs-NH_2 had -15.7 (±1.5) and 15.7 (±1.4) mV respectively. The MWCNTs-2 had a value of -17.6 (±1.4) mV (Figure 5.9).

ZP values in pure Milli-Q water ranged from -15.6 (±12.8) for SWCNTs to -33.2 (± 0.9) in MWCNTs-2 type. Figure 5.9 represents these results.

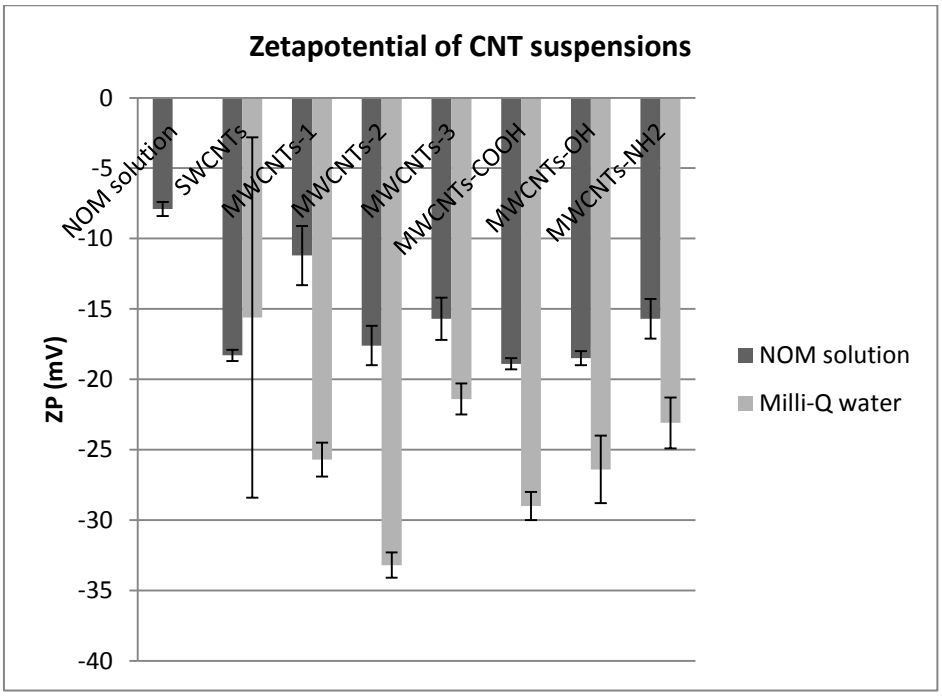

Figure 5.9. Results of zeta potential measurements of CNTs in pure Milli-Q water and NOM solution

The error bars show standard deviation. N= 2, 4, 3, 3, 2, 4, 4, 2 respectively for NOM solutions and 4, 3, 3, 3, 3, 2, 2, 4 respectively for Milli-Q water.

Largest average particle size measured was 2536 nm, for SWCNTs. The MWCNTs-1 and MWCNTs-2 had comparable particle sizes, 2190 and 2170 nm respectively. The MWCNTs-3 and MWCNTs-NH2, MWCNTs-OH had the values 410, 503 and 360 nm respectively. The smallest particle size measured was 286 nm for MWCNTs-COOH. The standard deviations for these measurements ranged from 462 to 14, the highest in the case of MWCNTs-1 and the lowest for MWCNTs-COOH. Figure 5.10 represents these results.

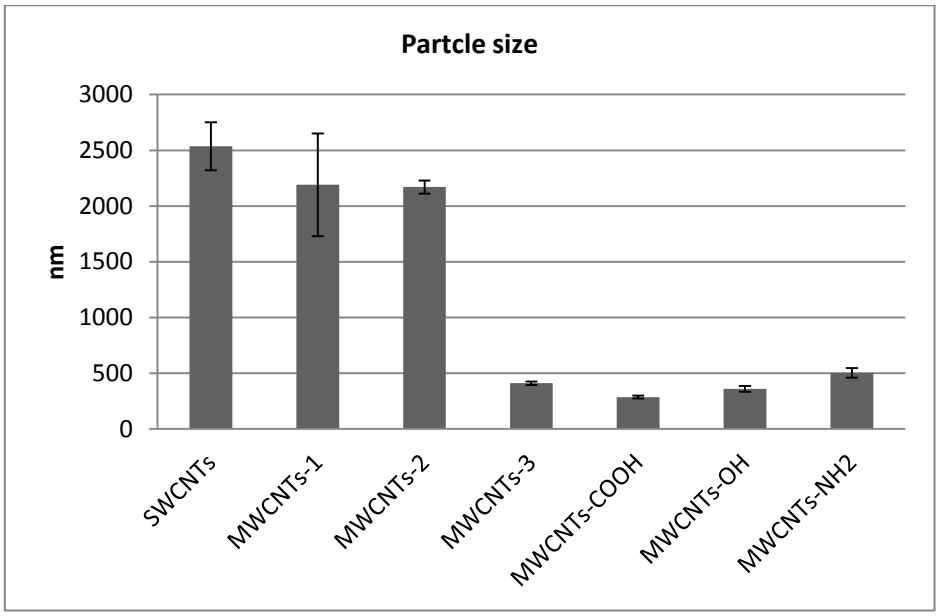

Figure 5.10. Results of particles size measurements of CNTs in NOM solution (sonicated).

The error bars show standard deviations. N= 2, 2, 3, 2, 3, 3, 2 respectively.

5.1.5 Summary:

Error! Reference source not found. summary of CNTs characterization results

	SSA (BET) m^2/g	OD (nm)	V_T (cm^3/g)	ZP(mV) in NOM	ZP(mV) milli-Q water	Particle size (nm) NOM stabilized
SWCNTs	467	2.4	1.53	-18.3	-15.6	1268
MWCNTs-1	428	6	0.71	-11.2	-25.7	1095
MWCNTs-2	140	14.8	1.28	-17.6	-33.2	1085
MWCNTs-3	175	16.6	1.31	-15.7	-21.4	205
MWCNTs-COOH	137	20.3	1.33	-18.9	-29	143
MWCNTs-OH	161	14.3	1.24	-18.5	-26.4	180
MWCNTs-NH2	142	16.7	1.50	-15.7	-23.1	251

SSA=specific surface area, ZP=Zeta potential, OD=outer diameter, V_T= Total pore volume.

5.2 Study of partition equilibrium times for aqueous PAHs to PDMS coated SPME fibers.

For both phenanthrene and pyrene, the amount of target analyte extracted by the PDMS coated SPME fiber increased from time zero until the equilibrium was achieved. In the Figure 5.11 the SPME time is plotted against GC-MS responses for phenanthrene. The plot shows rapid increase rate in GC-MS responses in the beginning but that, over an increased extraction time, is decreased and approached equilibrium

after approximately 72 hr. The extraction profile for phenanthrene suggests an equilibrium time shortly after 72 hr.

The extraction profile for pyrene is shown in the Figure 5.12 and the plot in the figure suggests an equilibrium time for pyrene SPME sometime shortly after 6 days under experimental conditions.

The quality of data was assured by running replicates of the samples (n=2 or 3). The GC-MS analysis calibration curves for both phenanthrene and pyrene over the range of 0.001-5.0 µg/mL are given in the Appendix A.

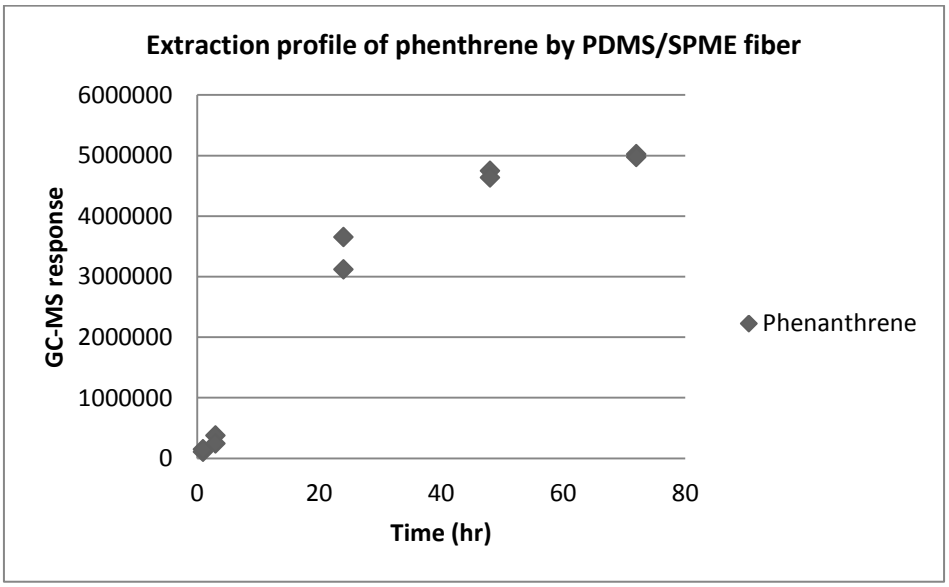

Figure 5.11. Extraction profile of phenanthrene by PDMS/SPME fiber at 125 rpm and 25 ˚C

The data shown in the chart corresponds to 1, 3, 24, 48 and 72 hr. N=2

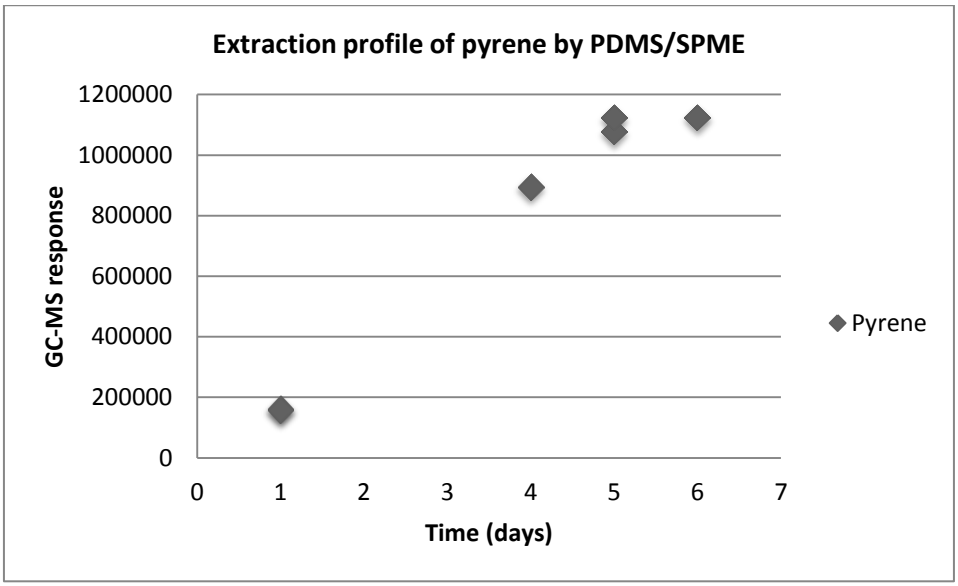

Figure 5.12. Extraction profile of pyrene by PDMS/SPME fiber at 125 rpm and 25 ˚C

The data shown in the chart corresponds to 1, 4, 5 and 6 days. N=2, 1, 2, 1 respectively.

5.3 Study of adsorption equilibrium time between CNTs and aqueous PAHs

To estimate the equilibrium time for adsorption of PAHs to the CNTs, two different concentrations of SWCNTs were used with slightly different methodologies (a and b):

(a). Phenanthrene detected at any of the exposure times was below the limit of quantification (0.001 µg/mL for the method described in 4.6 for PAHs). The obtained data and the GC-MS analysis calibration curve from this experiment can be found in the Appendix A.

The Figure 5.13 shows the GC-MS responses plotted against exposure time of 100 µg/L pyr to 0.5 mg/L SWCNTs. The GC-MS responses measured for pyrene in the n-hexane extract showed a random distribution. Samples collected after 1, 2 and 3 days adsorption exhibited very low amounts of adsorbed pyrene (GC-MS responses 63111, 56652, 50962 respectively). In contrast, samples collected after 4, 5 and 6 exhibited relatively much higher amounts of pyrene (GC-MS responses 1207180, 1092555 and 895372 respectively). The obtained data and the GC-MS analysis calibration curve from this experiment can be found in the Appendix A.

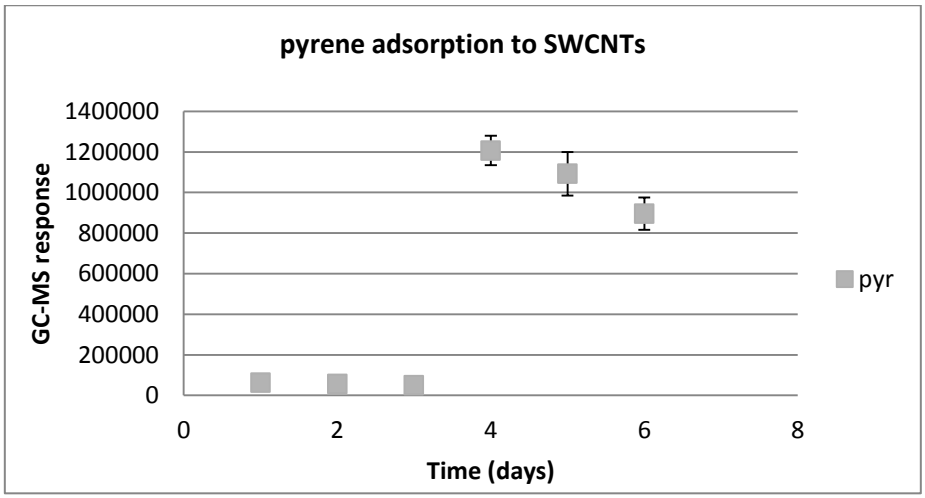

Figure 5.13. Adsorption profile of pyrene to SWCNTs

N=1, 2, 2, 2, 2, 2 respectively while error bars show standard deviations for GC-MS responses

5.4 Adsorption of phenanthrene to different CNT types

5.4.1 In MHRW:

The SWCNTs showed the highest adsorption of phenanthrene while MWCNTs-OH showed the least adsorption tendency. The observed adsorption potential of the CNTs for phenanthrene had the order; SWCNTs>MWCNTs-1>MWCNTs-2>MWCNTs-NH2>MWCNTs-COOH>MWCNTs-OH. The phenanthrene free (phe_{free}) concentration determined in SWCNTs sample at the end of experiment was found to be 33 µg/L while for MWCNTs-OH it was 88 µg/L. The phe_{free} concentration values determined for MWCNTs-1, MWCNTs-2, MWCNTs-NH2 and MWCNTs-COOH were 52, 67, 71 and 77 µg/L respectively. The measured value of phe_{free} for the control (100 µg/L in MHRW) was found to be 105 with a standard deviation of 5.63. Standard deviations of phe_{free} concentration determinations for all the CNT type samples varied from 0.18 to 4.62. Figure 5.14 shows the average phe_{free} concentrations for each CNT after 5 days adsorption, extracted by 5 days SPME and analyzed by GC-MS. The decrease in phe_{free} concentration in each CNT sample represents a measure of phenanthrene adsorption to the CNTs. The phe_{free} calibration curve, GC-MS analysis calibration curve, and summarized data for this experiment can be found in the Appendix A.

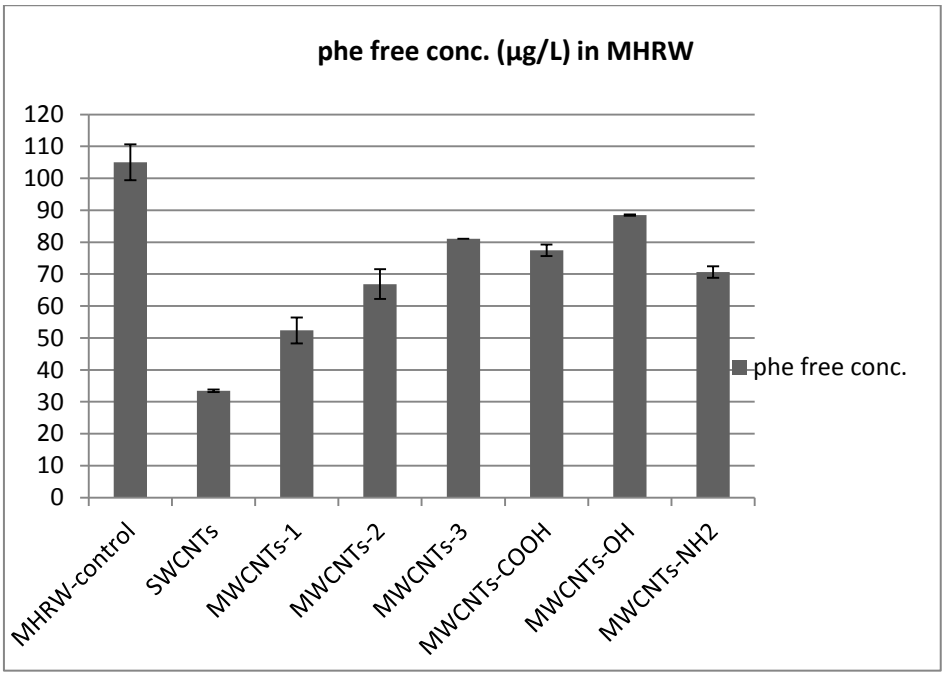

Figure 5.14. Phenanthrene free concentrations determined after adsorption to different CNTs in MHRW.

N= 3, 2, 3, 3, 3, 3, 2,3 respectively. The error bars represent standard deviation.

5.4.2 In NOM solution

Figure 5.15 shows average phe_{free} concentration for each CNT type after 5 days adsorption to CNTs in NOM solution. In this case phe_{free} concentrations determined ranged from 66.86 to 97.52 µg/ L, with the highest value being for SWCNTs and lowest for MWCNTs-COOH. In NOM solution, the SWCNTs in NOM solution also showed much higher adsorption as compared with other CNTs. The phe_{free} concentration for MHRW (no NOM and CNTs) and NOM controls (no CNTs) were determined to be 100.13 and 91.82 µg/L respectively. All functionalized CNTs showed higher phe_{free} measurements than the NOM control which were 94.01, 94.51 and 97.52 µg/L for MWCNTs-NH2, MWCNTs-

OH and MWCNTs-COOH respectively. Standard deviations for these measurements ranged from 1.32 to 12. 82. The highest standard deviation value observed was for the control in MHRW. The replicate measurements for NOM control were not available due to loss of the SPME during handling. Figure 5.15 represents these results.

The phe_{free} calibration curve, GC-MS analysis calibration curve, and summarized data for this experiment can be found in the Appendix A.

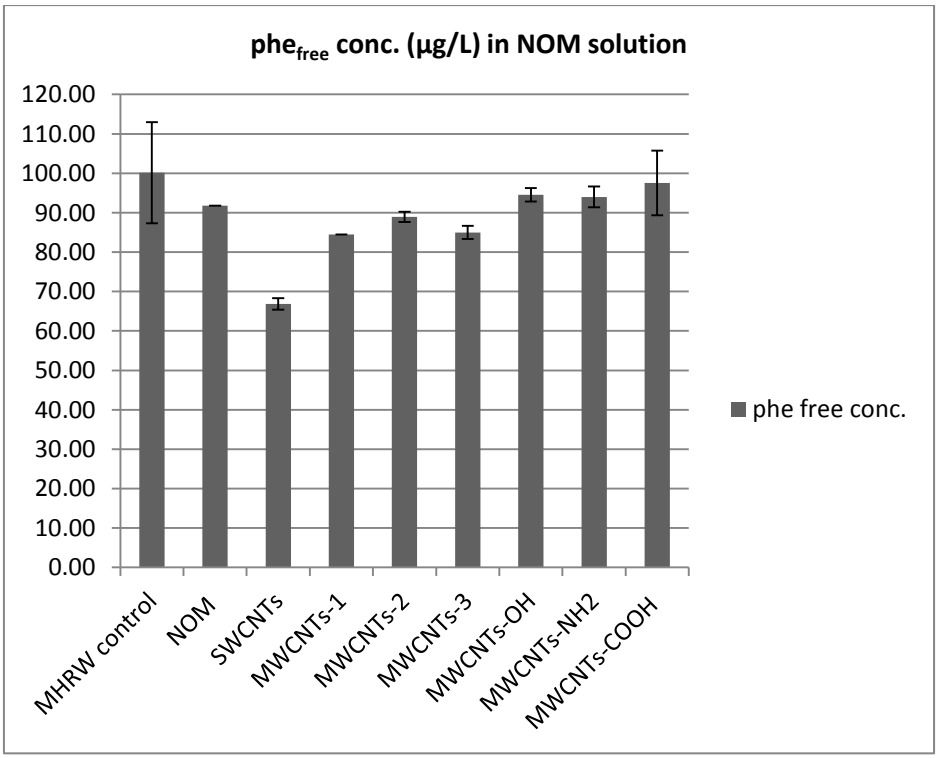

Figure 5.15. Phenanthrene free concentrations determined after adsorption to different CNTs in NOM solution.

N=2, 1, 3, 1, 3, 3, 3, 3, 3. The error bars represent standard deviations.

Chapter 6

Discussion

6.1 Characterization of CNTs:

The TEM image and EDX analysis raised a question on the quality of CNTs as claimed by the manufacturer. The presence of significant amount of impurities; MWCNTs in the SWCNTs specified sample, broken walls, open ends and graphitic material in MWCNTs-1, and failed CNTs, looking like concentric cones in MWCNTs-OH sample have already been described in the section 5.1.1. Percentage purity is still needed to be determined.

The diameters of CNTs also showed differences from those specified by the manufacturer. The differences might arise from the methods used. In the present study ODs of CNTs were measured from high resolution TEM images. The average values obtained in this method are dependent on the resolution of the TEM used and number of the tubes included in the measurement. OD of the CNTs in a sample is spread over a range. Information could not be obtained from the manufacturer what method exactly they have followed. OD determination using same methods can better give the differences from those specified by the manufacturer.

SWCNTs generally show higher surface areas per weight than MWCNTs. In MWCNTs as the number of walls increases, weight

increases but the exposed surface is the outer surface which is the only available surface for adsorption in perfect and closed CNTs. The CNTs which have open ends they can show higher surface areas because the inner surface of the tube can also be available for adsorption. Bundling of CNTs due to Van Der Waals forces results in lower surface areas (Peigney, Laurent et al. 2001). SSAs obtained by BET measurements differ from the ones given by the manufacturer. The manufacturer also determined SSA by BET method but the information about which instrument the manufacturer has used for their BET measurements, could not be available. However, the observed differences might not be explained by the instrumental variations alone. A more plausible explanation is that the manufacturer has specified BET measurements for individual CNTs rather than the aggregates. This is why the manufacturer's specified values are generally higher than the ones measured in this study. The SSA values measured in this study and given by the manufacturer are shown in Table 6.1. For MWCNTs-3 the measured BET value is higher than specified by the manufacturer. This might be explained by the defects in walls and broken CNTs in which case the internal surface of a CNT could have been available for the adsorption. The internal CNT diameter (1.2-3 nm) is larger than N_2 molecules (0.3nm) (Kennedy, Hull et al. 2008) so the inner sides of the walls can also be available for adsorption if the wall is broken or is with open ends.

Lower Zeta potential (ZP) values in NOM solution than in Milli-Q water for CNTs have also been reported by other researchers. Kennedy and colleagues have reported lower ZP values for MWCNTs-COOH and

MWCNTs-OH in NOM solution than in Milli-Q water (Kennedy, Hull et al. 2008).

Table 6.1. CNTs specific surface area and outer diameters measured in this study and as given by the manufacturer

	SSA (BET) m2/g		**OD (nm)**	
	Manufacture	measured	Manufacture	measured
SWCNTs	>380	467	<2	2.4
MWCNTs-1	>500	428	<8	6
MWCNTs-2	>233	140	8-15	14.8
MWCNTs-3	>110	175	20-30	16.6
MWCNTs-COOH	>233	137	8-15	20.3
MWCNTs-OH	>233	161	8-15	14.3
MWCNTs-NH2	>233	142	8-15	16.7

Average particle sizes for nearly all the CNTs were biased and greatly influenced by a very small number of very large particles. The representative values were much lower than the average particle size. The high variations between measurements might arise due to agglomeration of CNTs in suspensions. The independent measurements taken in this study were 2 or 3 which is very limited. International Standard on DLS ISO13321 recommends 12 independent measurements (International organization for standardization 1996). Sonication of the samples greatly affects the size of the suspensions of CNTs (Zhang, Kah et al. 2012). The CNTs were sonicated during sample preparation for DLS measurements. This is another reason that these values cannot be the representation of actual particle sizes of CNTs

suspensions in the adsorption experiments in this study where no sonication was performed. The CNTs were kept suspended simply by agitation. The measured particle sizes may just represent the aggregation tendency of the CNTs can just be a clue for particle size comparison of CNTs under the experimental conditions.

The presence of metals in CNT samples is because of their addition as catalysts in the CNTs synthesis process (Prasek, Drbohlavova et al. 2011). The transition metal impurities detected in CNT samples may not influence significantly the adsorption studies but they are very important for toxicity studies. Transition metals like, Fe, Ni, Co and Cr have been repeatedly reported toxic depending on their concentration to living cells (Nies 1999; Yadav 2010).

It is very important that the adsorption studies involving CNTs should always involve a through characterization of CNTs as the data from the manufacturer may not represent the actual characteristics of a particular batch. The adsorption results can then be correlated to actual characteristics of the CNTs. It can better help environmental impacts and risk assessment studies of the CNTs.

6.2 Phenanthrene and pyrene partition equilibrium times towards PDMS/SPME:

Hu and colleagues (Hu, Liu et al. 2008) reported that equilibrium is achieved between a PDMS coated fiber with same specifications and phenanthrene within 48 hr at 20 ˚C and 200 rpm. The prolonged

equilibrium times in the present study could be due to the low mass transfer rates resulting from use of lower shaking speed, 125 rpm in the present study. Extraction rate or equilibrium time in SPME is determined by the agitation conditions (Pawliszyn 1997).

The overall higher extraction efficiency of pyrene than of phenanthrene is because of the higher hydrophobicity of pyrene. Lower partitioning equilibrium time of phenanthrene is because of its lower molecular weight which resulted in higher diffusion rate and hence shorter partitioning equilibrium time to the PDMS coating (Philip Mayer P. 2000).

The quality of the data was assured by running replicates of the samples (n=2 or 3).

6.3 Adsorption equilibrium times of phenanthrene and pyrene to CNTs:

Shortly after the phenanthrene was spiked, nearly all phenanthrene was adsorbed to the CNTs and the remaining freely dissolved concentration partitioned to the PDMS/SPME fiber was below the limit of quantification. The detection of phenanthrene below the limit of quantification can be because of the relatively much higher concentration of CNTs in the samples.

This result suggested that the CNT concentration to be used should be relatively much lower than 50 mg/L CNTs used in this experiment. Due to time restrictions it was not possible to repeat the same experiment with phenanthrene at lower concentration of CNTs. However, based on

these results the experimental method to determine the equilibrium time for pyrene was modified. In this case 100 µg/ L pyrene was present with the CNTs at a concentration of 0.5 mg/L. The results from this study are difficult to explain (results shown as chart in Figure 5.13). There should have been a decrease in the free concentration detected as the adsorbed quantity increases when more time has passed. The randomness of the values might be because of blocking of PDMS/SPME fiber due to adsorption of the CNTs to the fiber. Some fibers got more adsorption of CNTs and some less which led different gain of pyrene due to different surface areas available for pyrene to enter PDMS coating. But the free concentrations of pyrene detected after 1, 2 and 3 days have much lower values than 4, 5 and 6 days (Figure 5.13). It should have been other way around. This experimental method also failed in giving the adsorption equilibrium times between pyrene and the CNTs in the aqueous system.

6.4 Adsorption of phenanthrene to different CNT types

The adsorption behavior and potential of CNTs towards polycyclic aromatic hydrocarbons in natural fresh water systems is better understood when the physical and chemical properties of carbon nanotubes and the chemistry of the water system are taken in consideration. A number of CNTs physical and chemical properties determine the adsorption behavior of CNTs to a particular PAH. It is unlikely that a single property alone can be discriminating. If one factor favors the adsorption, another factor may counteract adsorption

simultaneously to more or lesser extent. The findings in the present study support this fact.

The comparison of adsorbed phenanthrene to different sets of CNTs and the differences in the surface chemistries and physical properties of each set of CNTs may help in understanding the role of each parameter.

The SWCNTs showed the highest adsorption potential. Significantly higher phenanthrene adsorption towards SWCNTs than MWCNTs has been reported by Apul and colleagues in a similar study. The greater adsorption potential of SWCNTs was attributed to its greater SSA (Apul, Shao et al. 2012). SSA has been reported as the most important characteristic of CNTs which controls adsorption capacities of CNTs (Yang, Zhu et al. 2006).

An increase in OD and decrease in SSA from MWCNTs-1 to MWCNTs-2 have demonstrated 18 % less adsorption of phenanthrene towards MWCNTs-2. A Comparison of characteristics of CNTs and adsorption potential is presented in Table 6.2. The decrease in adsorption potential can be attributed to 67% lower SSA of MWCNTs-2 than MWCNTs-1. Total pore volume ($V_{T)}$ increases the adsorption potential by providing more pores as adsorption sites (Su and Lu 2007), so increased V_T along with increased diameter counteracted the effect of decreased SSA, otherwise such a large decrease in SSA could have resulted in much lower adsorption potential of MWCNTs-2. Apul and colleagues reported that increased diameter of MWCNTs results in increased adsorption potential of MWCNTs. Increase in diameter offers less curved surface of the CNTs And better contact to the planar

organic molecules leading towards greater adsorption (Apul, Shao et al. 2012).

Table 6.2. Comparison of CNTs characteristics and adsorption

Decrease in adsorption potential	Decrease in adsorption %	Change in SSA	Change in OD	Change in V_T	ZP in Milli-Q water mV	Particle size (nm)
From MWCNTs-1 to MWCNTs-2	18	67 % decrease	59 % increase	44 % increase	-25.7 -33.2	2536 2190
From MWCNTs-2 to MWCNTs-3	16	20 %increase	11 % increase	2 % increase	-33.2 -21.4	2170 410
From MWCNTs-2 to MWCNTs-NH2	5	1 %increase	11 % increase	17 %increase	-33.2 -23.1	2170 503

CNTs characteristics comparison is made by using **Error! Reference source not found.** and adsorption comparison is made from the values given in Table 6.3 of CNTs characteristics SSA= Specific surface area, OD= Outer diameter, V_T= total pore volume, ZP= zeta potential

A decrease of 16 % adsorption to MWCNTs-3 than MWCNTs-2 is observed even though the SSA is increased to 20 %, V_T to 2 % and the surface charge is decreased as shown by ZP value (Table 6.2) while ODs remain comparable (**Error! Reference source not found.**). All these parameters suggest higher adsorption capacity of MWCNTs-3 than MWCNTs-2. The comparative decrease in adsorption potential of MWCNTs-3 can be explained by its adsorption affinity. The MWCNTs-3 particles in suspension have much higher charge density than MWCNTs-2. Both CNTs have comparable ZP values but the average

particle size has dropped from 2170 for MWCNTs-2 to 410 nm for MWCNTs-3. The increased charged density of the MWCNTs-3 particles lowered its adsorption affinity towards phenanthrene. The observed adsorption potential is the net effect of its adsorption capacity and adsorption affinity.

The slight differences of adsorption potential between MWCNTs-2 and MWCNTs-NH_2 can also be explained by the differences in adsorption affinity. Both CNT types have comparable SSAs. Greater V_T suggests a higher adsorption capacity for MWCNTs-NH_2 but due to the decreased particle size MWCNTs-NH2 particles have higher charge density and lower adsorption affinity. But the difference of observed adsorption potential between MWCNTs-2 and MWCNTs-NH_2 is less than the difference between MWCNTs-2 and MWCNTs-3. Greater V_T of MWCNTs-NH_2 than MWCNTs-3 has given some compensation for the decreased adsorption affinity of MWCNTs-NH_2 resulting in lower adsorption differences between MWCNTs-2 and MWCNTs-NH_2 than MWCNTs-2 and MWCNTs-3.

Functionalization enables better dispersion of CNTs as shown by the hydrodynamic diameters of functionalized CNTs compared with MWCNTs-2 (particle sizes as measured by DLS are given in Figure 5.10). The adsorption potential order MWCNTs-2 >MWCNTs-NH_2 >MWCNTs-COOH >MWCNTs-OH (Table 6.3) shows that increased functionalization has resulted in decreased adsorption potential of the CNTs. These CNTs have comparable SSA, V_T and ODs. Surface functionalization of MWCNTs as –COOH, -OH and –NH_2 enabled better dispersion of functionalized MWCNTs as shown by the hydrodynamic diameters of

functionalized CNTs and MWCNTs-2 (**Error! Reference source not found.**). Significantly smaller particle sizes with comparable ZP values, resulted in high charge density of the particles, and reduced the phenanthrene adsorption affinity of functionalized MWCNTs than MWCNTs-2.

From the results of this study, no clear correlation can be established between the adsorption potential of the MWCNTs and a specific single parameter like surface area (SSA), outer diameter (OD), total pore volume (V_T), number of walls or length of the MWCNTs. The main reason for this is either no information is available about a parameter for all CNT types or the lack of systematic variation in CNT characteristics. From the specifications available from manufacturer the CNTs were choose to make this study systematic but the characterization of the CNTs done in this study showed that there is less systematic variation among the parameters of the CNTs than we expected.

Effect of NOM on the adsorption behavior of CNTs

The order for adsorption potential of CNTs in the NOM solution was SWCNTs > MWCNTs-1 > MWCNTs-3> MWCNTs-2 > MWCNTs-NH2 > MWCNTs-OH > MWCNTs-COOH which is different from that observed in MHRW. The presence of NOM reduced phenanthrene adsorption towards CNTs from 26-88 % of what was observed in MHRW. Table 6.3 compares the adsorption of phenanthrene towards CNTs in MHRW and in NOM solution. The CNTs were affected by the NOM in the following order; The MWCNTs-COOH > MWCNTs-2 > MWCNTs-1 > MWCNTs-OH

> SWCNTs > MWCNTs-3 > MWCNTs-NH2. The MWCNTs-COOH were affected most and showed ~88% less phenanthrene adsorption while MWCNTs-3 were least affected With a ~27% less phenanthrene adsorption of in NOM than in MHRW.

Significantly decreased adsorption towards CNTs in NOM solution than in MHRW shows that NOM adsorbs to CNTs. Lower adsorption values for functionalized CNTs in NOM solution than NOM alone show decreased availability of adsorption sites offered by both, NOM and CNTs separately (Table 6.3). The overall effect of NOM on the adsorption towards CNTs has been reported as a net result of two opposite effects. Better dispersion of CNTs creates more adsorption sites and NOM also competes with hydrophobic organic compounds for adsorption towards CNTs which reduces the observed adsorption potential of CNTs (Hyung and Kim 2008). The results of this study suggest that the latter effect is the dominant one. These results are in agreement with the findings of Zhang and colleagues (Zhang, Shao et al. 2011).

Comparison of decrease in adsorption potential of functionalized CNTs with MWCNTs-2 suggests that the adsorption potential of CNTs is affected by the type and extent of functionalization. The MWCNTs-2 type is the non-functionalized analogue of the functionalized MWCNTs according the manufacturer. If the manufacturer's specifications about the extent of functionalization represent the given batch then NOM decreases the adsorption potential of CNTs in the order MWCNTs-NH2 > MWCNTs-COOH > MWCNTs-OH with respect to the type of functionalization.

Table 6.3. Comparison of adsorption of phenanthrene to different CNT types in MHRW and in NOM

CNT type	% Adsorption in MHRW	Ads in NOM %	% decrease
NOM	-	8	-
SWCNTs	67	33	51
MWCNTs-1	45	16	65
MWCNTs-2	37	11	70
MWCNTs-3	21	15	27
MWCNTs-COOH	22	3	88
MWCNTs-OH	15	6	61
MWCNTs-NH2	32	6	81

A maximum depletion of phenanthrene from the aqueous CNTs systems was found ~ 1% in both adsorption experiments under the experimental conditions. This is <5% and falls under the criteria of negligible depletion proposed by Vaes and colleagues (Vaes, Urrestarazu Ramos et al. 1996). Depletion was calculated by dividing the total amount of phenanthrene extracted by the fiber for 100 µg/L MHRW control with its initial quantity present in the sample volume.

Conclusions

The primary conclusions from this study are followings.

- From the results of this study, no clear correlation can be established between the adsorption potential of the MWCNTs and a specific parameter like surface area (SSA), outer diameter (OD), total pore volume (V_T), number of walls or length of the MWCNTs.
- The SWCNTs have much higher adsorption potential than MWCNTs.
- The study suggested that increased diameter of MWCNTs might have supporting effect for the adsorption potential of CNTs for phenanthrene.
- Functionalization (-COOH, -OH and $–NH_2$) reduces the adsorption potential of CNTs towards hydrophobic compounds like phenanthrene.
- The presence of NOM reduced phenanthrene adsorption towards the CNTs from 26 to 88 % of what was observed in MHRW.
- According to literature NOM affects CNTs in two ways. (i) NOM competes for adsorption towards CNTs or blocks the adsorption sites and decreases the adsorption potential of CNTs (ii) More adsorption sites are created because of better dispersions of CNTs in the presence of NOM. The results of this study suggest that the former effect of NOM is more dominant for the adsorption of phenanthrene towards CNTs.
- The results showed that adsorption potential of CNTs is affected by the type and extent of functionalization. NOM decreases the adsorption potential of CNTs in the order MWCNTs-NH2 > MWCNTs-COOH > MWCNTs-OH with respect to the type of functionalization.

Suggestions and future work

Following future work is recommended and suggestions are given for performing future study.

1. Different SWCNTs and MWCNTs with considerably different number of walls, diameters and lengths and functionalized CNTs with different extents of functionalization of each functional group are recommended to be included in further study. This can make study more systematic and effect of each parameter can better be studied.
2. A through characterization of CNTs should be performed as the specifications given by the manufacturer may not represent the batch under study.
3. Principal component analysis (PCA) of the adsorption results is recommended. It may give better correlation and effect of each parameter for the adsorption potential of CNTs.
4. Multipoint adsorption data for each CNT type is recommended as is done in the most studies because it allows validity of the data by adsorption isotherms and reveals more information about the adsorption behavior of CNTs.
5. A concentration 100 µg/L phenanthrene may not be environmentally relevant. Adsorption studies with lower concentrations can make the data more environmentally relevant.
6. SPME should be performed protecting the PDMS fiber. A Cellulose hollow fiber membrane is suggested while studying the adsorption towards CNTs. Because the cellulose is hydrophilic and CNTs are unlikely to adsorb on cellulose surface and block the pores for the in and out

diffusion controlled mass transfer of PAH molecules for partition to the PDMS fiber. It can help in avoiding the fouling of the SPME fiber because of the CNTs if adsorbed to the SPME fiber which may also add phenanthrene to the *n*-hexane during extraction from the SPME fiber leading to erroneous results. This fouling of SPME fiber by CNTs has already been reported by in the literature. Use of much lower concentrations of CNTs up to 0.5 mg/L also decreased this effect.

References

Apul, O. G., T. Shao, et al. (2012). "Impact of carbon nanotube morphology on phenanthrene adsorption." Environ Toxicol Chem **31**(1): 73-78.

Aqel, A., K. M. M. A. El-Nour, et al. (2012). "Carbon nanotubes, science and technology part (I) structure, synthesis and characterisation." Arabian Journal of Chemistry **5**(1): 1-23.

Chen, B., E. J. Johnson, et al. (2005). "Sorption of Polar and Nonpolar Aromatic Organic Contaminants by Plant Cuticular Materials: Role of Polarity and Accessibility." Environmental Science & Technology **39**(16): 6138-6146.

Chen, W., L. Duan, et al. (2007) "Adsorption of polar and nonpolar organic chemicals to carbon nanotubes." Environ Sci Technol **41**, 8295-8300.

Cui, D., F. Tian, et al. (2005). "Effect of single wall carbon nanotubes on human HEK293 cells." Toxicol Lett **155**(1): 73-85.

Ding, Y. "Fundamental Theory of Transmission Electronic Microscopy."

Ebbesen, T. W. (1997). "Carbon nanotubes, preparation and properties." CSR press, Boca Raton, Fla USA: 139.

Edmond de Hoffman (2007). "Mass spectrometry principles and applications ": 15.

Egerton, R. F. (2005). "Physical principles of electron microscopy: An introduction to TEM, SEM and AEM." 11, 78-82.

Egerton, R. F. (2005). "Physical principles of electron microscopy: An introduction to TEM, SEM and AEM." 17, 125-128.

Egerton, R. F. (2005). "Physical principles of electron microscopy: An introduction to TEM, SEM and AEM." 19.

Gohlke, R. and F. McLafferty (1993). "Early gas chromatography/mass spectrometry." Journal of the American Society for Mass Spectrometry **4**(5): 367-371.

Goodge, J. (2013). "Back-scattered Electron Detector (BSE)."

Gorecki, T. and J. Pawliszyn (1997). "Effect of sample volume on quantitative analysis by solid-phase microextraction. Part 1. Theoretical considerations." Analyst **122**(10): 1079-1086.

Gottschalk, F., T. Sonderer, et al. (2009). "Modeled Environmental Concentrations of Engineered Nanomaterials (TiO2, ZnO, Ag, CNT, Fullerenes) for Different Regions." Environmental Science & Technology **43**(24): 9216-9222.

Gottschalk, F., T. Sonderer, et al. (2010). "Possibilities and limitations of modeling environmental exposure to engineered nanomaterials by probabilistic material flow analysis." Environ Toxicol Chem **29**(5): 1036-1048.

Heringa, M. B. and J. L. M. Hermens (2003). "Measurement of free concentrations using negligible depletion-solid phase microextraction (nd-SPME)." TrAC Trends in Analytical Chemistry **22**(9): 575-587.

Hirsch, A. and O. Vostrowsky (2005). "Functionalization of carbon nanotubes." Functional Molecular Nanostructures **245**: 193-237.

Holbrook, R. D., C. N. Kline, et al. (2010). "Impact of Source Water Quality on Multiwall Carbon Nanotube Coagulation." Environmental Science & Technology **44**(4): 1386-1391.

Holler, Skoog, et al. (2007). "Principles of Instrumental Analysis." 788- 815.

Hu, H., P. Bhowmik, et al. (2001). "Determination of the acidic sites of purified single-walled carbon nanotubes by acid–base titration." Chemical Physics Letters **345**(1–2): 25-28.

Hu, X., J. Liu, et al. (2008). "Impacts of some environmentally relevant parameters on the sorption of polycyclic aromatic hydrocarbons to aqueous suspensions of fullerene." Environmental Toxicology and Chemistry **27**(9): 1868-1874.

Hyung, H. and J. H. Kim (2008). "Natural organic matter (NOM) adsorption to multi-walled carbon nanotubes: effect of NOM characteristics and water quality parameters." Environ Sci Technol **42**(12): 4416-4421.

Iijima, S. (1991). "Helical Microtubules of Graphitic Carbon." Nature **354**(6348): 56-58.

In-Youp Jeon, Dong Wook Chang, et al. (2011). "Functionalization of carbon nanotubes."

International organization for standardization (1996). "Particle size analysis-photon correlation spectroscopy, ISO 13321." **Part 8**.

Journet, C., W. K. Maser, et al. (1997). "Large-scale production of single-walled carbon nanotubes by the electric-arc technique." Nature **388**(6644): 756-758.

Katsnelson, M. I. (2007). "Graphene: carbon in two dimensions." Materials Today **10**(1–2): 20-27.

Kennedy, A. J., M. S. Hull, et al. (2008). "Factors influencing the partitioning and toxicity of nanotubes in the aquatic environment." Environ Toxicol Chem **27**(9): 1932-1941.

Kiang, C. H., M. Endo, et al. (1998). "Size Effects in Carbon Nanotubes." Physical Review Letters **81**(9): 1869-1872.

Krumeich, F. "Properties of Electrons, their Interactions with Matter and Applications in Electron Microscopy."

Li, Y.-H., S. Wang, et al. (2002). "Lead adsorption on carbon nanotubes." Chemical Physics Letters **357**(3–4): 263-266.

Long, R. Q. and R. T. Yang Carbon nanotubes as superior sorbent for dioxin removal, J Am Chem Soc. 2001 Mar 7;123(9):2058-9.

Malver Instruments. "Zeta potential measurement using laser Doppler electrophoresis (LDE)."

Mawhinney, D. B., V. Naumenko, et al. (2000). "Surface defect site density on single walled carbon nanotubes by titration." Chemical Physics Letters **324**(1–3): 213-216.

McNair H.M. and Miller J.M (2011). "Basic Gas Chromatography." 1-9.

Miller J.M. (2005). "Chromatography: Concepts and Contrasts." 161-166.

Miller J.M. (2009). "mass spectrometry: instrumentation, interpretation and applications ": 49-50.

Miralles, P., E. Johnson, et al. (2012). "Multiwalled carbon nanotubes in alfalfa and wheat: toxicology and uptake." Journal of The Royal Society Interface **9**(77): 3514-3527.

Nies, D. H. (1999). "Microbial heavy-metal resistance." Appl Microbiol Biotechnol **51**(6): 730-750.

NORON Instruments. "Energy dispersive X-ray microanalysis; nn Introduction,." 1-2.

Ouyang, G. and J. Pawliszyn (2008). "A critical review in calibration methods for solid-phase microextraction." Anal Chim Acta **627**(2): 184-197.

Pan, B. and B. Xing (2008). "Adsorption Mechanisms of Organic Chemicals on Carbon Nanotubes." Environmental Science & Technology **42**(24): 9005-9013.

Particle analyticle (2013). "Brunauer, Emmett and Teller (BET) Theory."

Patel, V. (2011). "Global carbon nanotubes market - industry beckons."

Pawliszyn, J. (1997). "Solid Phase Micro extraction : Theory and practice." 89.

Pawliszyn., J. (1997). "Solid phase microextraction : Theory and practices,."

Peigney, A., C. Laurent, et al. (2001). "Specific surface area of carbon nanotubes and bundles of carbon nanotubes." Carbon **39**(4): 507-514.

Petersen, E., L. Zhang, et al. (2011). "Potential release pathways, environmental fate, and ecological risks of carbon nanotubes." Environ Sci Technol **45**(23): 9837-9856.

Poerschmann, J., Z. Zhang, et al. (1997). "Solid Phase Microextraction for Determining the Distribution of Chemicals in Aqueous Matrices." Analytical Chemistry **69**(4): 597-600.

Poole C.F. (2003). "The Essence of Chromatography." 71-72, 80, 83-85, 226-229, 733-735.

Prasek, J., J. Drbohlavova, et al. (2011). "Methods for carbon nanotubes synthesis-review." Journal of Materials Chemistry **21**(40): 15872-15884.

Rolf Ekman, Dominic M. Desiderio, et al. (2002). "Mass Spectrometry - Instrumentation, Interpretation, and Applications." 50.

Sakshat Virtual Labs "Principles of Zeta potential."

Sander, M. and J. J. Pignatello (2005). "Characterization of Charcoal Adsorption Sites for Aromatic Compounds: Insights Drawn from Single-Solute and Bi-Solute Competitive Experiments." Environmental Science & Technology **39**(6): 1606-1615.

Shi Kam, N. W., T. C. Jessop, et al. (2004). "Nanotube molecular transporters: internalization of carbon nanotube-protein conjugates into Mammalian cells." J Am Chem Soc **126**(22): 6850-6851.

Su, F. and C. Lu (2007). "Adsorption kinetics, thermodynamics and desorption of natural dissolved organic matter by multiwalled carbon nanotubes." J Environ Sci Health A Tox Hazard Subst Environ Eng **42**(11): 1543-1552.

Thermo Scientific "Overview of Mass Spectrometry."

Throck Watson J. (2007). "Introduction to Mass Spectrometry ": 3.

U.S. Environmental Protection Agency (1993). "Methods for measuring the acute toxicity of effluents and receiving waters to freshwater and marine organisms."

University of Wisconsin, M. M. r. s. a. e. c. (2008). "Carbon Nanotubes & Buckyballs."

Vaes, W. H. J., E. Urrestarazu Ramos, et al. (1996). "Measurement of the Free Concentration Using Solid-Phase Microextraction: Binding to Protein." Analytical Chemistry **68**(24): 4463-4467.

Warheit, D. B., B. R. Laurence, et al. (2004). "Comparative pulmonary toxicity assessment of single-wall carbon nanotubes in rats." Toxicol Sci **77**(1): 117-125.

Yadav, S. K. (2010). "Heavy metals toxicity in plants: An overview on the role of glutathione and phytochelatins in heavy metal stress tolerance of plants." South African Journal of Botany **76**(2): 167-179.

Yang, K. and B. Xing (2007). "Desorption of polycyclic aromatic hydrocarbons from carbon nanomaterials in water." Environ Pollut **145**(2): 529-537.

Yang, K., L. Zhu, et al. (2006). "Adsorption of Polycyclic Aromatic Hydrocarbons by Carbon Nanomaterials." Environmental Science & Technology **40**(6): 1855-1861.

Zhang, S., T. Shao, et al. (2009). "The Impacts of Aggregation and Surface Chemistry of Carbon Nanotubes on the Adsorption of Synthetic Organic Compounds." Environmental Science & Technology **43**(15): 5719-5725.

Zhang, S., T. Shao, et al. (2010). "Adsorption of synthetic organic chemicals by carbon nanotubes: Effects of background solution chemistry." Water Research **44**(6): 2067-2074.

Zhang, S., T. Shao, et al. (2011). "The effects of dissolved natural organic matter on the adsorption of synthetic organic chemicals by activated carbons and carbon nanotubes." Water Res **45**(3): 1378-1386.

Zhang, X., M. Kah, et al. (2012). "Dispersion State and Humic Acids Concentration-Dependent Sorption of Pyrene to Carbon Nanotubes." Environmental Science & Technology **46**(13): 7166-7173.

APPENDIX A.

Data for section 4.8 (a).

Table1.1: Equilibrium time determination between phe and PDMS fiber

SPME Time (hrs)	GC-MS resp. 1	GC-MS resp. 2	Average	Std. dev.	% RSD
1	104183	146782	125482.5	30122.04177	24.00497422
3	375961	244031	309996	93288.59764	30.09348432
24	3121374	3653928	3387651	376572.5447	11.11603718
48	4744405	4637521	4690963	75578.4012	1.611148952
72	4972421	5023240	4997830.5	35934.45951	0.719001165

Table1.2 GC-MS analysis calibration data for phe

std. conc. (µg/mL)	GC-MS responses
0.1	147431
0.5	791532
1	1488673
2.5	4671515

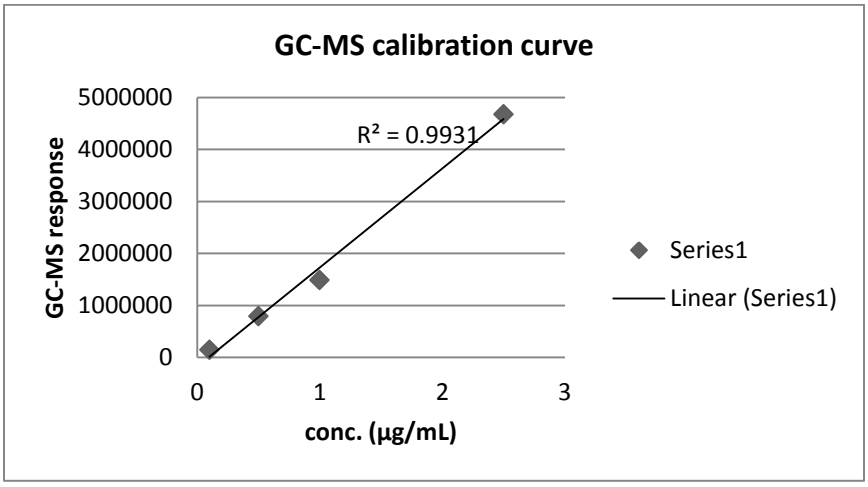

Data for 4.8 (b).

Table1.3: Equilibrium time determination for aqueous pyr to PDMS fiber for DI-SPME

SPME time (days)	GC-MS resp 1	GC-MS resp 2	Average	Std. dev.	% RSD
1	160328	157221	160328	2196.980769	1.370303858
4	8958920	NA	8958920	NA	NA
5	10779700	11243100	10779700	327673.2824	3.039725432
6	11247100	NA	11247100	NA	NA

Table1.4 GC-MS analysis calibration data for pyr

std conc. µg/mL	GC-MS responses
0.001	8198
0.01	13905
0.05	59210
0.1	124716
1.00	1398930
2.50	4471500
5	7956790

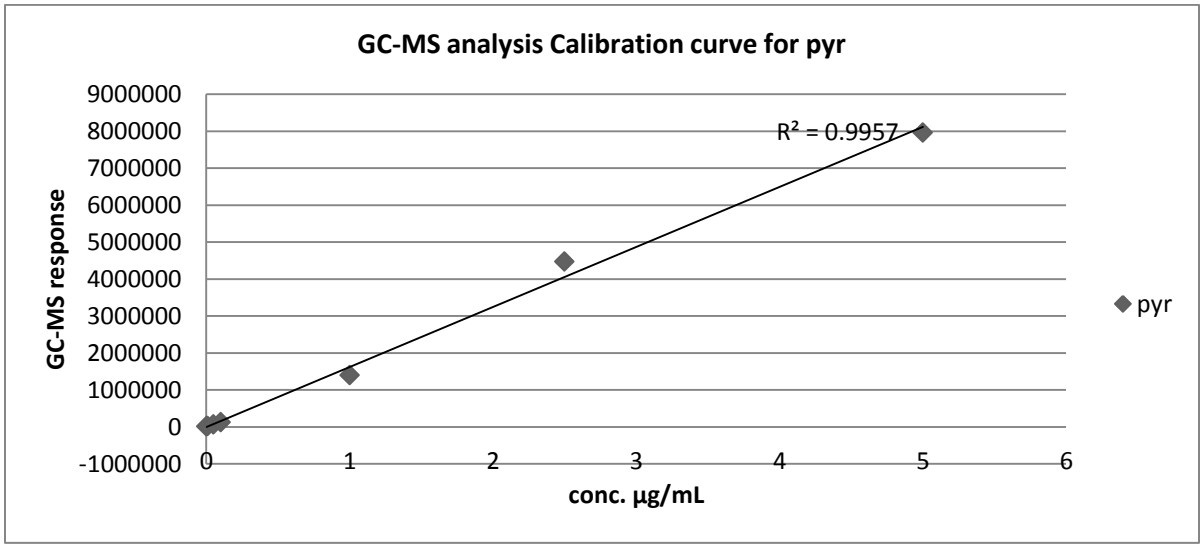

Data for section 4.9

Study of equilibrium time for adsorption between PAHs and CNTs

Table2.1 Study of equilibrium time for adsorption between Phenanthrene and CNTs

Sorption Time(CNT/Phe)	GC-MS response 1	GC-MS response 2	GC-MS response 3	Average	Std. dev.	%RSD
2.00	770	625	585	660	79.48	12.04
4	421	467	389	425.67	32.01	7.52
26	375	372	352	366.33	10.21	2.79
50	357	324	295	325.33	25.33	7.79
72	304	306	255	288.33	23.58	8.18
96	486	328	356	390.00	68.84	17.65
120	281	367	NA	324	60.81	18.77
148	1283	514	350	715.67	406.71	56.83

Table2.2 GC-MS calibration standards for phenanthrene

Std. conc. µg/mL	GC-MS responses
0.001	1132
0.01	4861
0.05	19500
0.1	38396
0.5	202739
1	336641
2.5	1092537
5	2305051

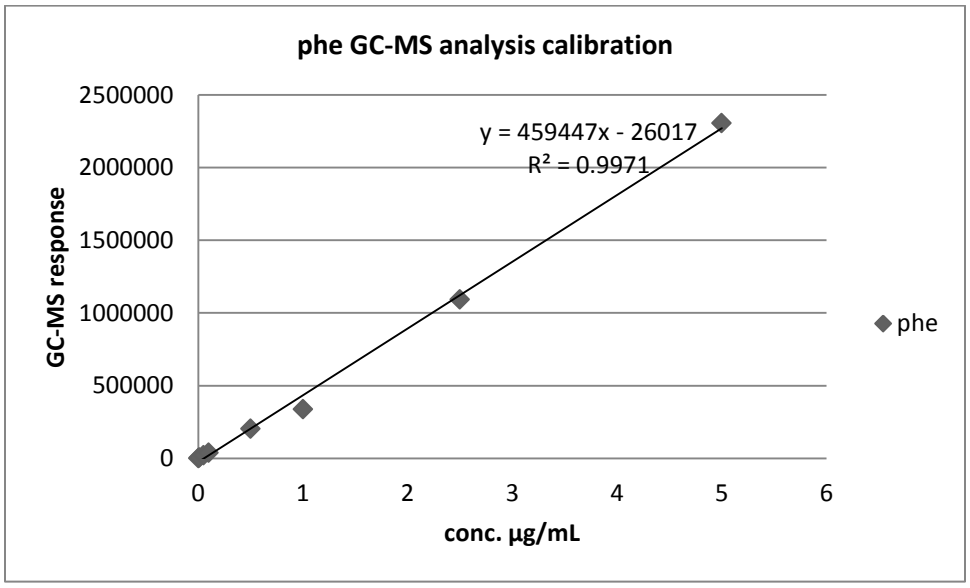

Table 2.3. Investigation of adsorption equilibrium times between pyr and SWCNTs (100 µg/L pyr and 0.5 mg/L SWCNTs)

Ads. Time (days)	GC-MS response 1	GC-MS response 2	Average	std. dev.	%RSD
1	63111	NA	63111	0	0
2	36302	77002	56652	28779.25	50.80
3	55729	46194	50961.5	6742.26	13.23
4	1155860	1258500	1207180	72577.44	6.01
5	1016500	1168610	1092555	107558.01	9.84
6	839081	951663	895372	79607.50	8.89
6 (CNTs blank)	1373	206			

Table2.4 GC-MS analysis calibration curve for pyrene

std conc. µg/mL	GC-MS responses
0.001	8198
0.01	13905
0.05	59210
0.1	124716
1.00	1398930
2.50	4471500
5	7956790

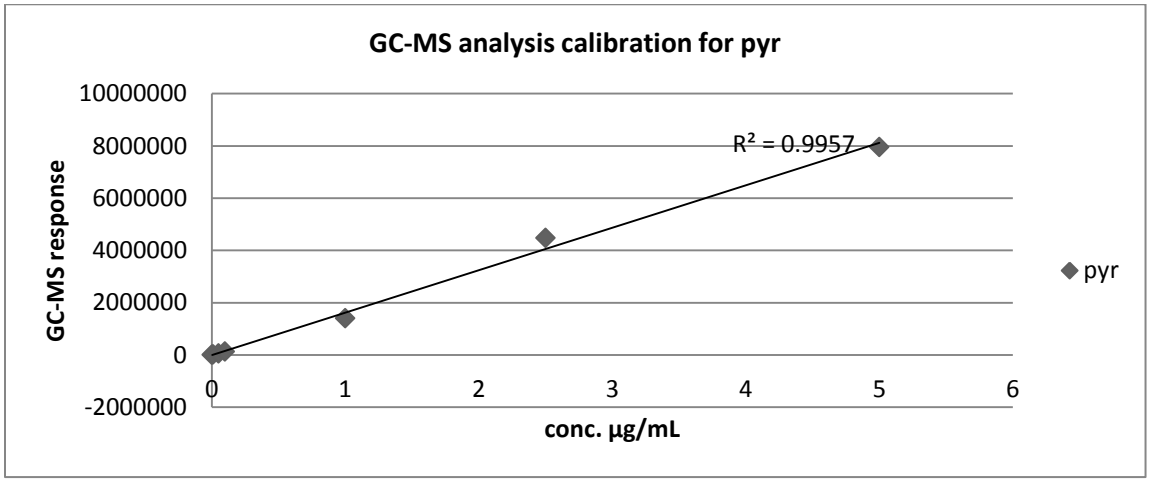

Data for section 4.10

Adsorption of phe to CNTs

Table.3.1 phe free conc. determination after adsorption to CNTs in MHRW

	Replicate 1 (µg/L)	Replicate 2 (µg/L)	Replicate 3 (µg/L)	Average (µg/L)	Std.dev	%RSD
MHRW (Control)	100.39	111.31	103.48	105.06	5.63	5.36
SWCNTs	33.12	33.73	NA	33.43	0.43	1.29
MWCNTs-1	51.48	57.24	48.42	52.38	4.07	7.78
MWCNTs-2	71.89	65.35	63.37	66.87	4.62	6.92
MWCNTs-3	82.2	82.19	78.77	81.05	0.01	0.01
MWCNTs-COOH	83.16	80.57	68.62	77.45	1.83	2.36
MWCNTs-OH	88.34	88.6	NA	88.47	0.18	0.21
MWCNTs-NH2	72.87	70.32	68.65	70.61	1.80	2.55

Table. 3.2 Phe free conc. Calibration data by SPME-MC-MS

Standard conc. (µg/L)	GC-MS responses	Average (µg/L)	std. dev.	%RSD
0	267			
25	17571	17458.5	159.10	0.91
25	17346			
50	37005	36648	504.87	1.38
50	36291			
75	58412	55670	2527.28	4.54
75	55164			
75	53434			
100	75404	77961.5	3860.76	4.95
100	75293			
100	83524			
100	77625			
150	118871	111346	10641.96	9.56
150	103821			

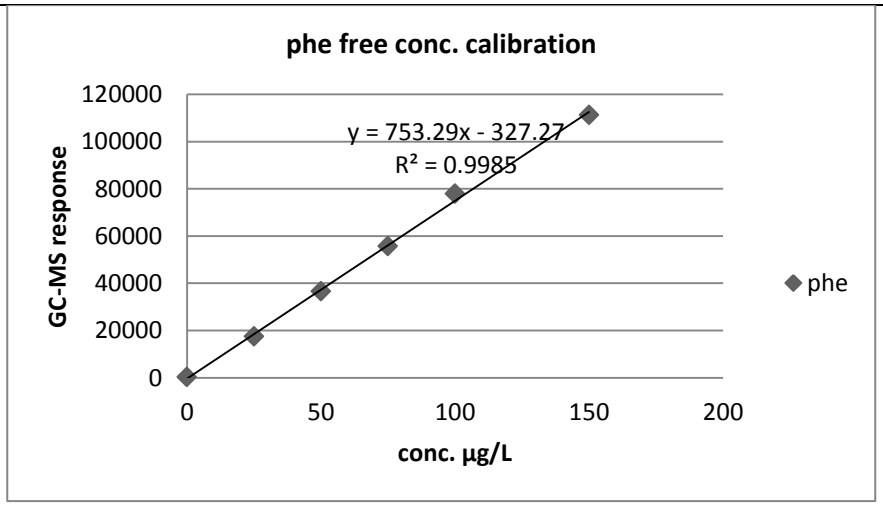

Table.3.3 GC-MS calibration data

GC-MS analysis calibration data	
Std. conc. (µg/mL)	**GC-MS response (peak area)**
0.01	12020
0.05	61412
1	1469310
2.5	3712800
5	7614510

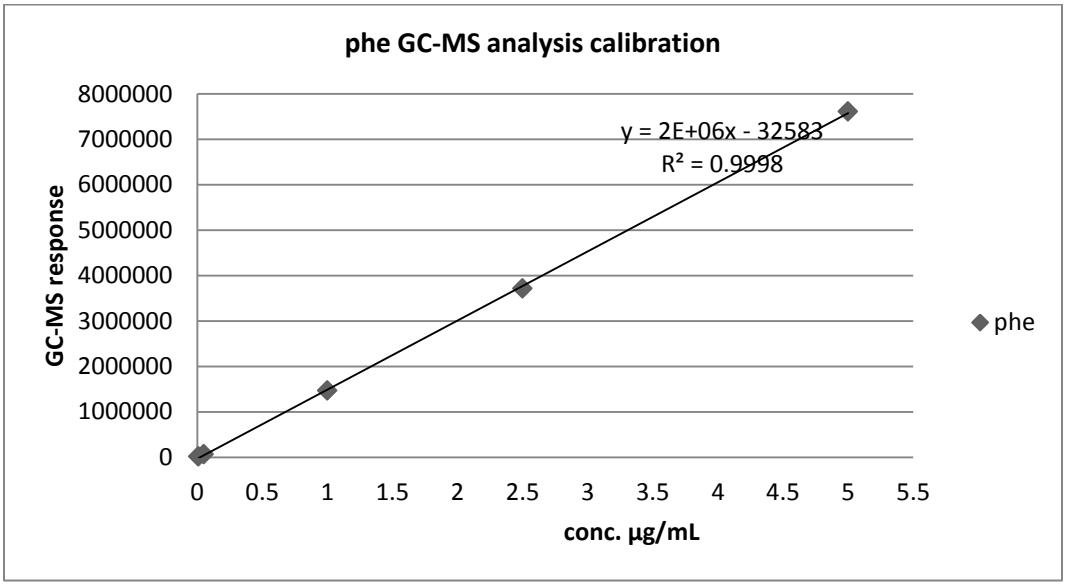

Table. 3.4 phe free conc. determined after adsorption to CNTs suspended in NOM solution

	replicate 1	replicate 2	replicate3	Average	Std. dev.	% RSD
MHRW control	91.06	**109.19**	**NA**	100.13	12.82	12.80
NOM	91.82	NA	NA	91.82	0	0
SWCNTs	68.46	66.48	65.63	66.86	1.45	2.17
MWCNTs-1	84.51	NA	NA	84.51	0	0
MWCNTs-2	88.64	90.37	87.78	88.93	1.32	1.48
MWCNTs-3	86.91	84.31	83.77	85.00	1.68	1.98
MWCNTs-OH	96.45	93.79	93.32	94.52	1.69	1.79
MWCNTs-NH2	97.02	92.16	92.84	94.01	2.63	2.80
MWCNTs-COOH	88.11	102.82	101.7	97.54	8.19	8.39

Phe free conc. Calibration data

Cfree (µg/L)	GC-MS responses 1	GC-MS responses 2	Average	Std. dev.	%RSD
1	858	979	918.5	85.56	9.32
2	1593	1430	1511.5	115.26	7.63
5	3446	3713	3579.5	188.80	5.27
10	7607	7522	7564.5	60.10	0.79
100	88593	106440	97516.5	12619.73	12.94

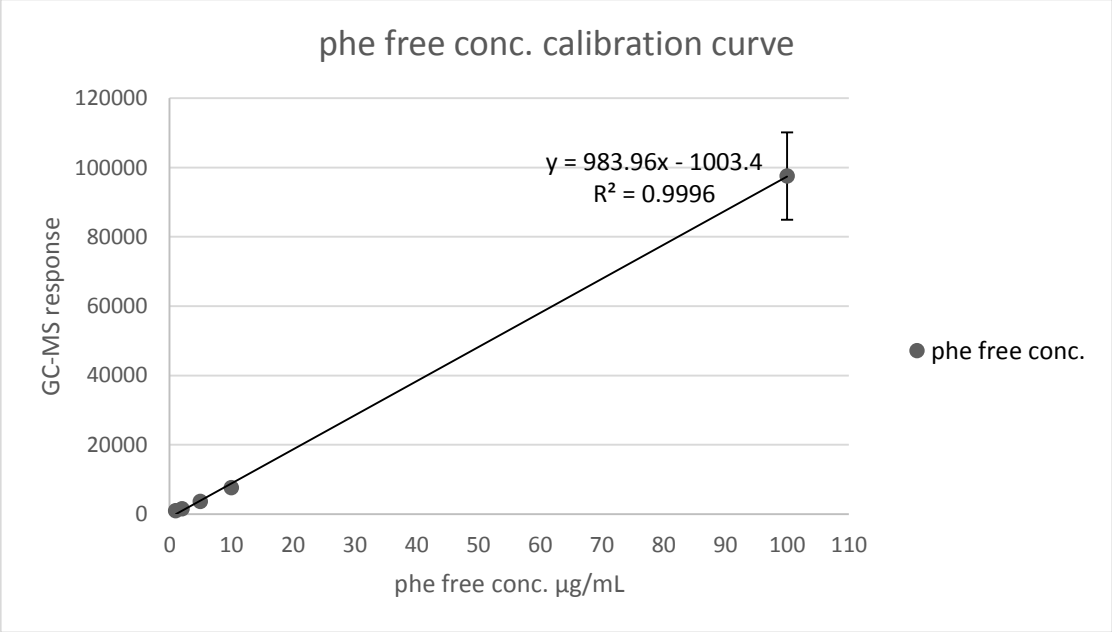

Table 3.5 GC-MS analysis calibration data

Std. conc. (µg/mL)	GC-MS response
0.001	1668
0.01	15916
0.05	80335
0.1	168261
0.5	868397
1	1850110
2.5	4762690
5	9677030

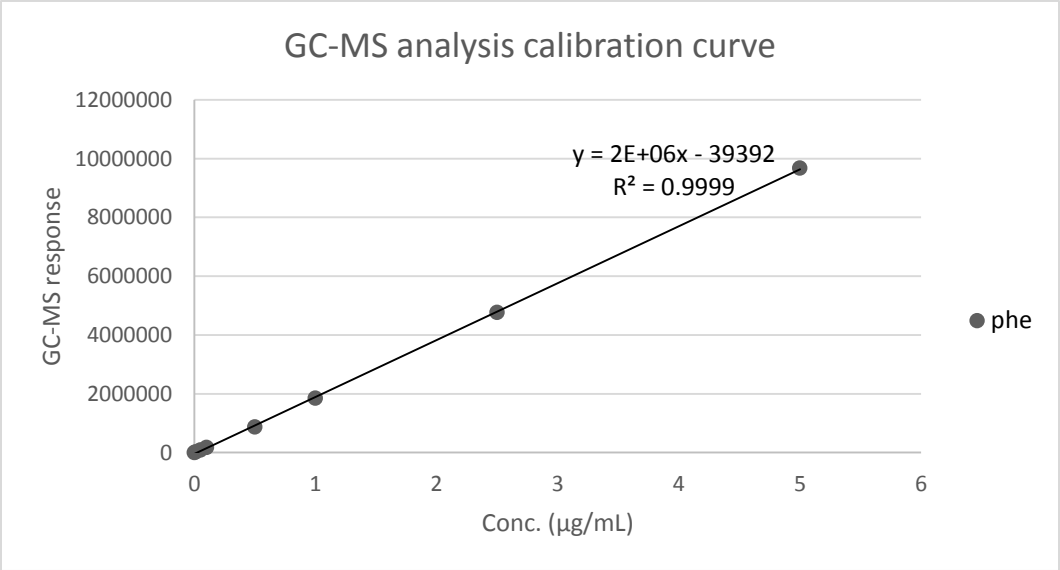

APPENDIX B

Data for diameter measurement from TEM images

MWCNT-1	
Nr counted	70
Average diameter (nm)	6.0
Std.av	2.2
Rel. Std.av	36.0
Max (nm)	14.7
Min (nm)	2.5
Median (nm)	5.6

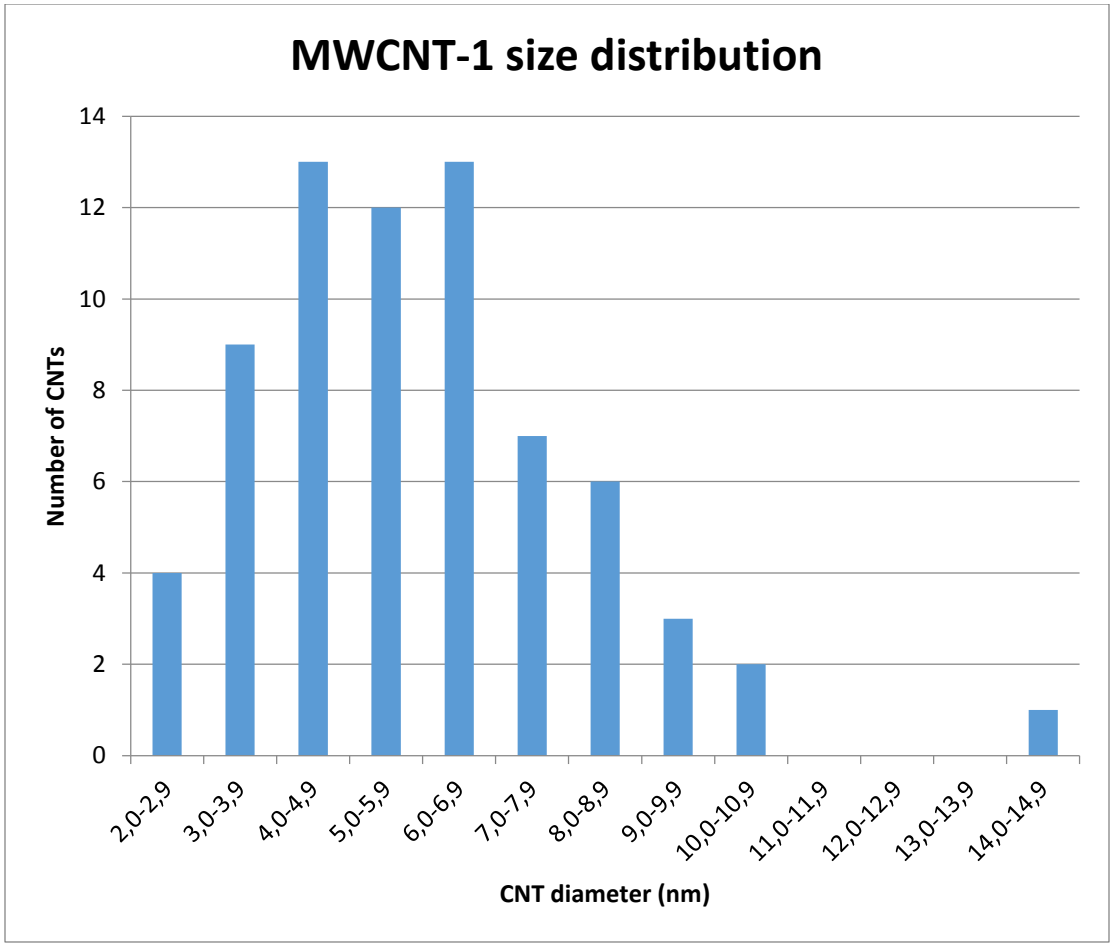

MWCNT-2	
Nr counted	332
Average diameter (nm)	14.8
Std.av	5.6
Rel. Std.av	37.6
Max (nm)	48.6
Min (nm)	5.2
Median (nm)	13.8

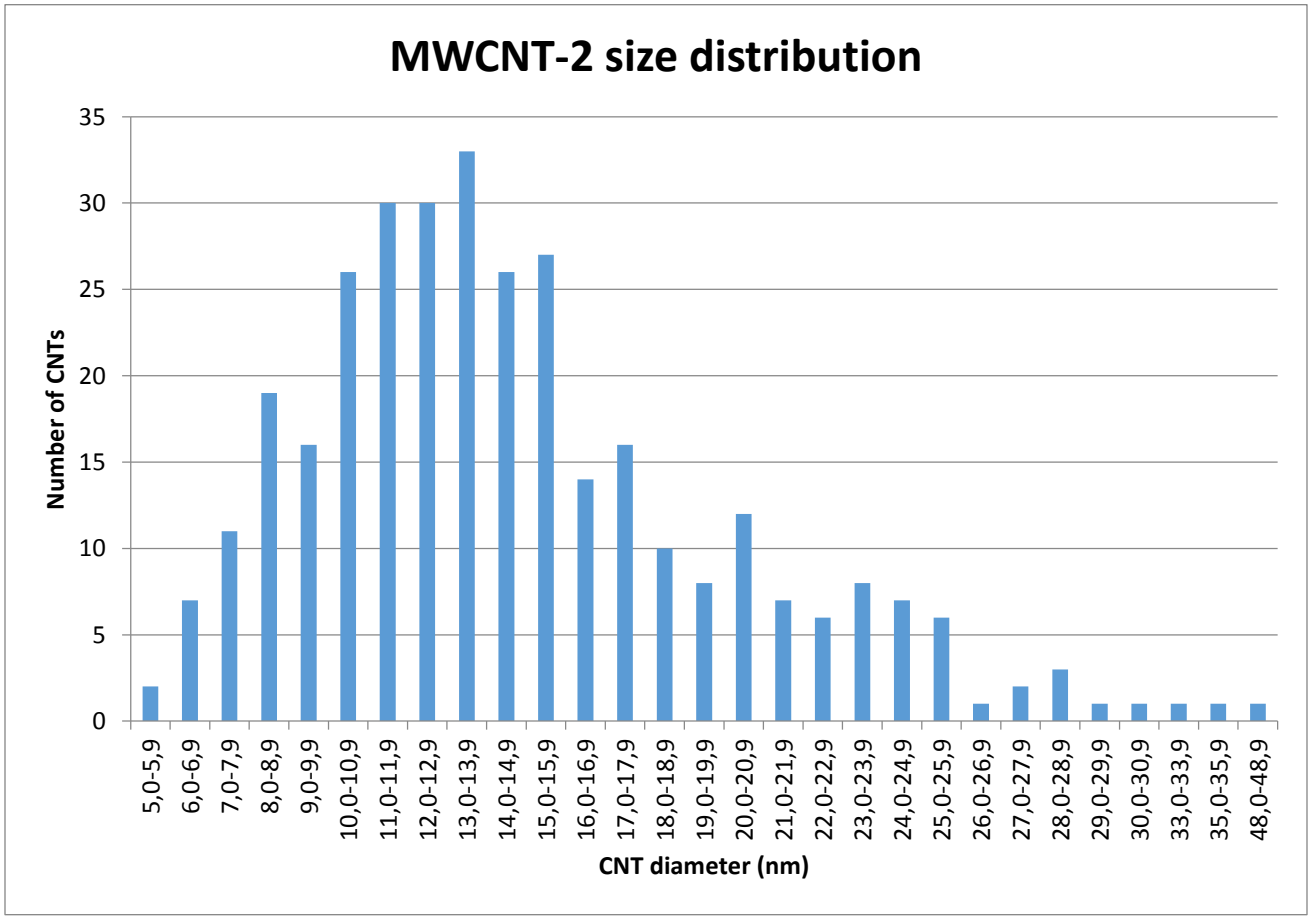

MWCNT-3	
Nr counted	200
Average diameter (nm)	16.6
Std.av	8.6
Rel. Std.av	51.9
Max (nm)	66.5
Min (nm)	5.9
Median (nm)	14.6

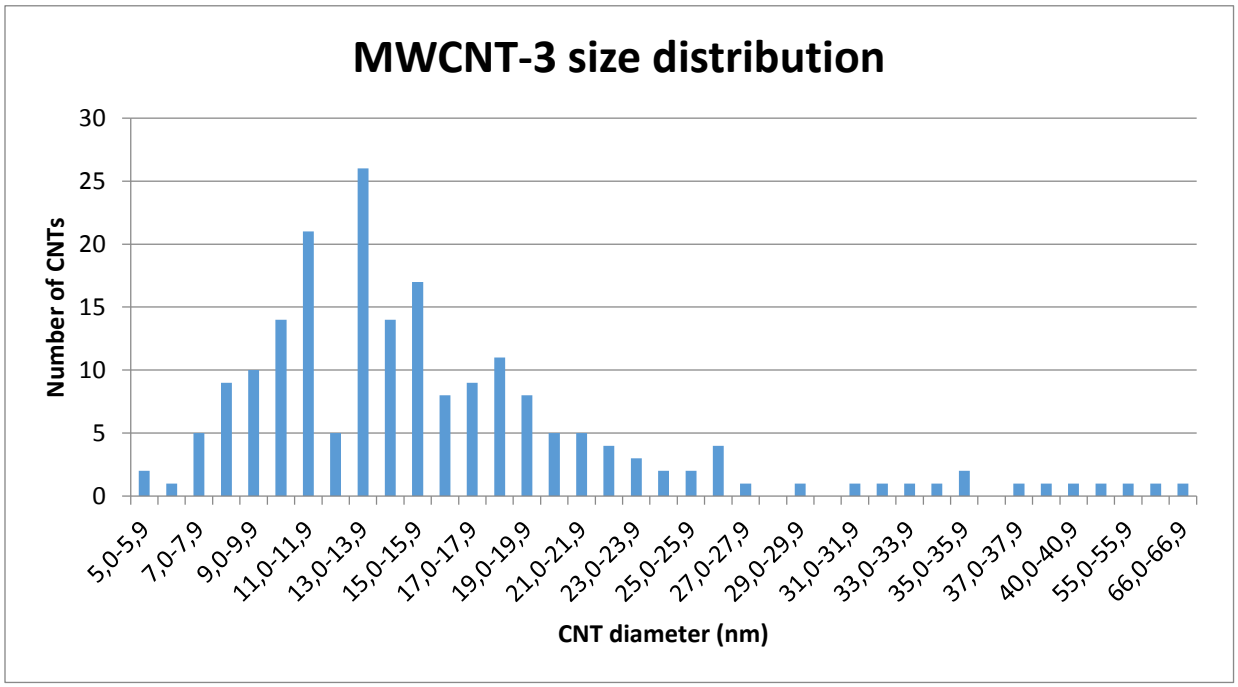

MWCNT-COOH	
Nr counted	241
Average diameter (nm)	20.3
Std.av	7.5
Rel. Std.av	36.8
Max (nm)	47.4
Min (nm)	5.9
Median (nm)	20.8

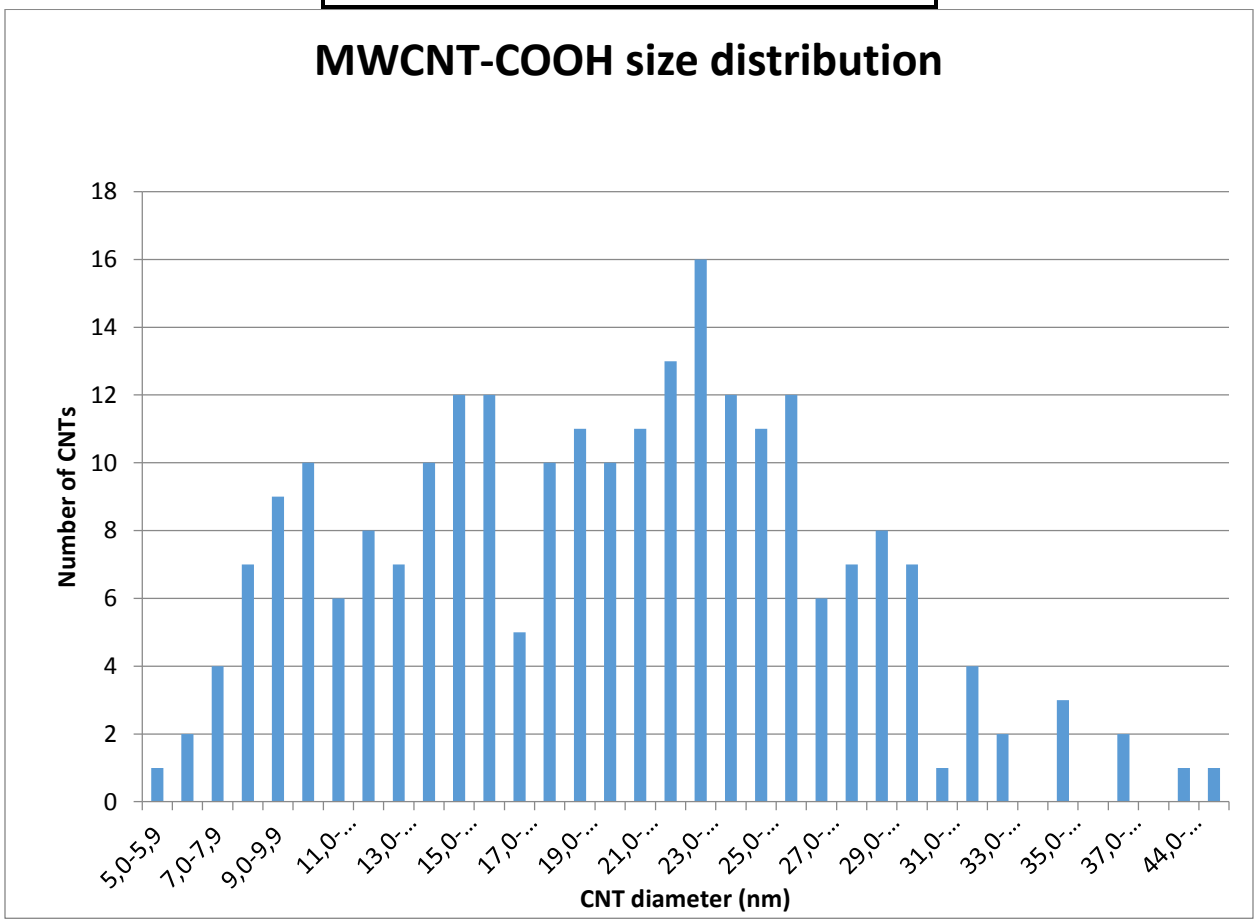

MWCNT-OH	
Nr counted	346
Average diameter (nm)	14.3
Std.av	5.8
Rel. Std.av	40.2
Max (nm)	45.8
Min (nm)	2.5
Median (nm)	13.1

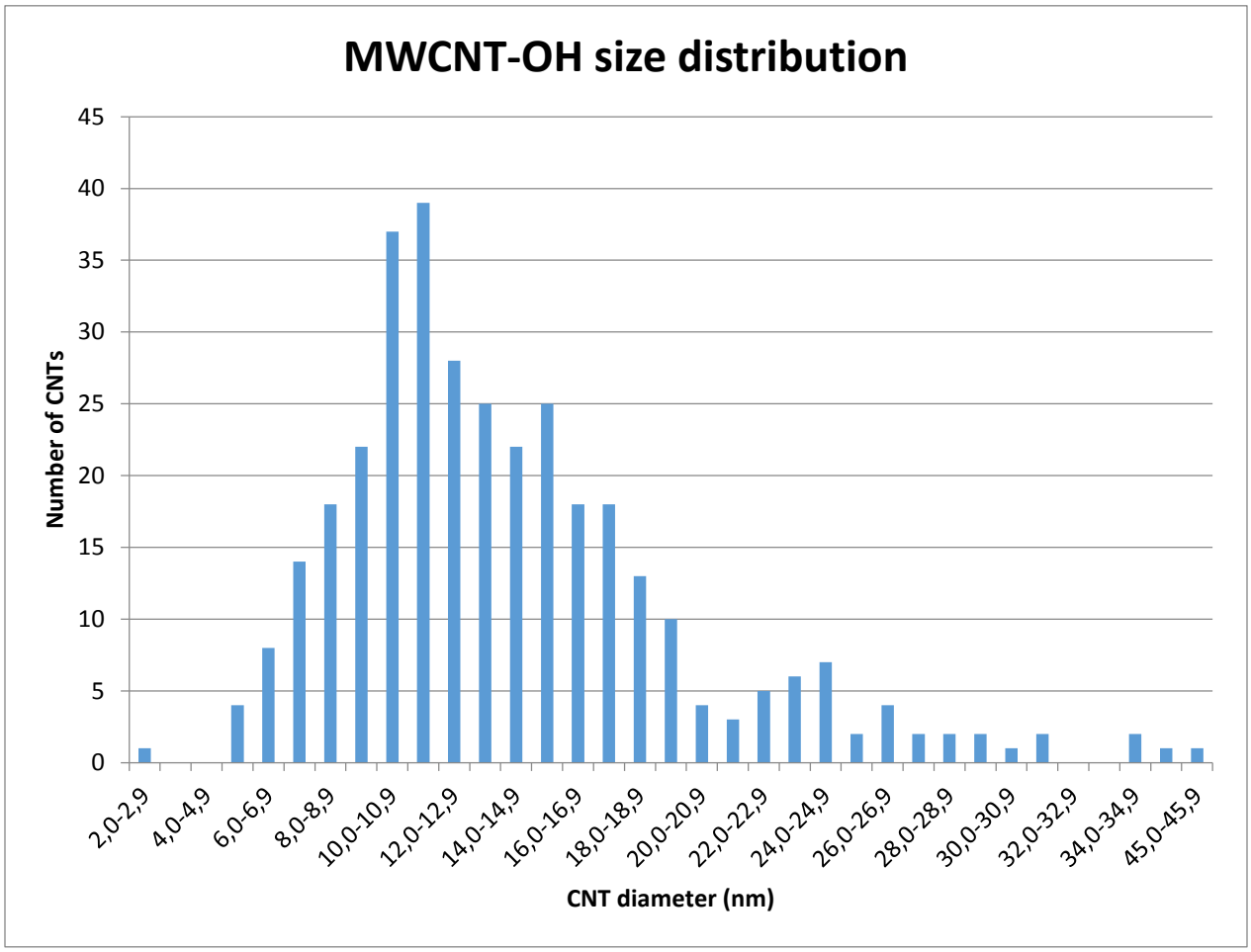

MWCNT-NH2	
Nr counted	346
Average diameter (nm)	16.7
Std.av	6.3
Rel. Std.av	37.4
Max (nm)	37.2
Min (nm)	6.2
Median (nm)	15.8

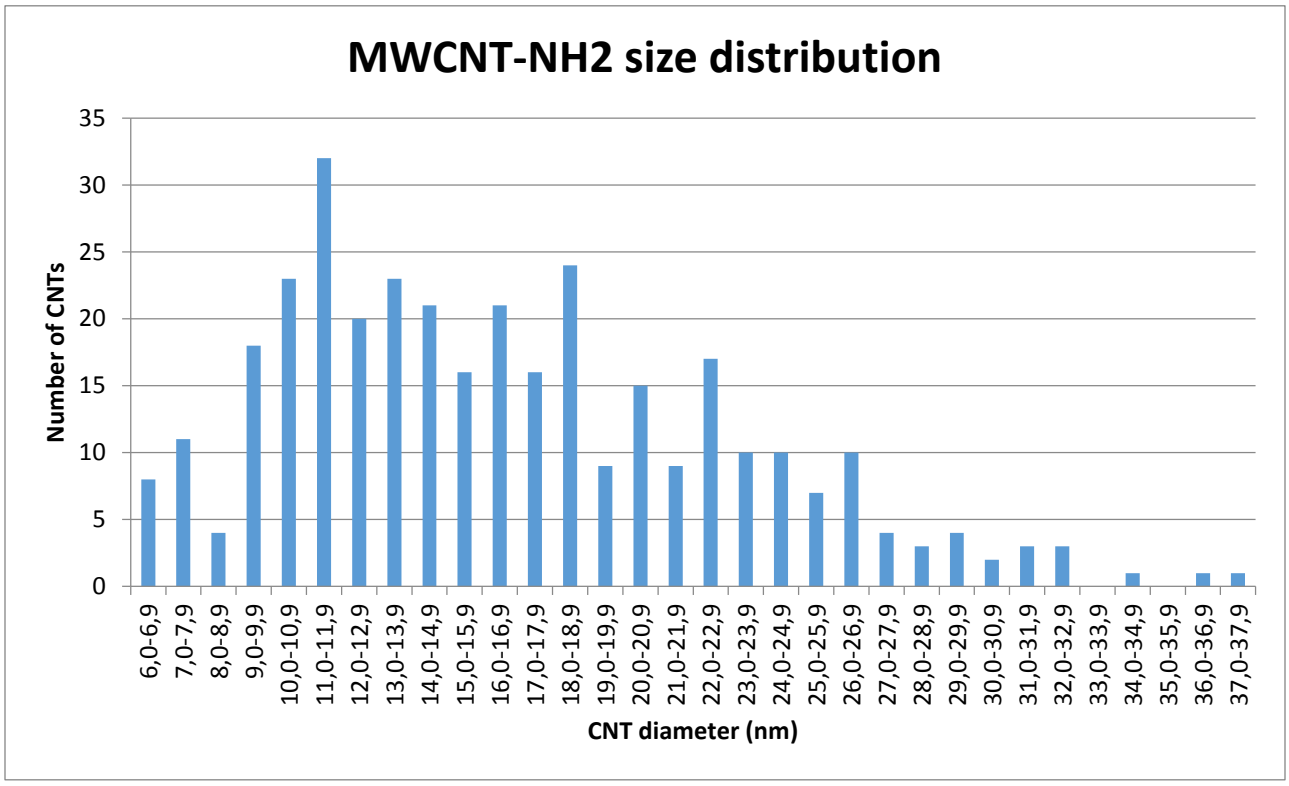

SWCNT	
Nr counted	59
Average diameter (nm)	2.4
Std.av	1.1
Rel. Std.av	45.6
Max (nm)	8.3
Min (nm)	0.9
Median (nm)	2.1

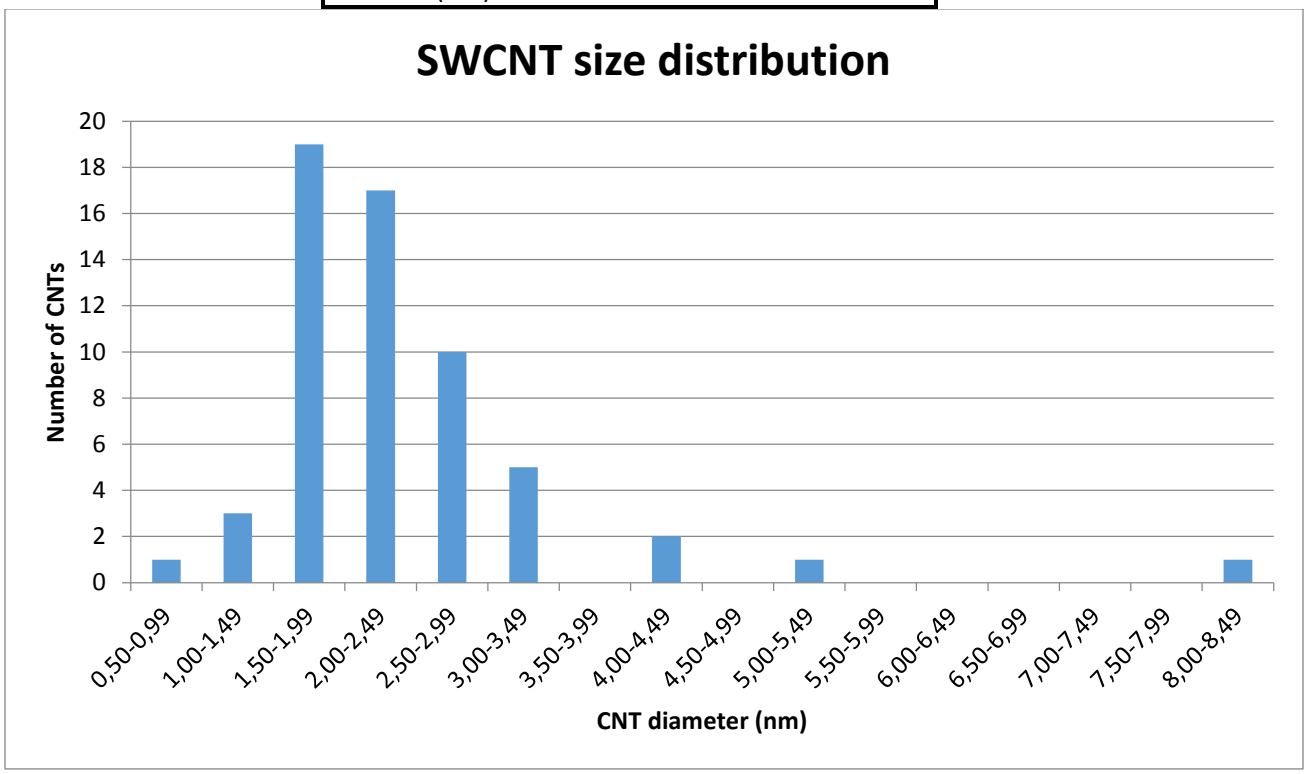

TEM images

SWCNTs

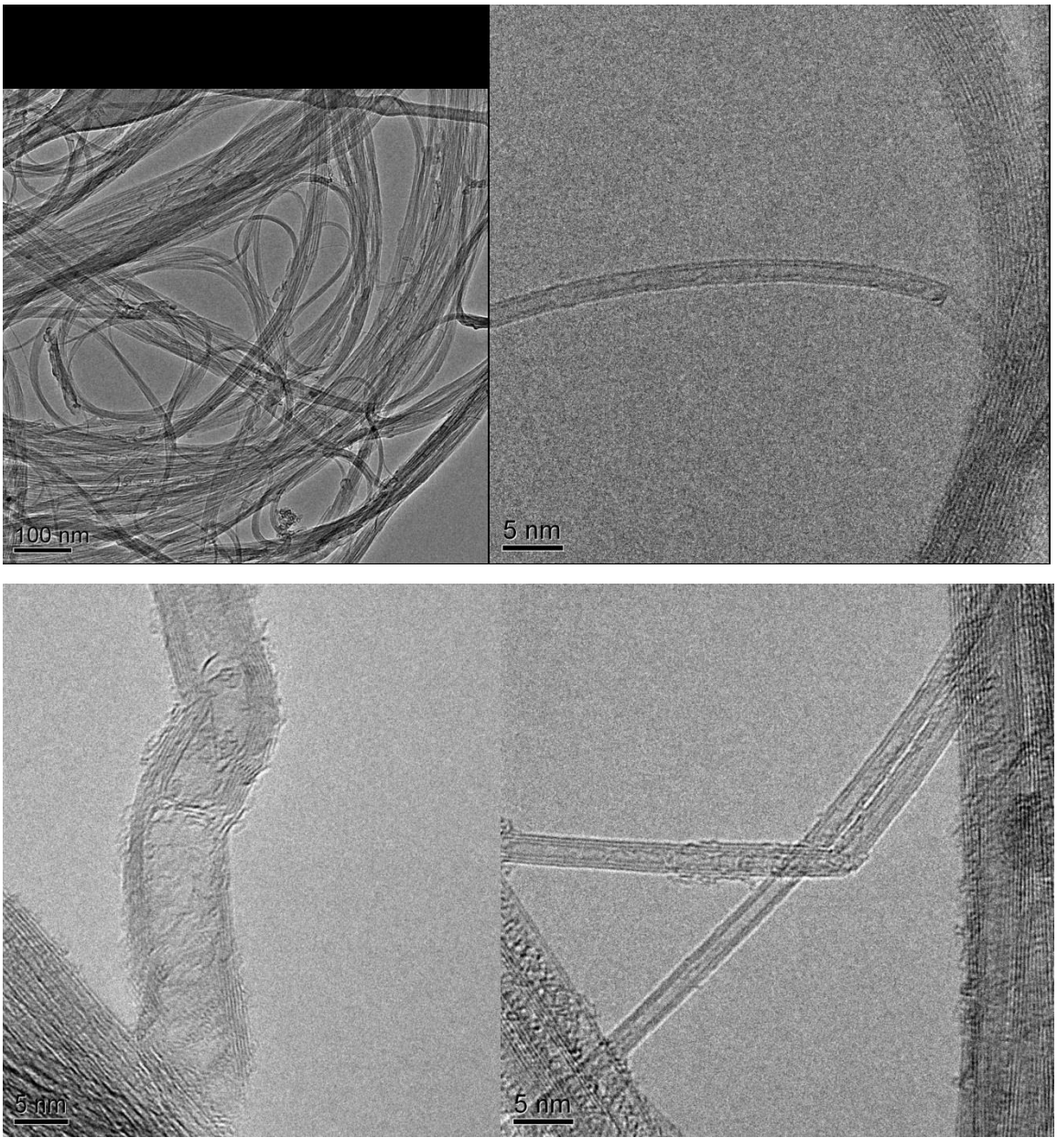

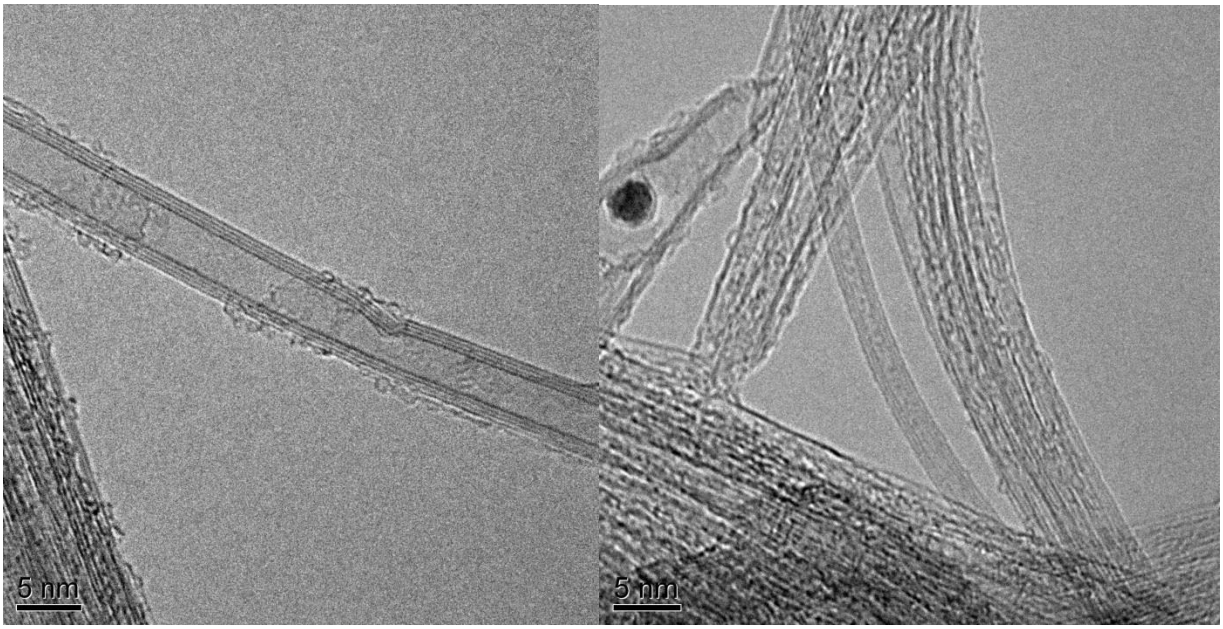
5 nm
5 nm

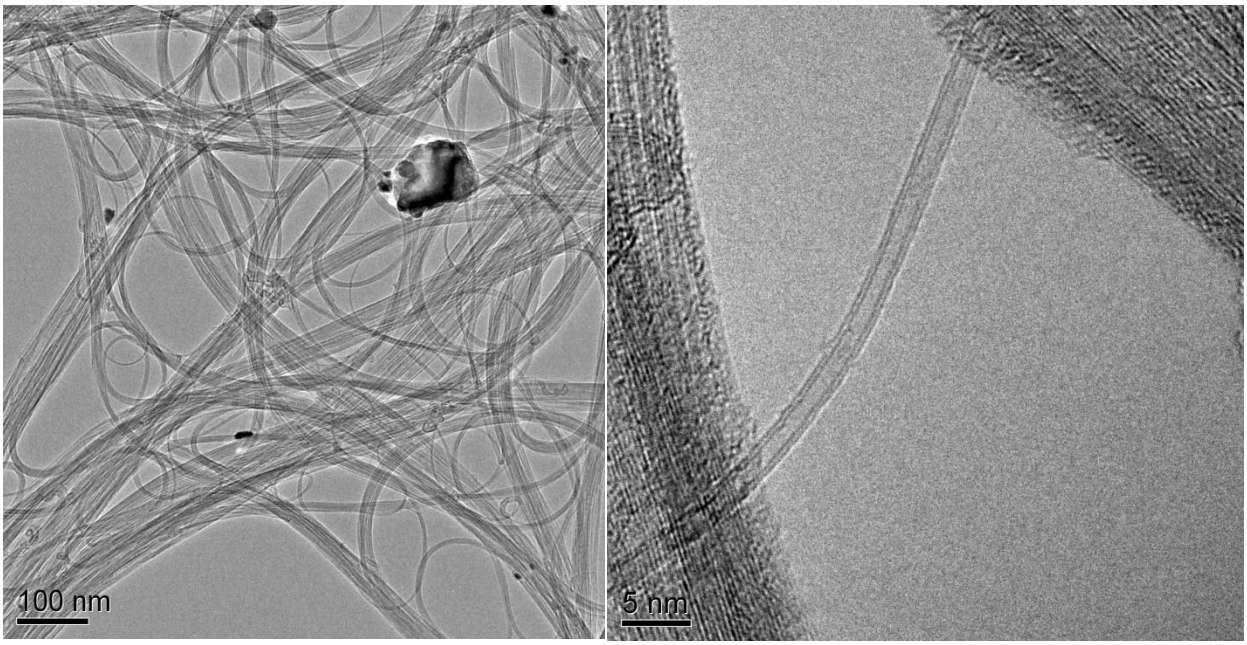
100 nm
5 nm

MWCNTs-1

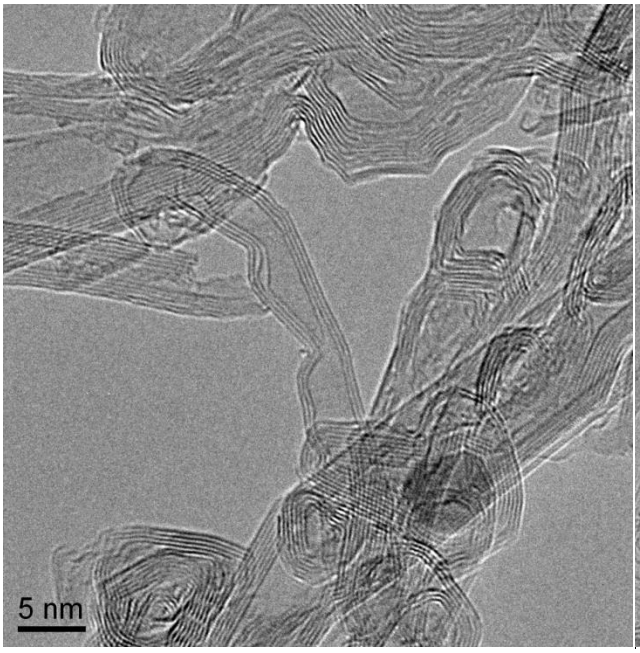

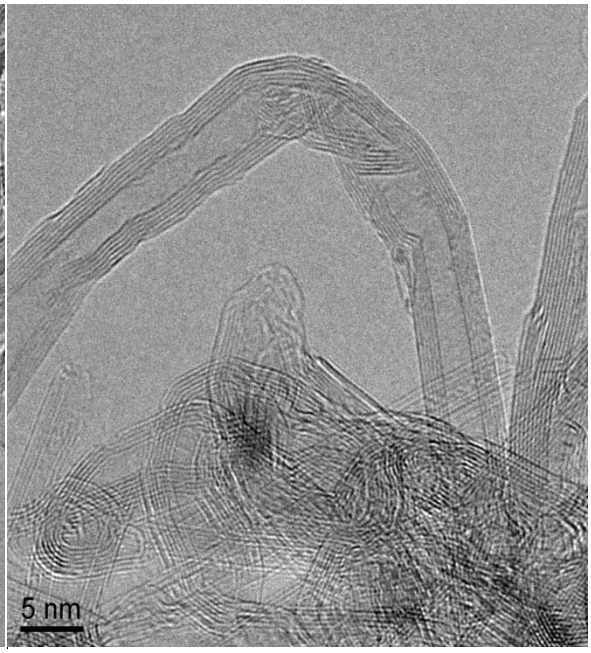

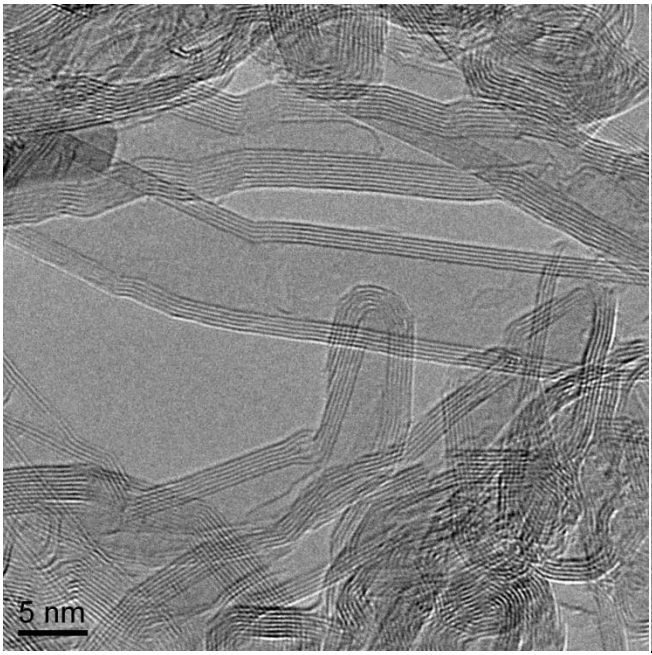

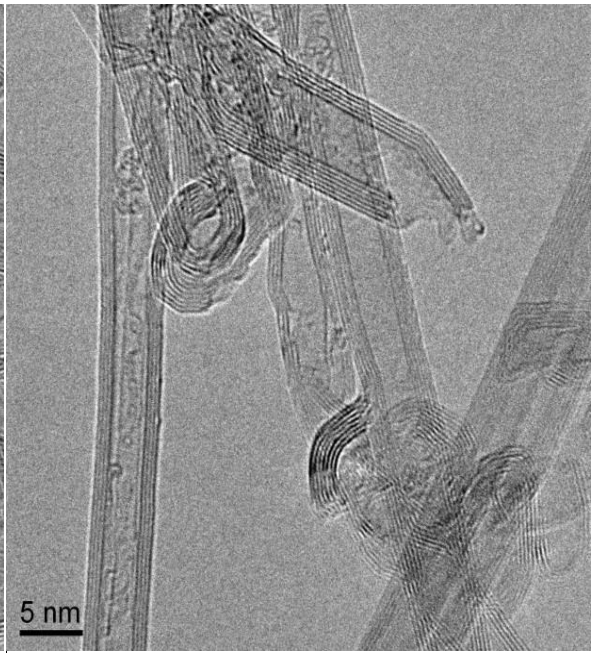

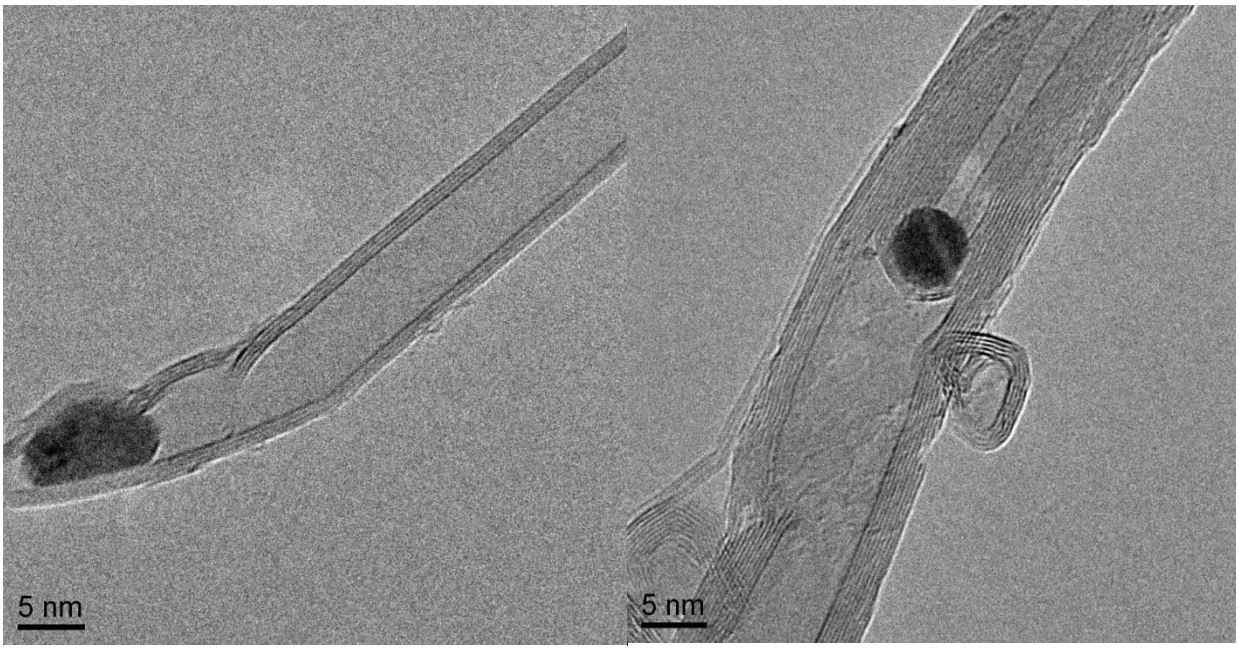

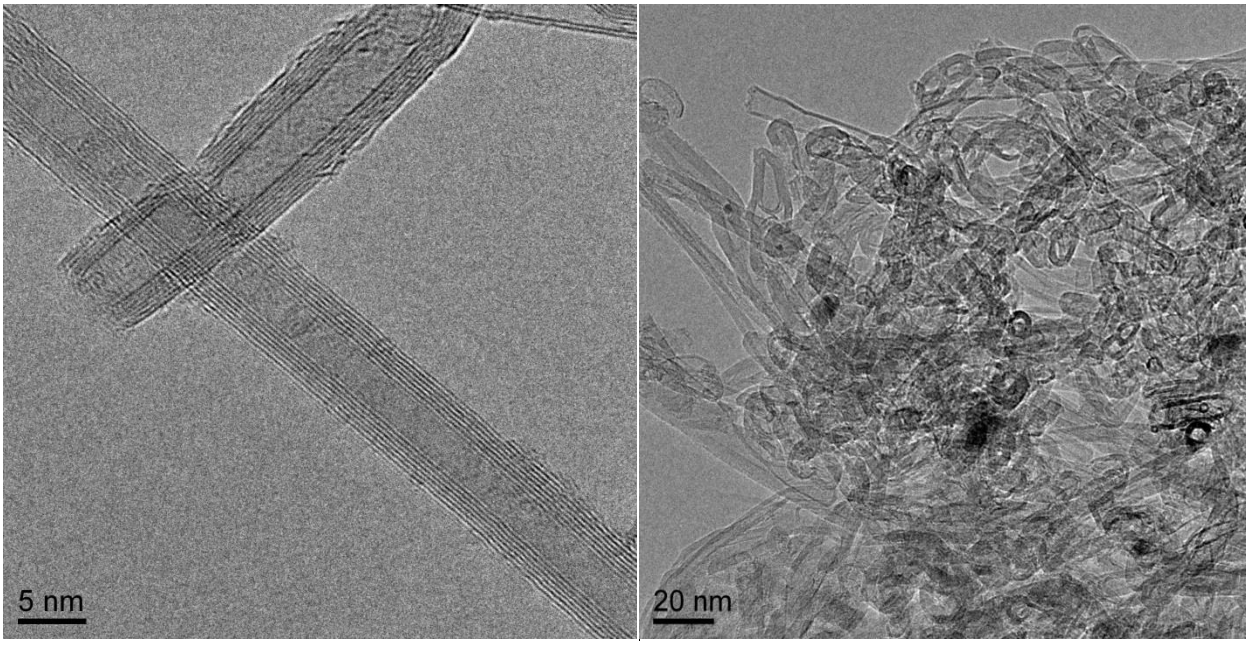

7 walled CNT in MWCNT-1 sample

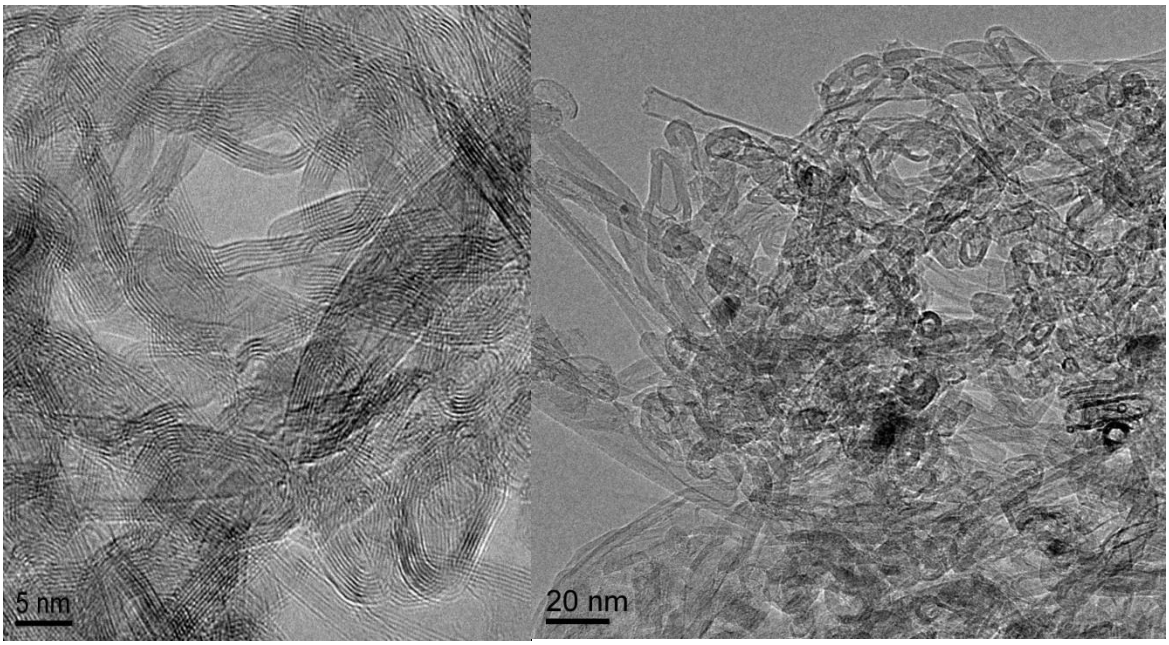
5 nm
20 nm

MWCNTs-2

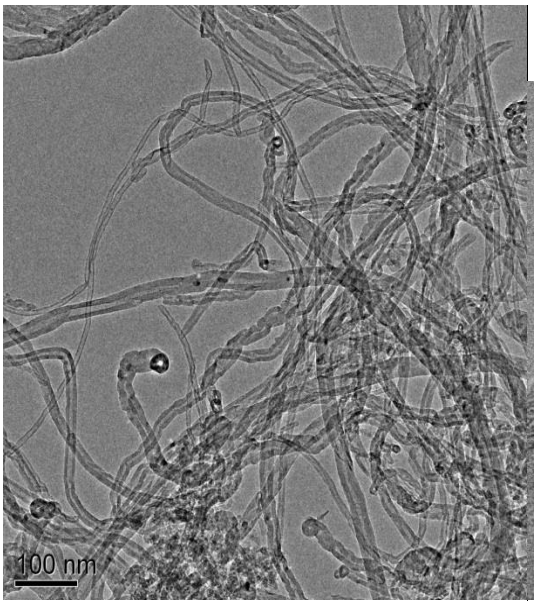

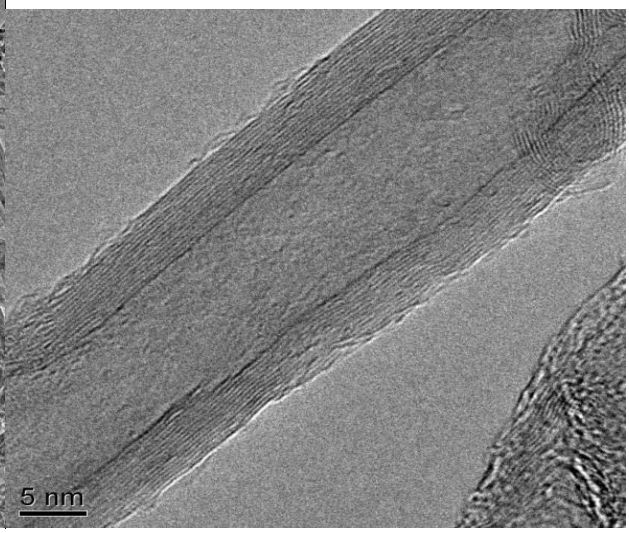

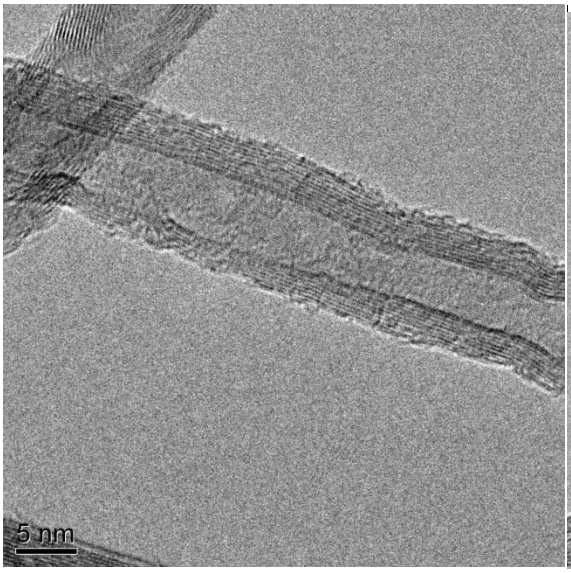

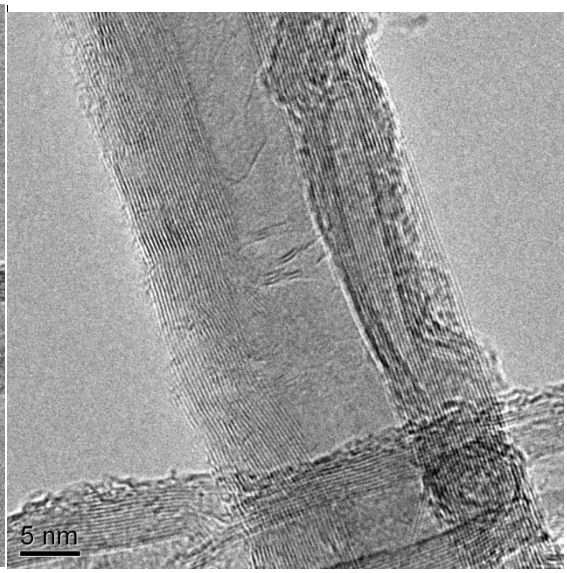

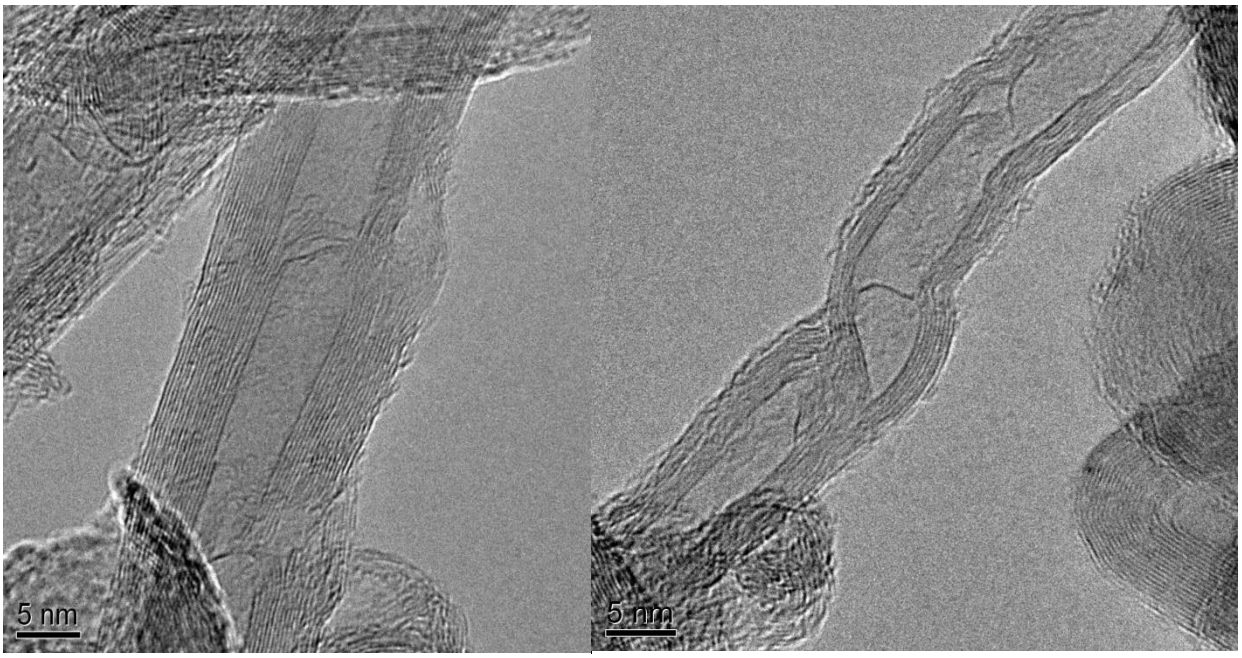
5 nm
5 nm

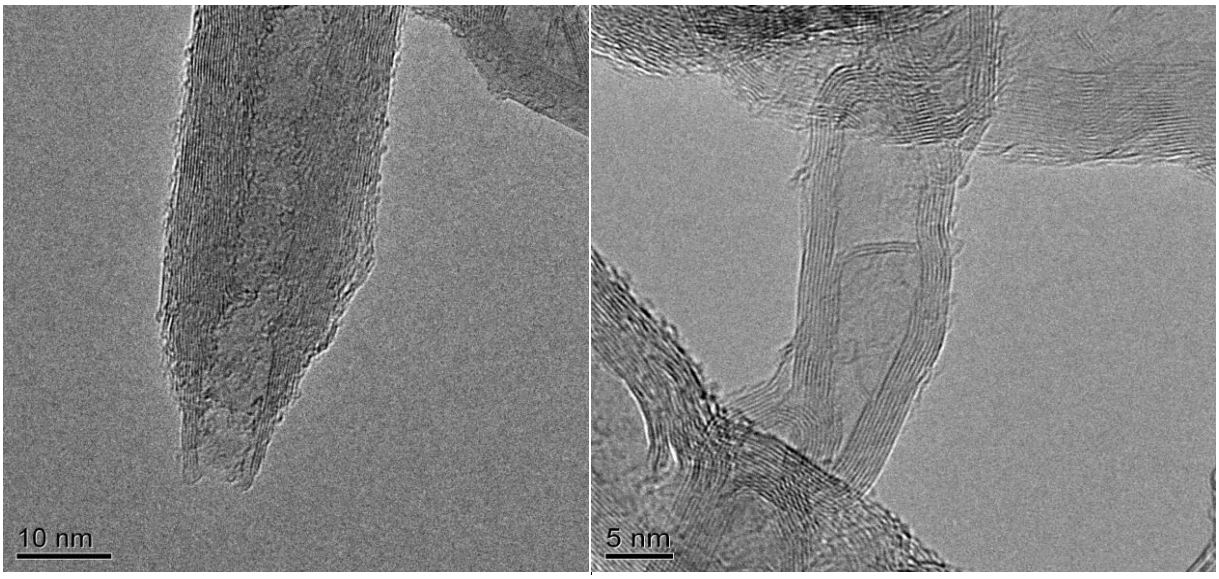
10 nm
5 nm

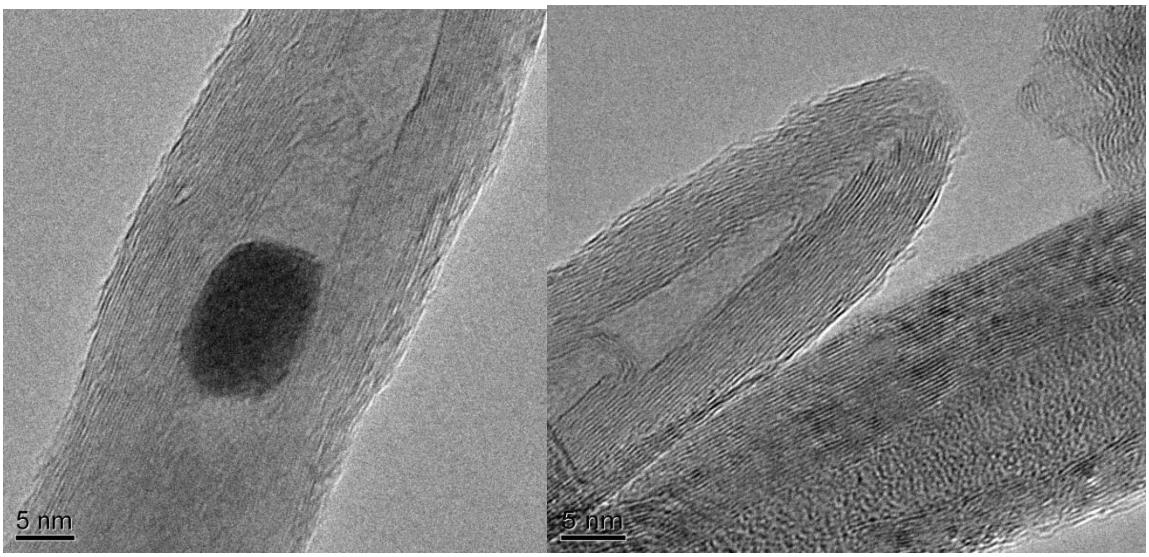
5 nm
5 nm

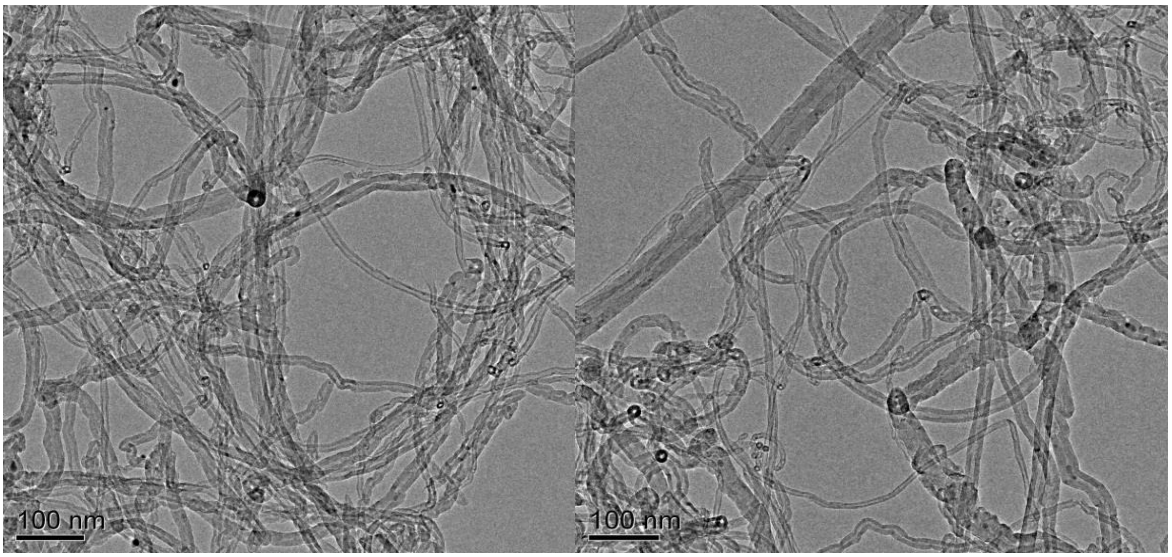
100 nm
100 nm

MWCNTs-3

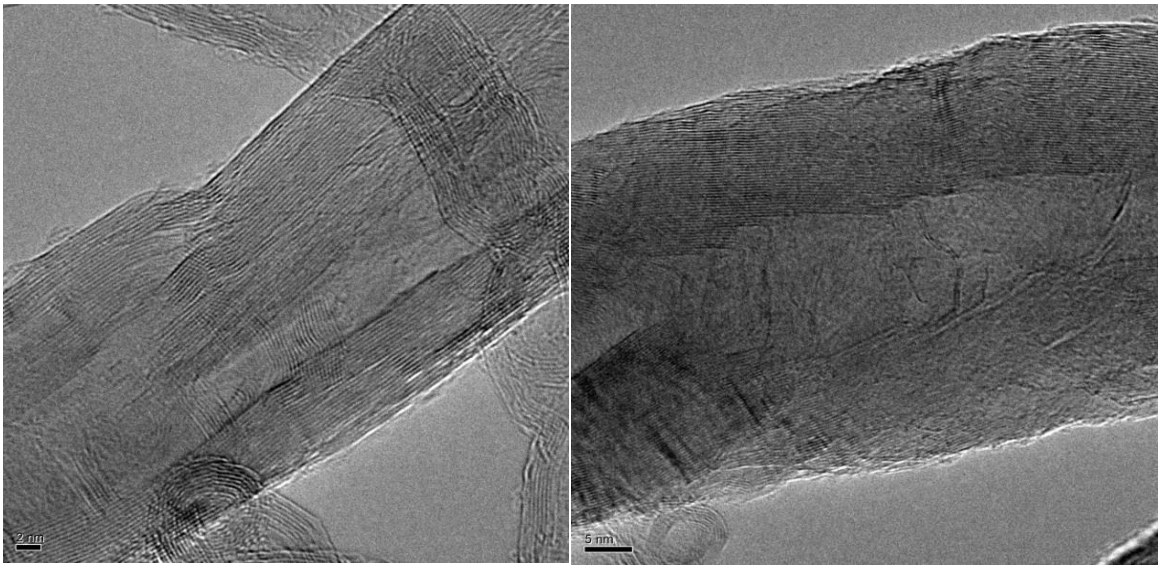

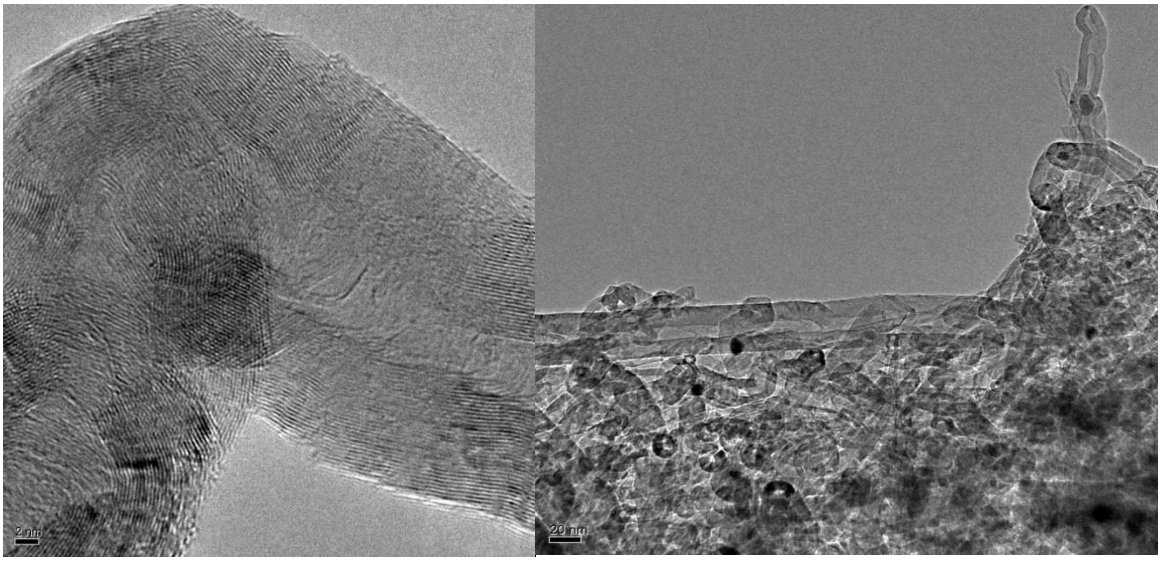

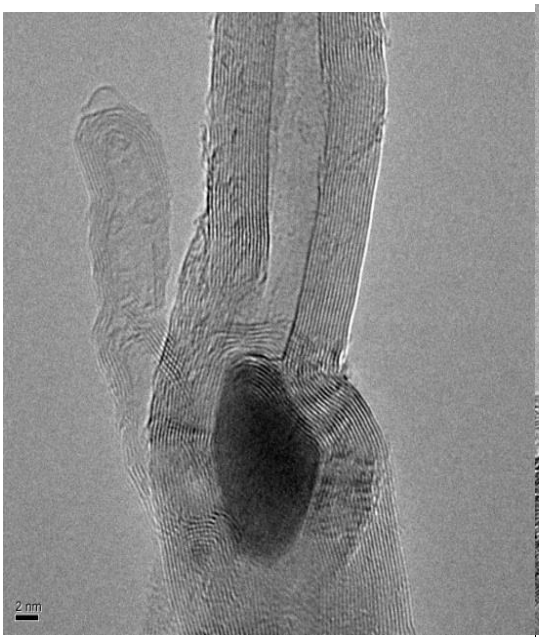
2 nm

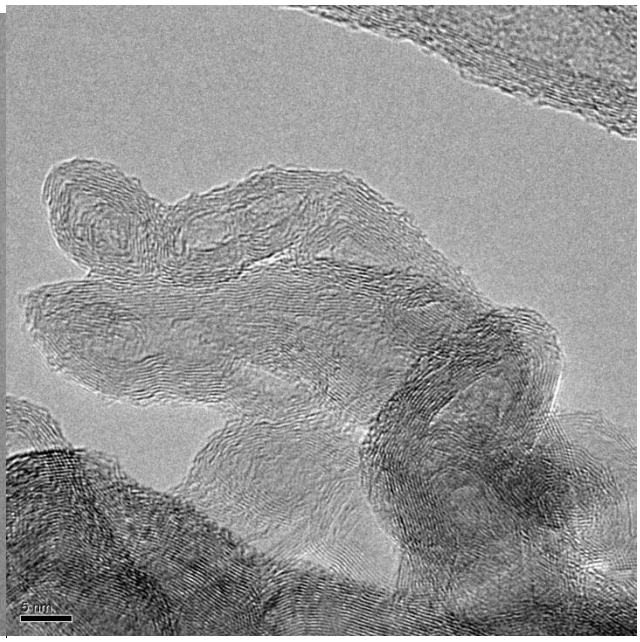
5 nm


50 nm

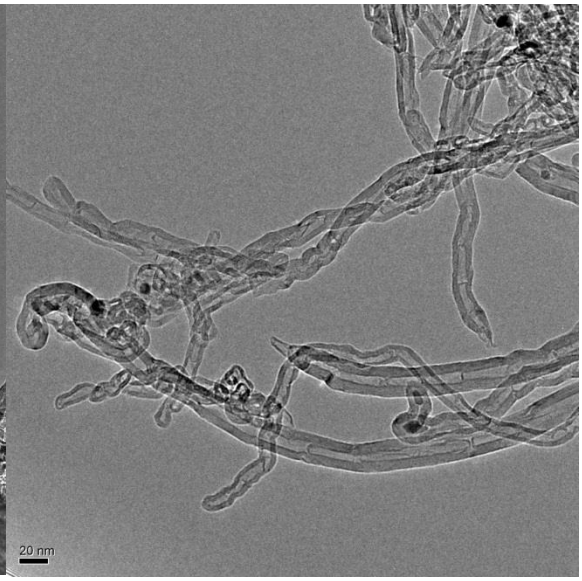
20 nm

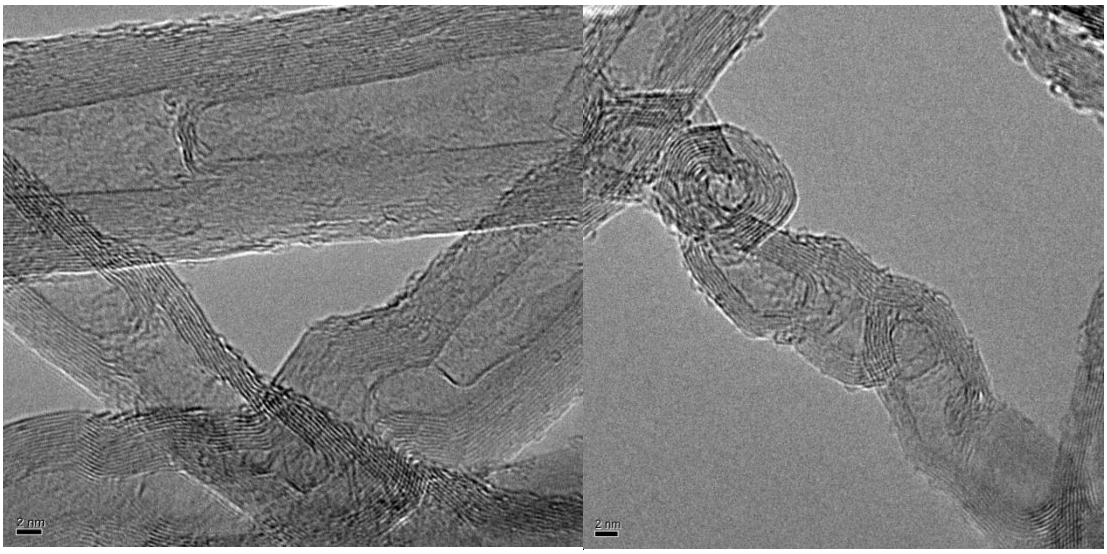
2 nm
2 nm

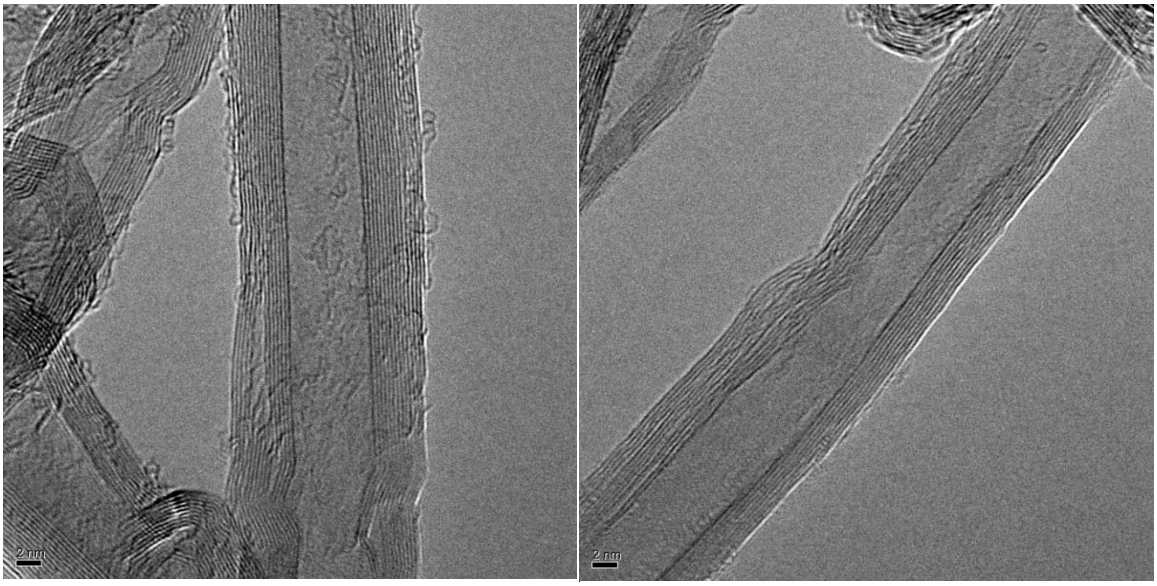
2 nm
2 nm

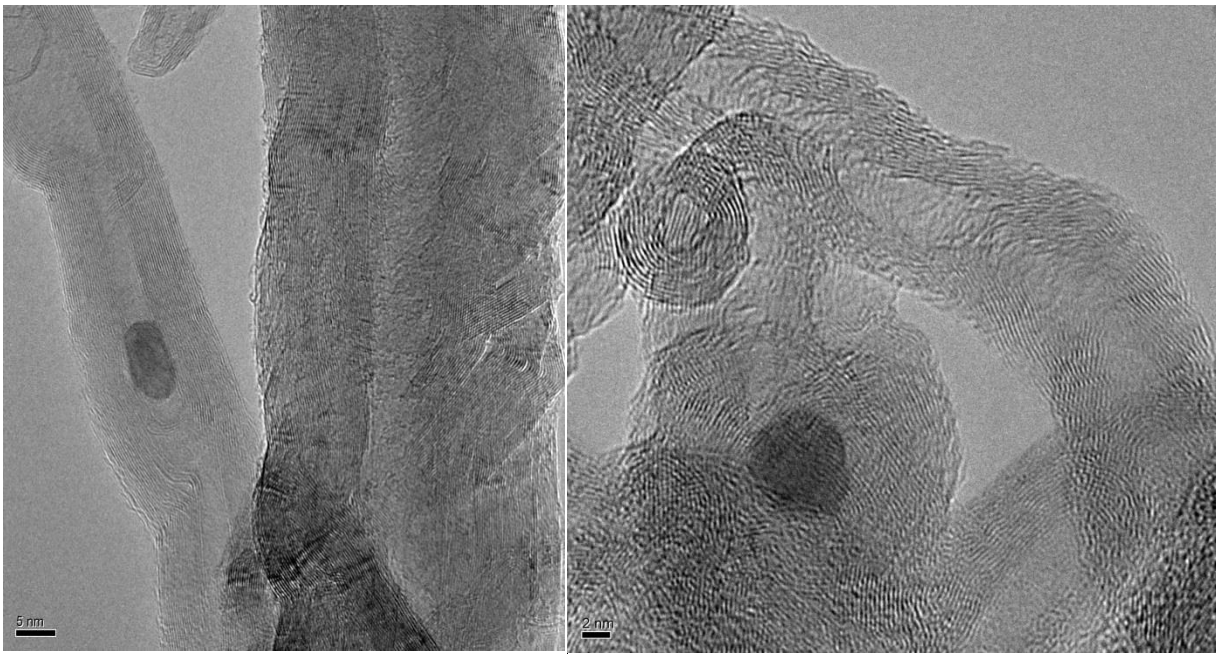
5 nm
2 nm

MWCNTs-COOH

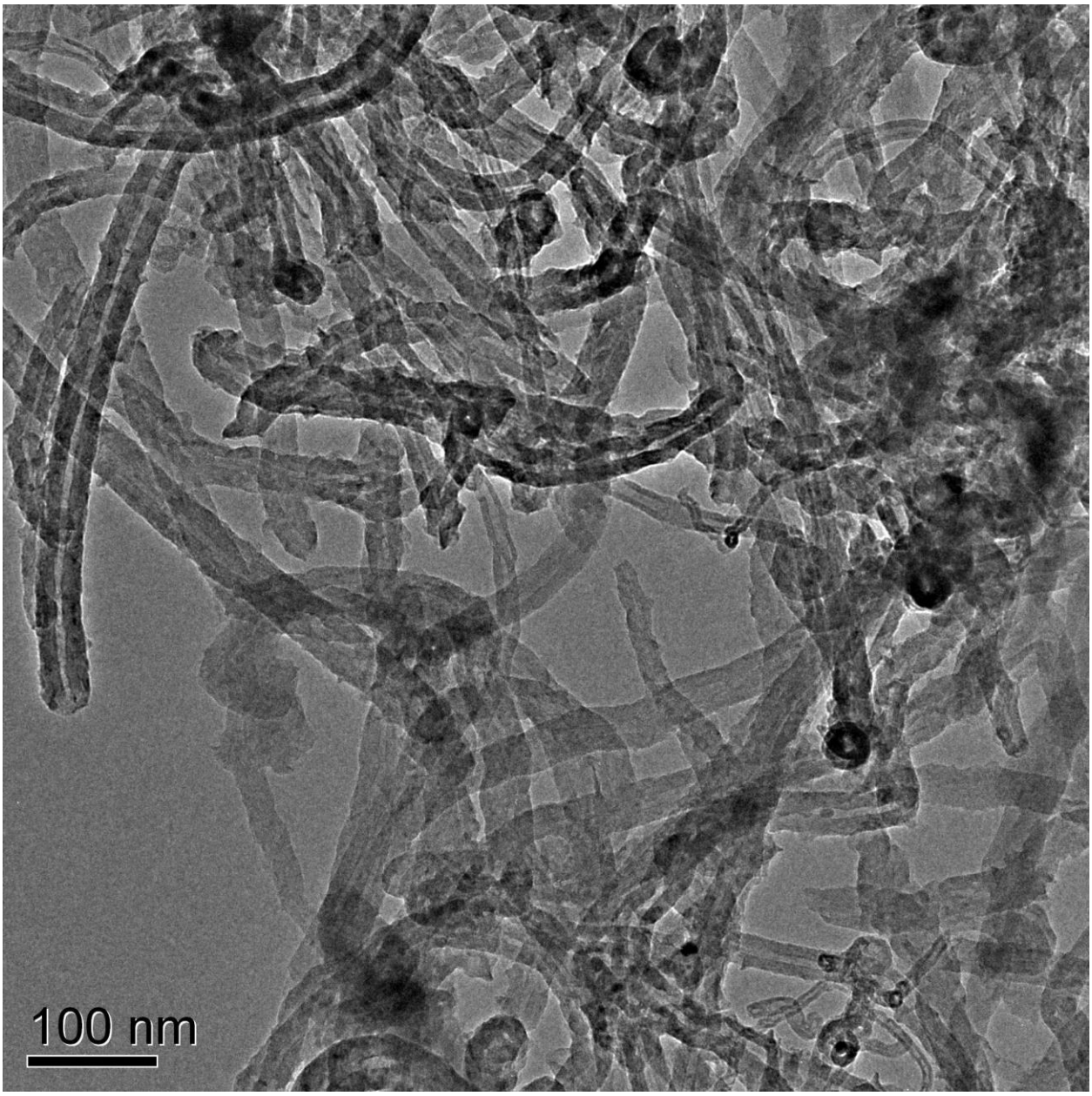

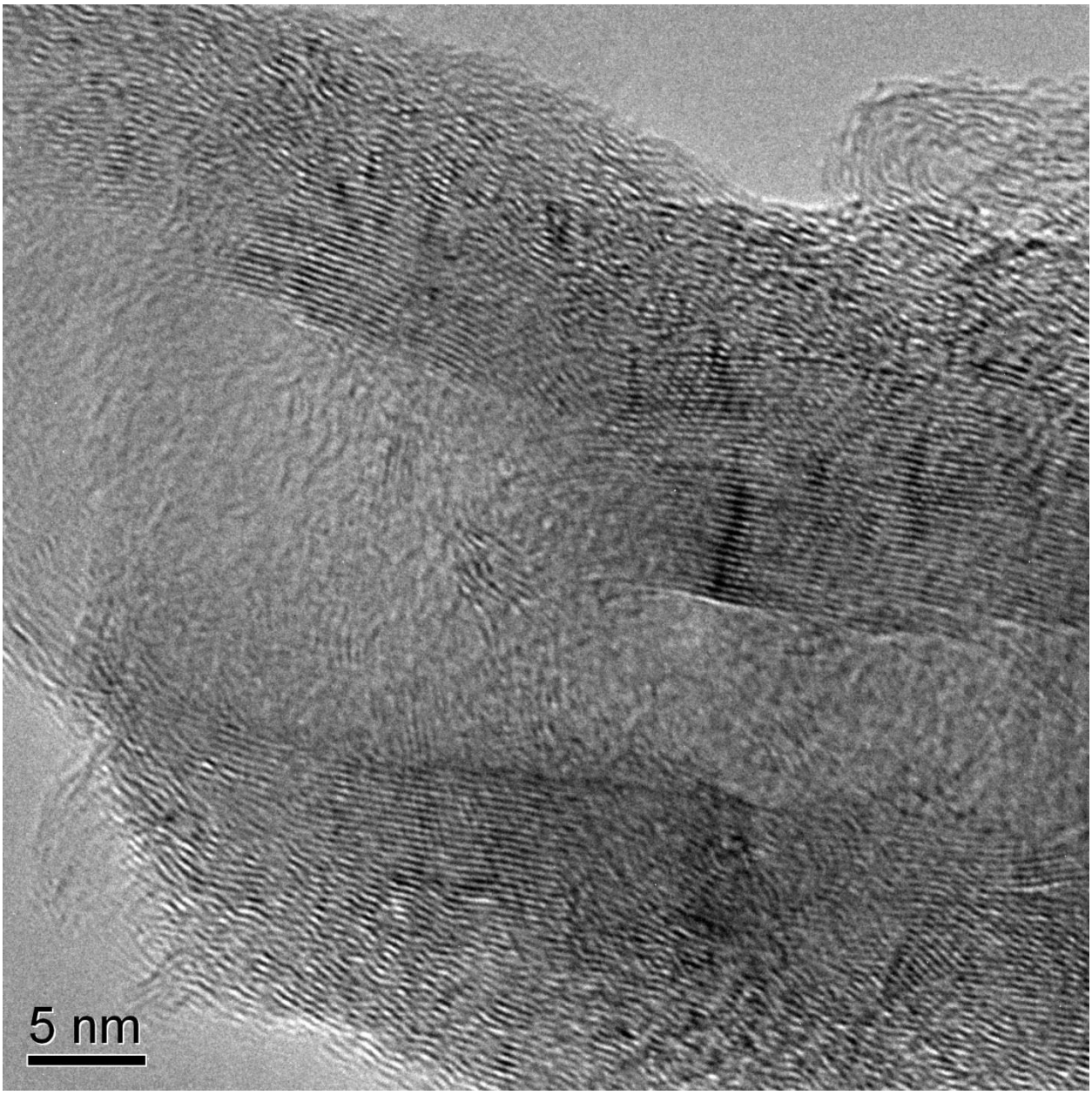
5 nm

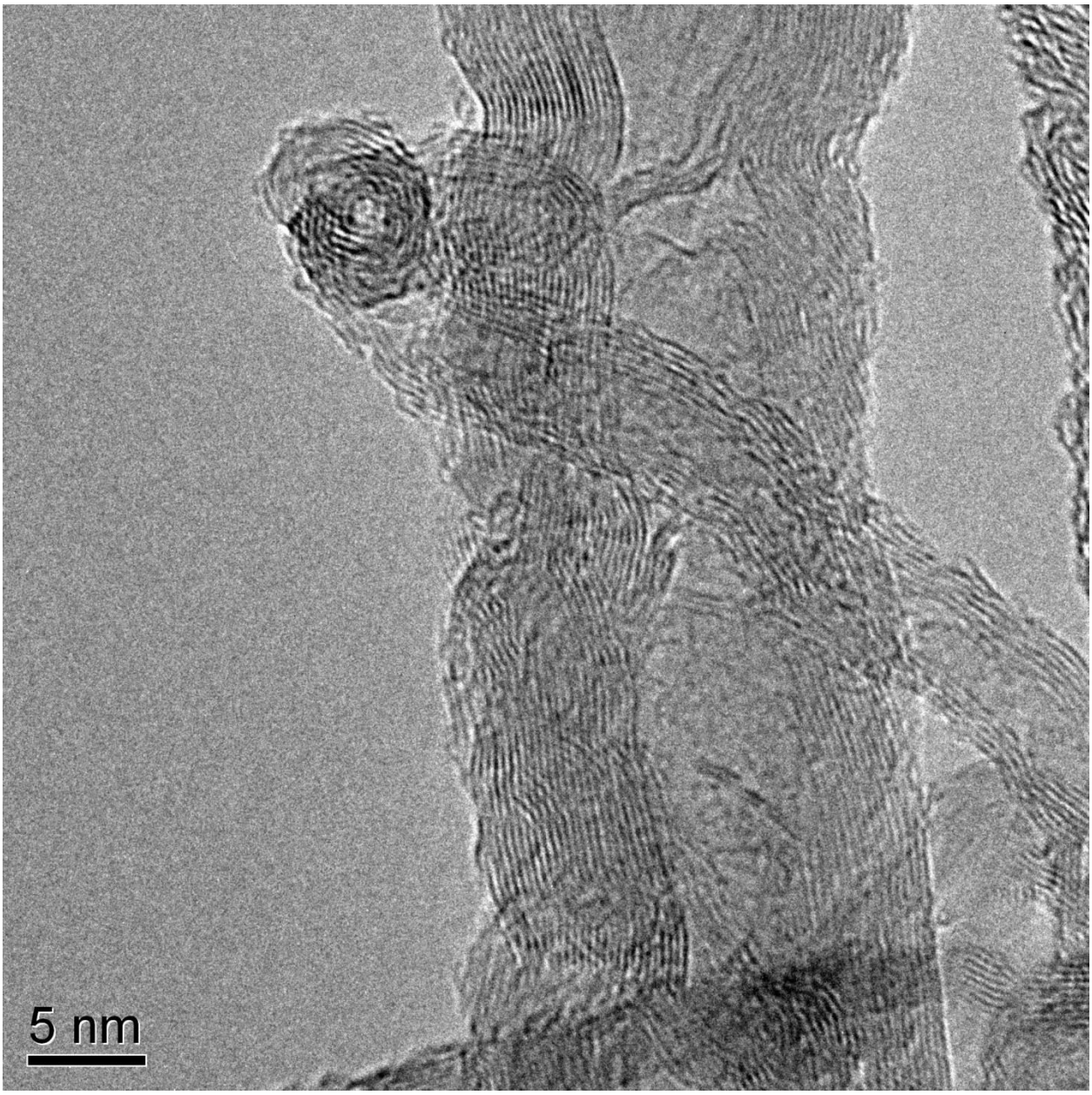
5 nm

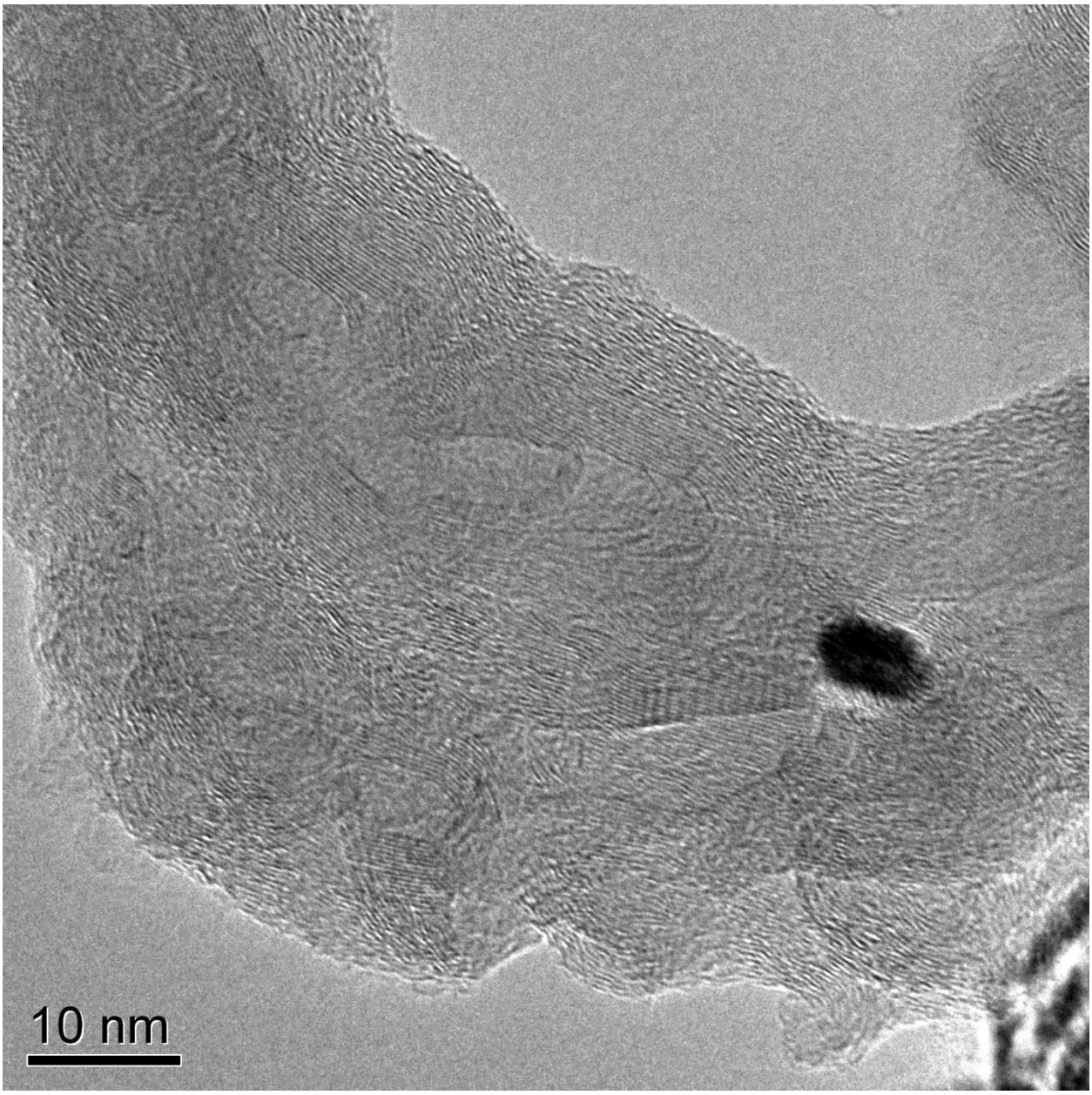
10 nm

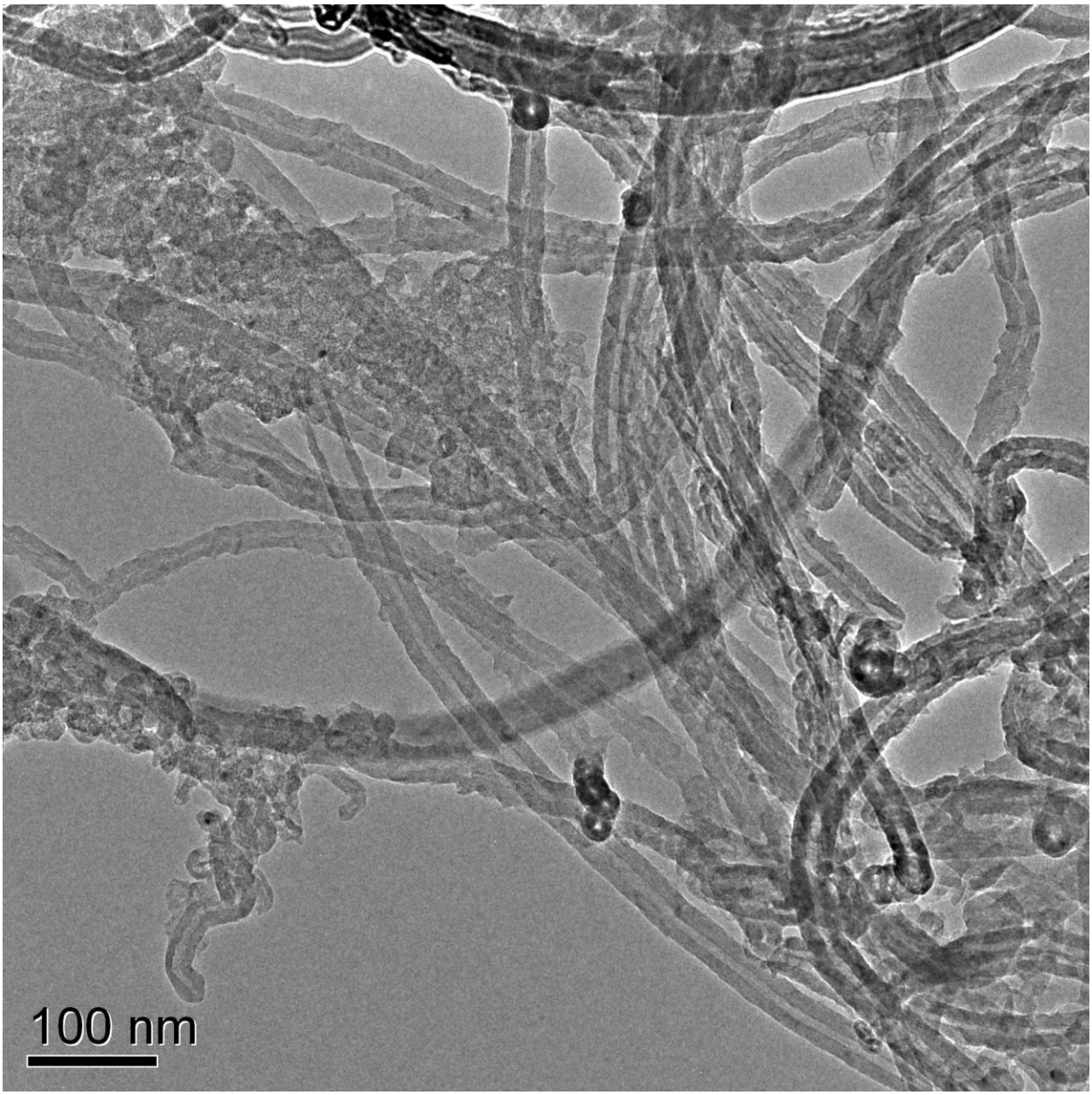
100 nm

MWCNTs-OH

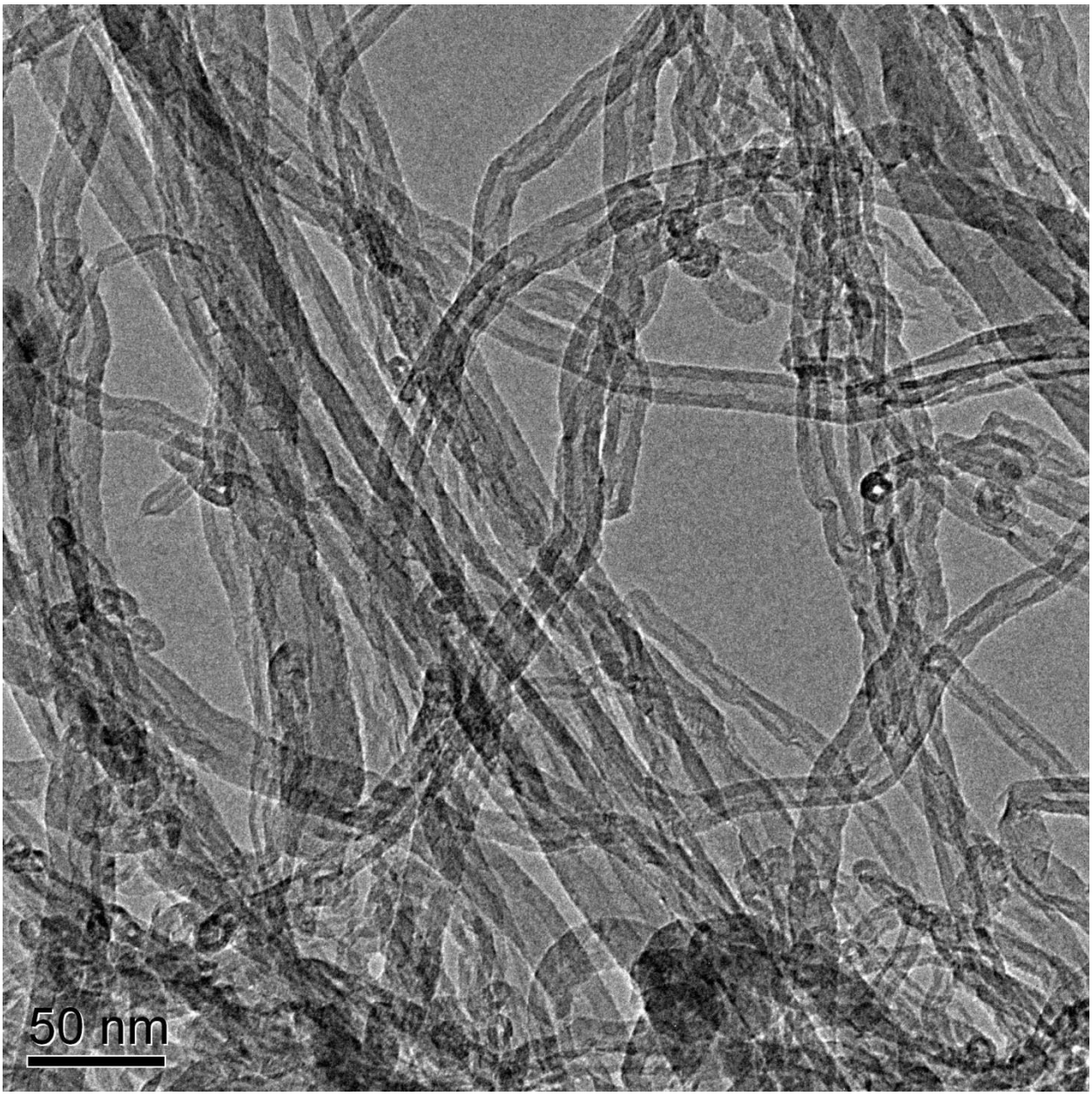

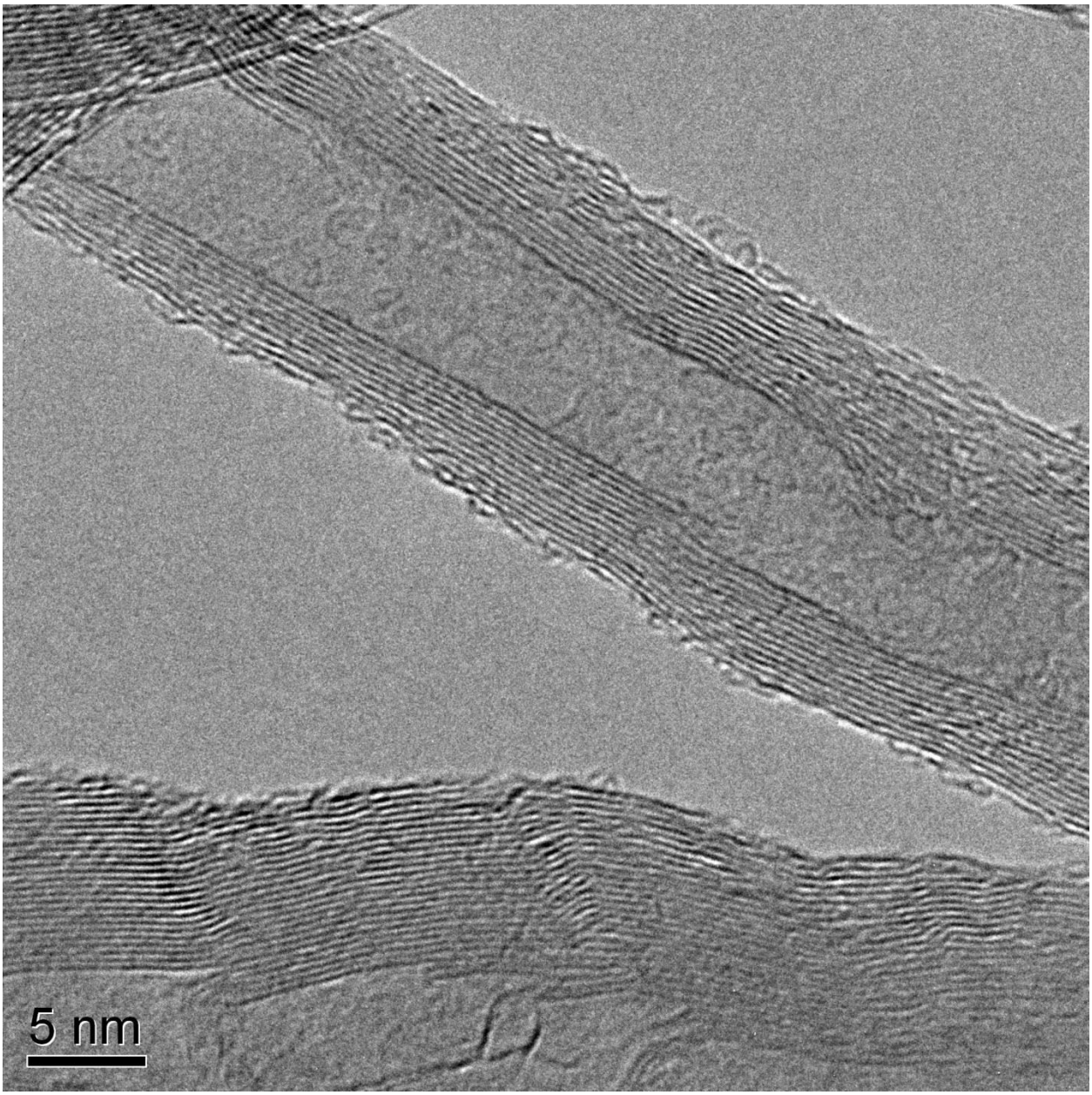
5 nm

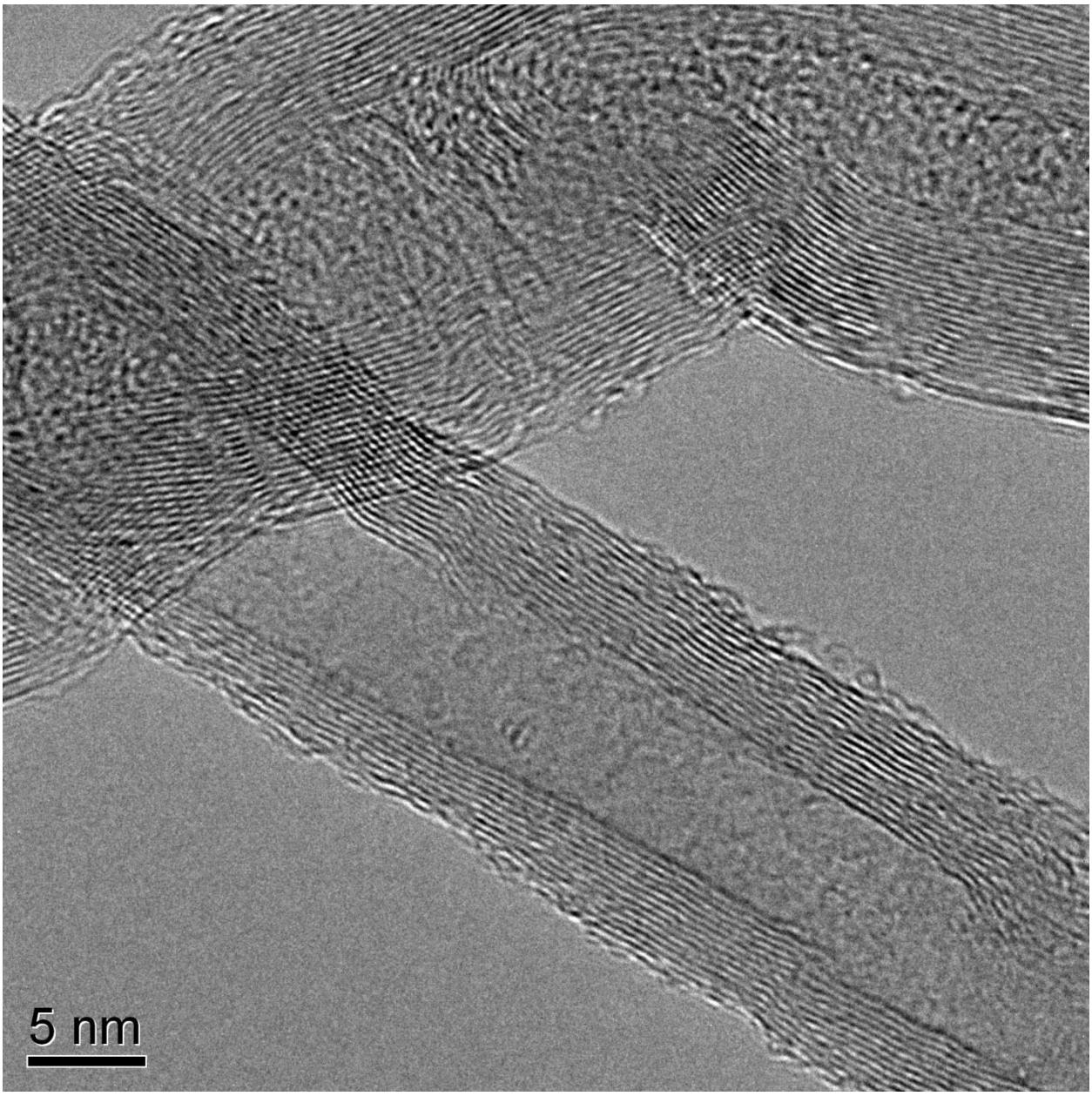
5 nm

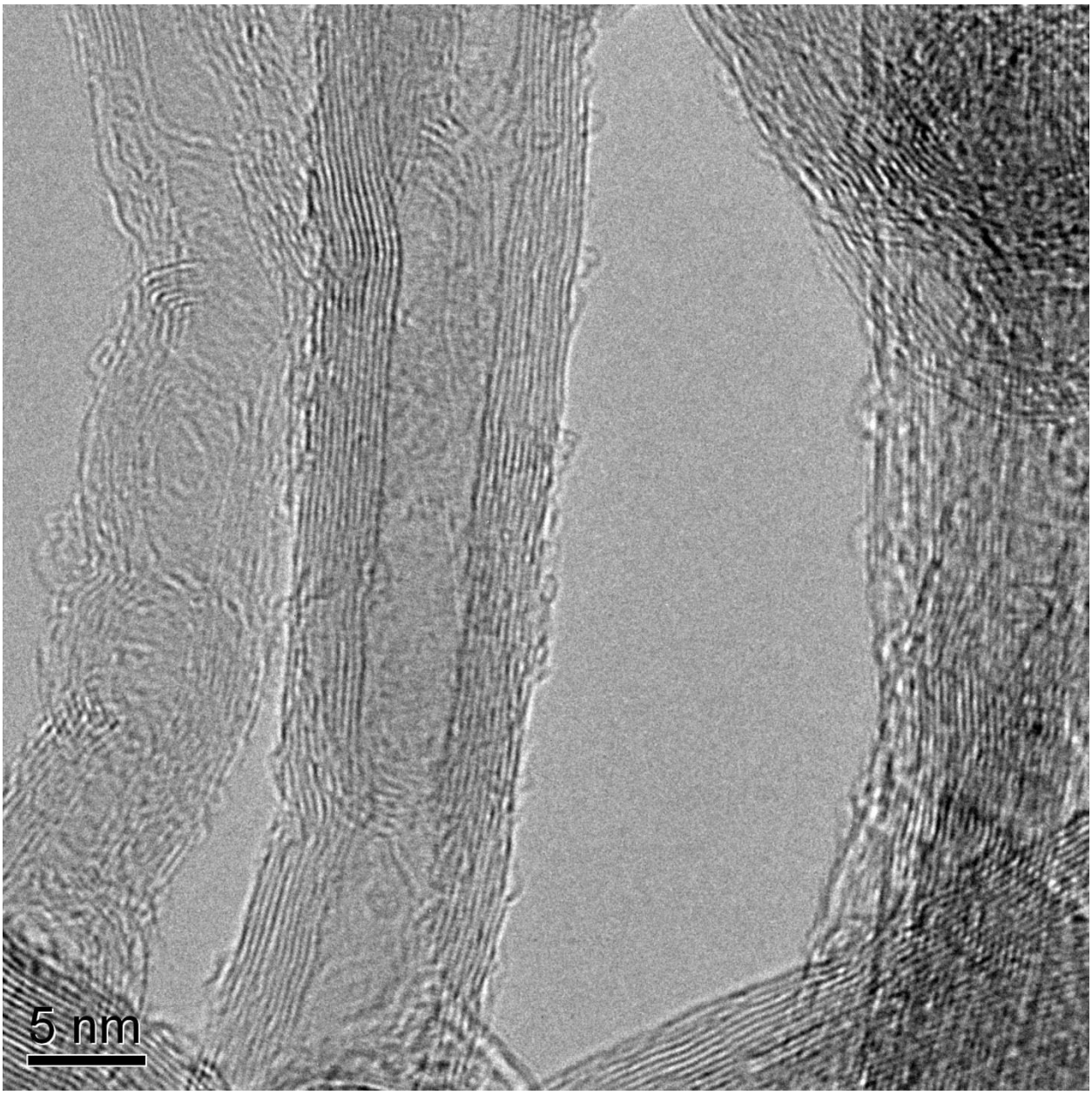
5 nm

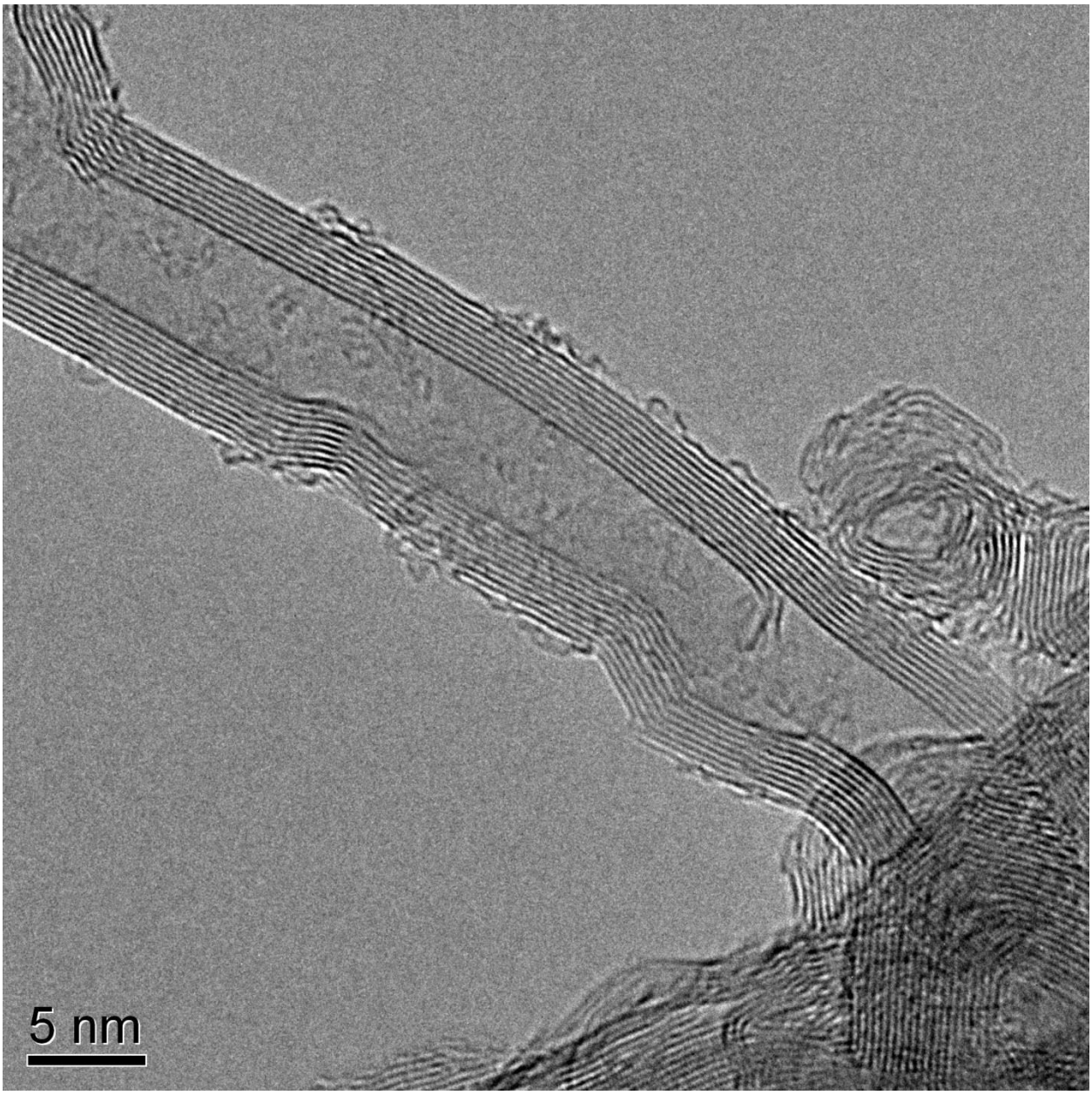
5 nm

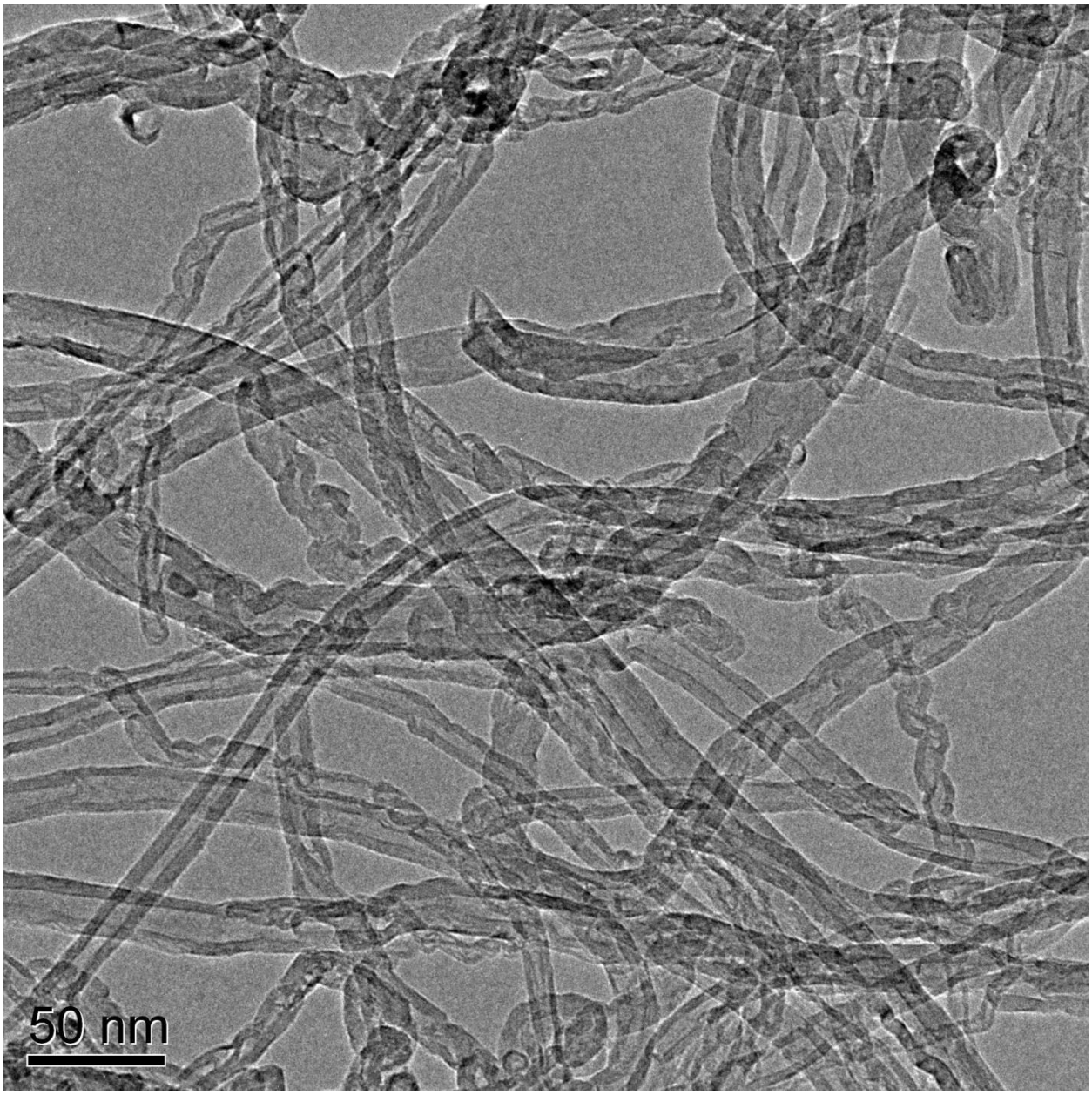
50 nm

MWCNTs-NH2

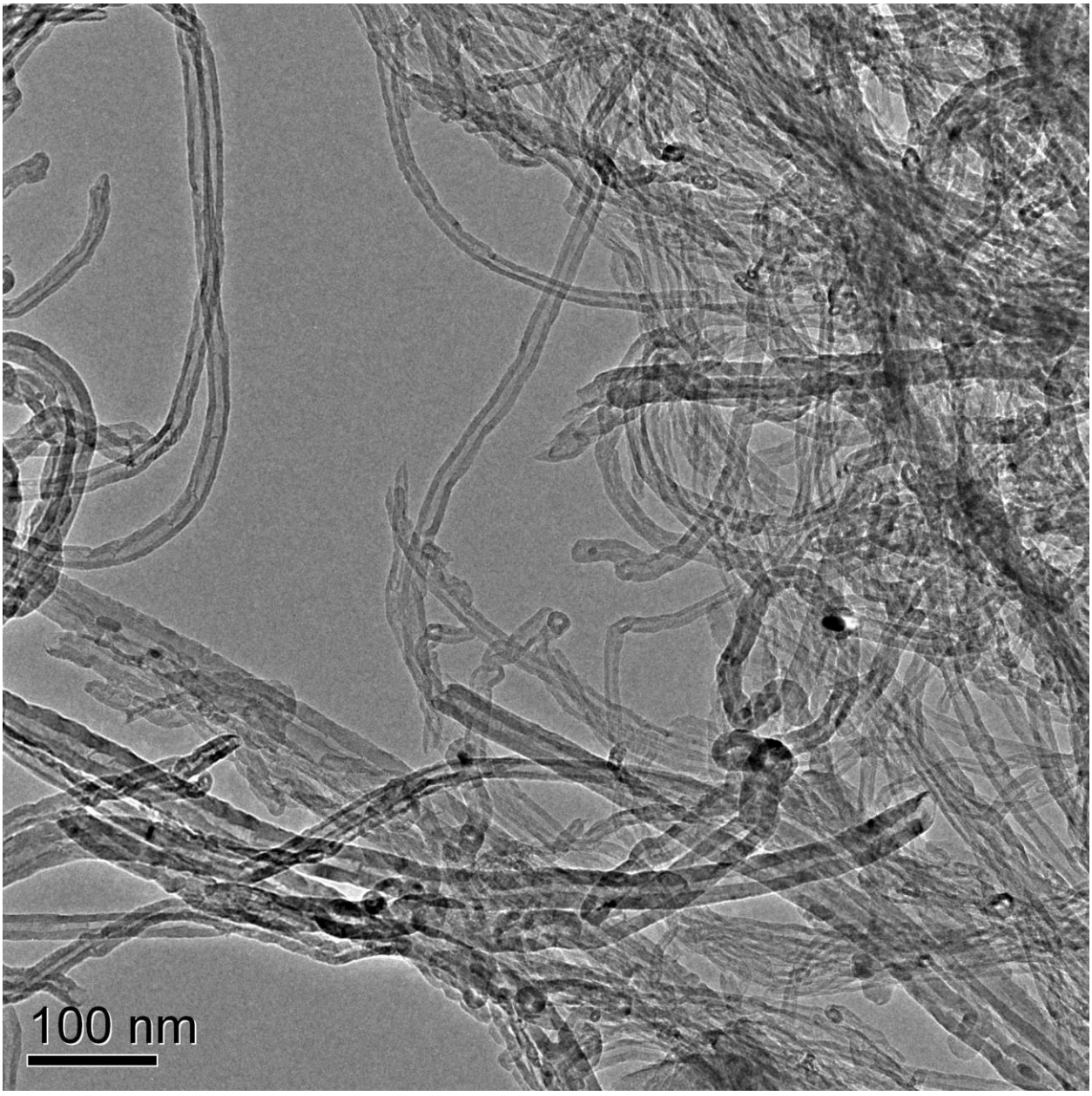

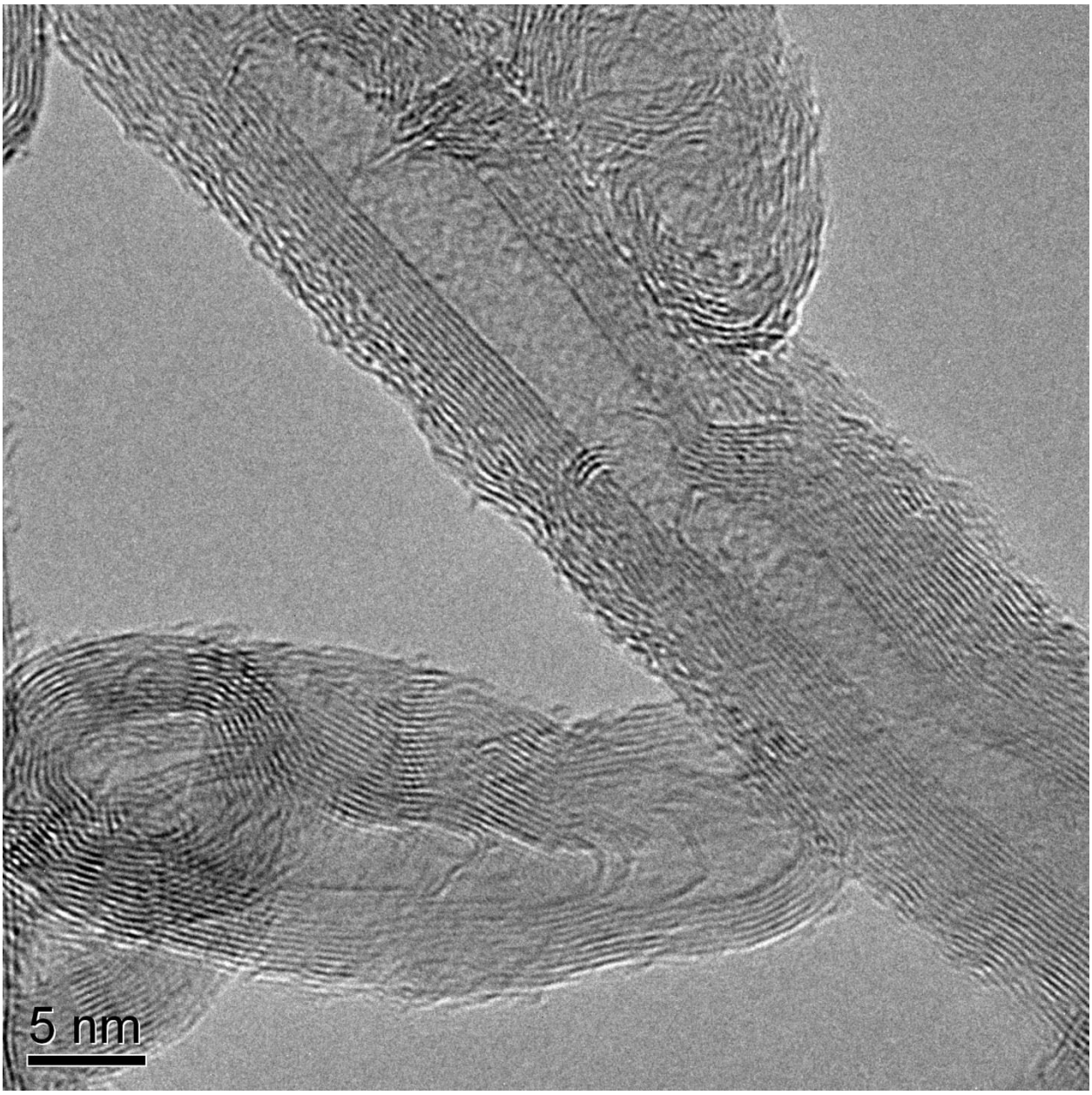
5 nm

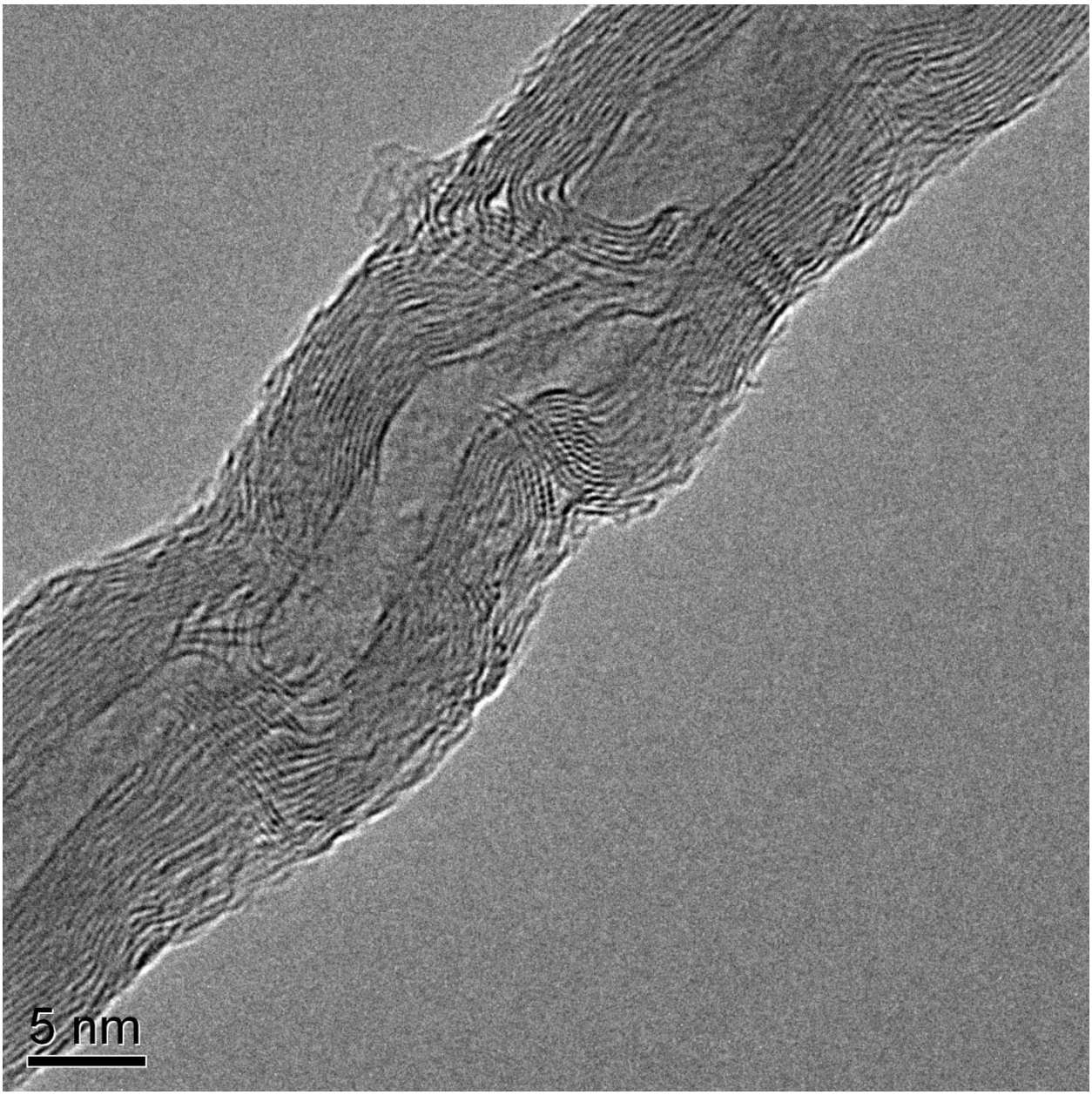
5 nm

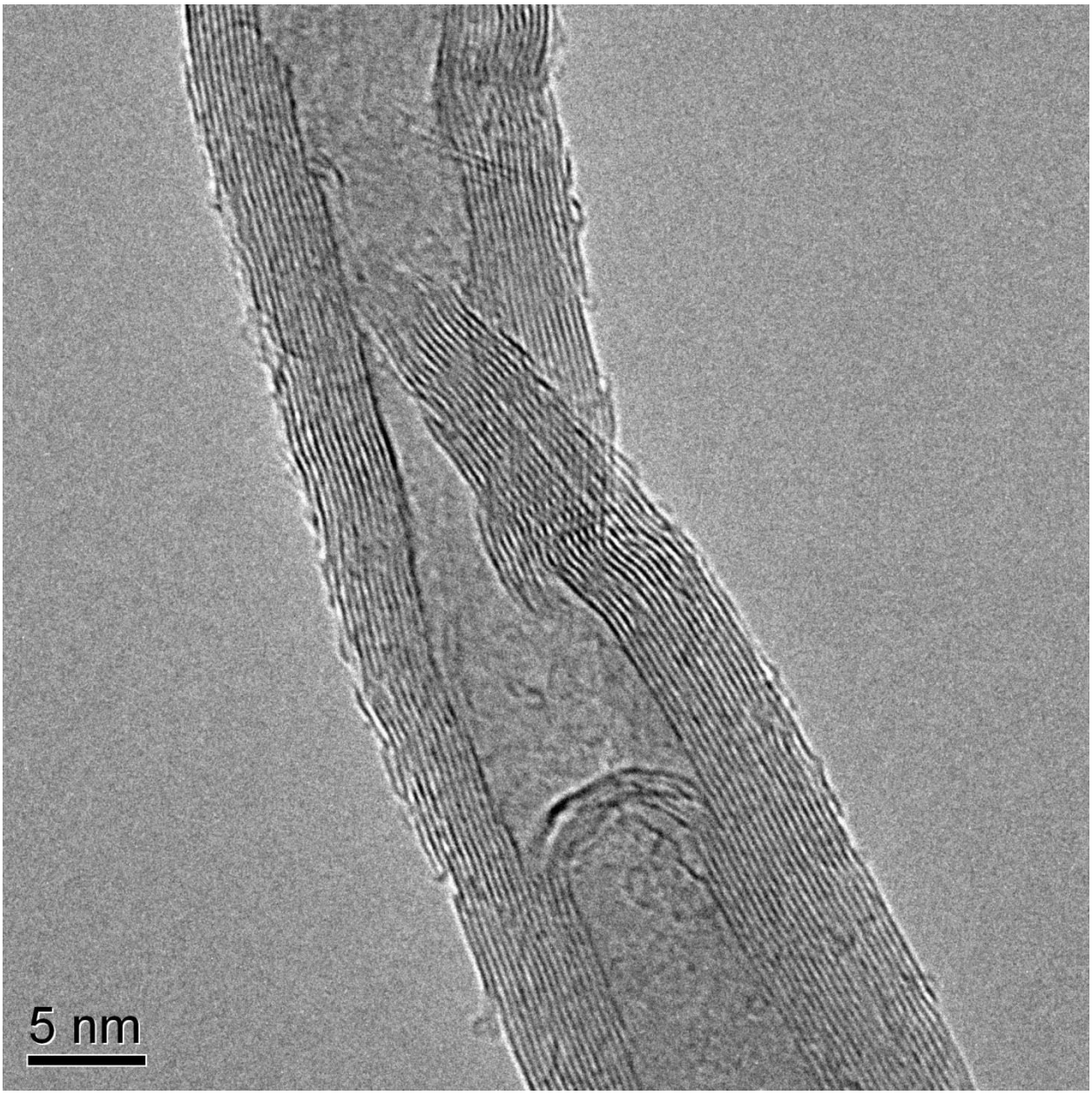
5 nm

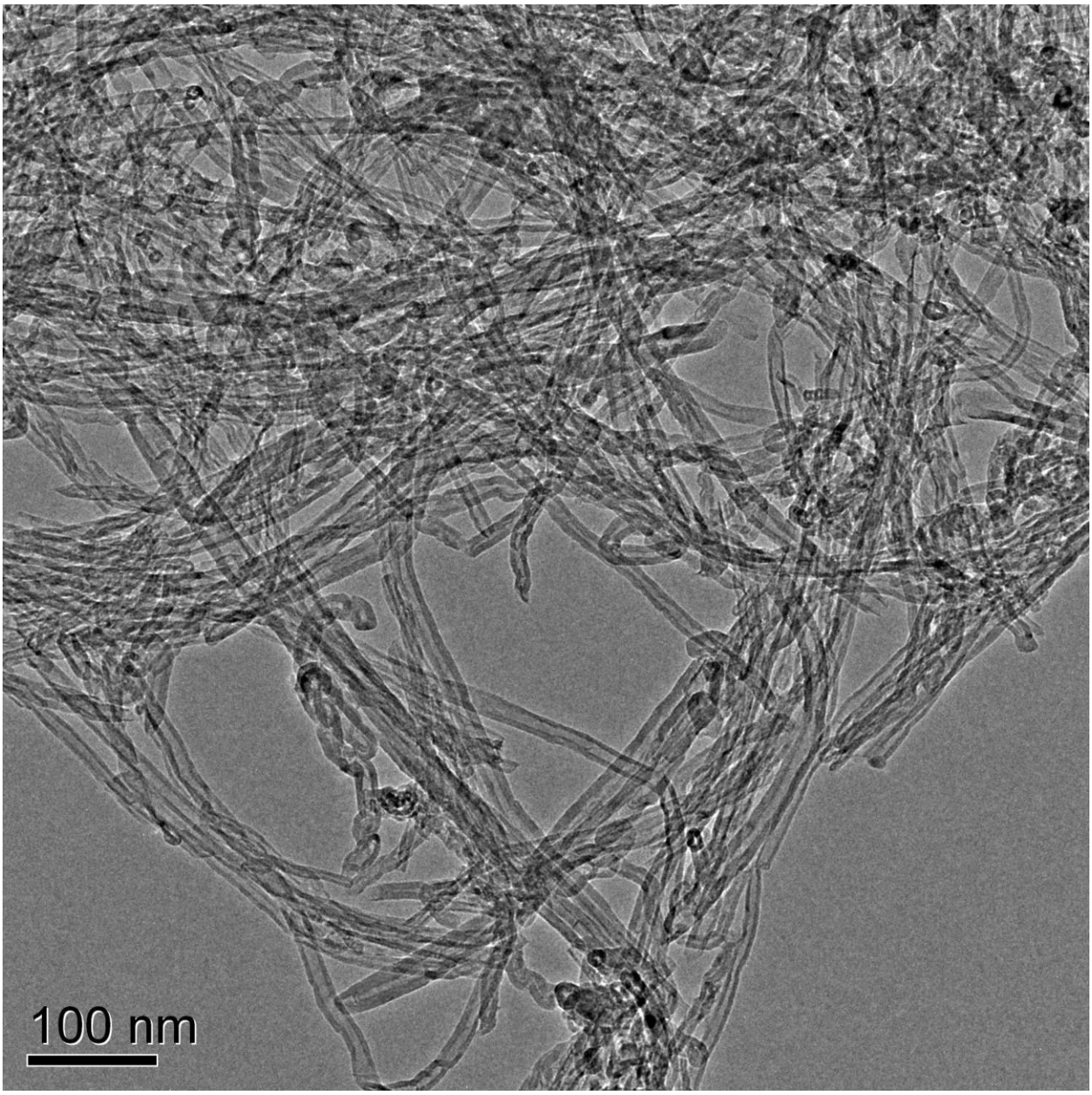
100 nm

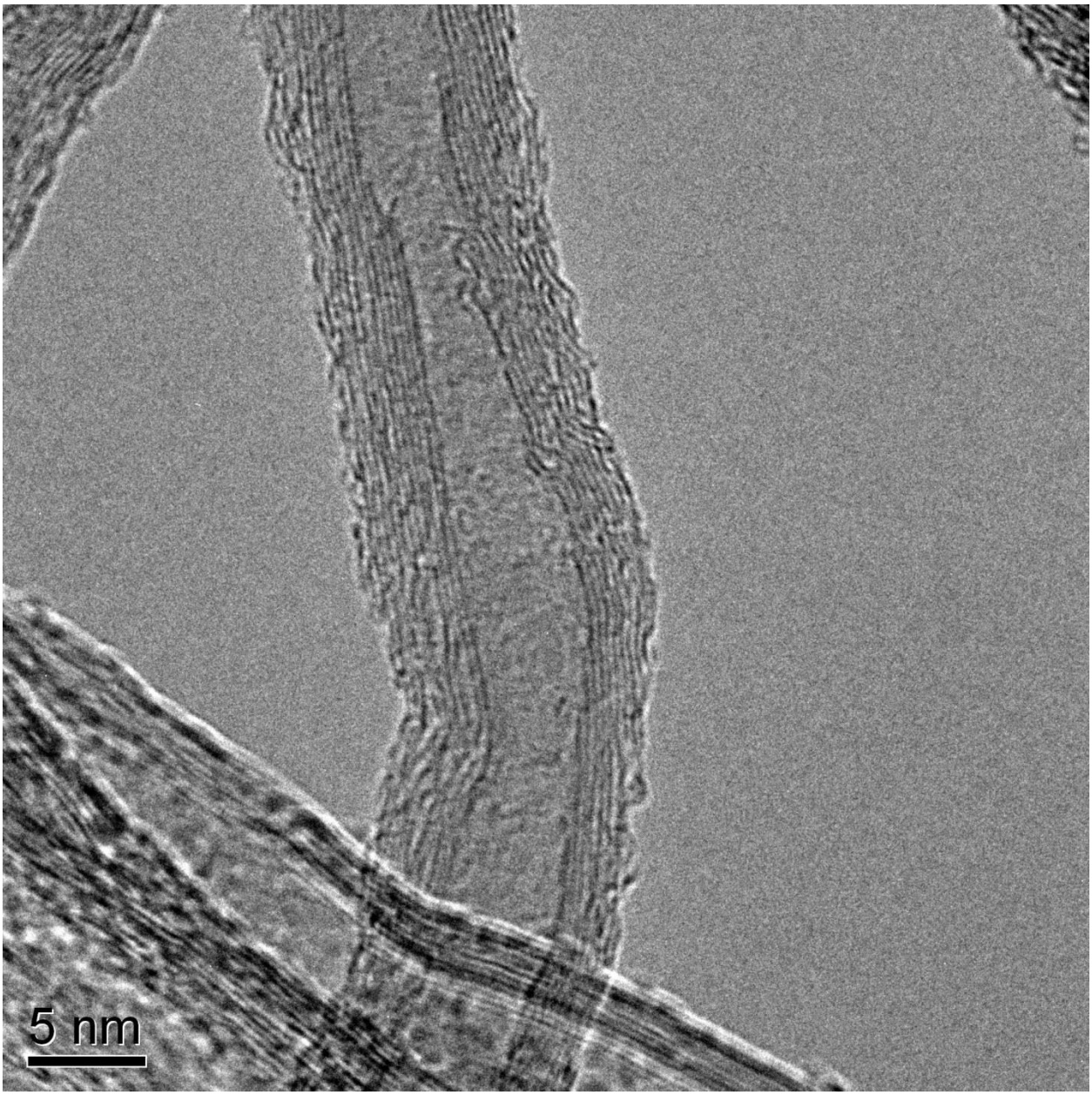
5 nm